POLITECNICO DI TORINO
Repository ISTITUZIONALE

Self-healing Polymers for Lithium Metal Batteries

(Article begins on next page)

12 June 2023

Doctoral Dissertation
Doctoral Program in Energy Engineering (XXXV Cycle)

Self-healing Polymers for Lithium Metal Batteries

By

Simone Siccardi

******

Supervisor:
Prof. Carlotta Francia

Doctoral Examination Committee:
Prof. Catia Arbizzani, Referee, University of Bologna
Prof. Maria Assunta Navarra, Referee, University of Roma "La Sapienza"
Prof. Marco Sangermano, Referee, Politecnico of Torino

Politecnico di Torino
2023

Declaration

I hereby declare that, the contents and organization of this dissertation constitute my own original work and does not compromise in any way the rights of third parties, including those relating to the security of personal data.

Simone Siccardi

2023

Acknowledgment

I did not make all this work alone so there are plenty of people I would like to say thank you for these three years of PhD.

First of all, I want to say thank you to prof. Silvia Bodoardo who gave me the chance for this great opportunity of research about electrochemistry studies and in particular for giving me the chance to use them in order to obtain self-healing capability in materials.

Thank you to dr. Julia Amici for giving me solid knowledge about the fundamentals of Electrochemistry. She has been my mentor and gave me lot of help on the experimental data collection, the submission of the paper, and in the end, for being always present and for all the support.

I also want to say thank you to professor Carlotta Francia, my supervisor, for the huge help she gave to me during this activity, even during the submission of the abstract for ISE of Prague and the speech in Lisbon, without her help and her support, everything would have been much more difficult and stressful.

A high thanks goes to prof. Luis Pereira and prof. Eliana Quartarone, for giving me the opportunity to work in their laboratory, in Lisbon and Pavia respectively; those experiences empowered my PhD results. Thank you, Tiago and Samuele, for their support in collecting research data when it was impossible for me to be in Turin to stay in the laboratory.

I also want to say thank you to all the people in the Electrochemistry group: Daniele, Davide, Laura, Sabrina, Matteo, Andrea, Roberto, Piera, Lucia, Federico, Mattia, Nadia, Anna, Claudia, Andrea, Riccardo, Giorgio, Elisa, Noemi, Sara; you made the laboratory very comfort and familiar place to me.

Thank you, Luisa, Giancarlo and Clara, for helping me with my difficult moments during these three years, for the nice experience of Iceland trip.

A big thank you to Laura, Matteo and Elena, my beloved neighbors. With your help I did not feel alone during the pandemic period, you've been like a "big family" to me and I felt so lucky to found you in a big city like Turin.

To Davide and Alessandro,

I will always fight for you.

"For Mum and Dad:
Love is the genesis of everything."

"Tommaso, sei stato bravo a resistere. Fai
così: sbaglia sempre per conto tuo. [...]
Fanno così le persone che vogliono essere
felici. Buongiorno, amore mio."

Summary

The abuse of fossil source of energy has increased the amount of greenhouse gasses in the atmosphere and as a consequence, the effects on the climate change became relevant in every-day life. Society is now implementing the storage technology based on renewable energy applied to vehicles moved by electrical propulsion engines. As a result, the production of large-scale lithium-ion batteries has increased. However, lithium ion batteries are approaching to the theoretical values, and the researchers are now focused on alternatives for increasing their features. Lithium metal batteries (LMBs) could be a valid choice because lithium anode possesses low gravimetric density and high theoretical specific capacity. However, the use of metallic lithium in these kinds of batteries brought up many problems of safety and poor cyclability, and those problems are mainly linked to a specific phenomenon which in literature is known as dendrite formation. The use of solid polymer swelled in commercial liquid electrolyte, called gel polymer electrolyte (GPEs) is one of the most relevant solutions for reducing dendrite growth and safety issues. GPEs with the capability of self-repairing could be a valid alternative to traditional polymers for increasing the life of lithium metal batteries. Self-healing process is mainly obtained by chemical interaction involving the formation of chemical bonds or secondary interactions. As we can assume LMBs can act like a closed system, the self-capability has to be spontaneously activated. For these reasons, hydrogen bond interactions are the most interesting chemical interaction and are mostly used in literature for this scope. By adding the self-capability process, with the introduction of an additive that can be introduced inside polymeric structures, it is very interesting to see that this solution is a valid strategy to obtain the self-healing reaction for gel polymer electrolyte in LMBs. In this PHD dissertation, the addition of a self-healing component ureidopyrimidinone methacrylate (UpyMa) is investigated in poly (ethylene glycol) methyl-ether-methacrylate reticulate structure. Since the self-healing additive is not commercialized, UpyMa must be synthesized by a coupling reaction involving methyl-isocytosine and 2-isocyanatoethyl methacrylate as reactants. The product is finally examined with spectroscopic analysis.

Two UpyMa-GPEs have been synthesized with a UV-polymerization without any solvents. Moreover, the polymers have been characterized for understanding the insertion of the additive inside the structure and their morphology. The self-healing properties are then evaluated at 50 °C and room temperature, in order to demonstrate its ability to repair after an external damage. In the last part of the dissertation, electrochemical characterization of the polymers has been carried out to assess GPE performances in lithium metal batteries.

Contents

List of Figures

List of Tables

Chapter 1

Preface

1.1 CO$_2$ Emissions and Climate Change

Climate change is one of the most important problems humanity has to solve in third millennium. A lot of human factors define climate change, but the most important is the emission in the atmosphere of greenhouse gasses, in particular CO$_2$ [1], which have a strong impact on the natural equilibria of the planet. CO$_2$ emissions in the atmosphere started since the first industrial revolution (1750), but after second world war it increased exponentially. Nowadays, the high concentration of CO$_2$ and other greenhouses gasses in the atmosphere determines an increase of temperature in all the world. The atmosphere temperature is in fact 1.5 °C higher than in 1970.

For these reasons, starting from III millennium, government of all countries in the world manage to find a solution. On this perspective, one of the most important environmental treaties is the Paris Agreement, signed on 2015, on 12th December at COP21 conference [2].

For these reasons two different scenarios have been described. The first one, with a global temperature higher no more than of 1.5 °C of the 1970s, the second one with 2.0 °C. In all the cases, as seen in Figure 1.1, it is important to stop the constant increasing of CO$_2$ of these last years.
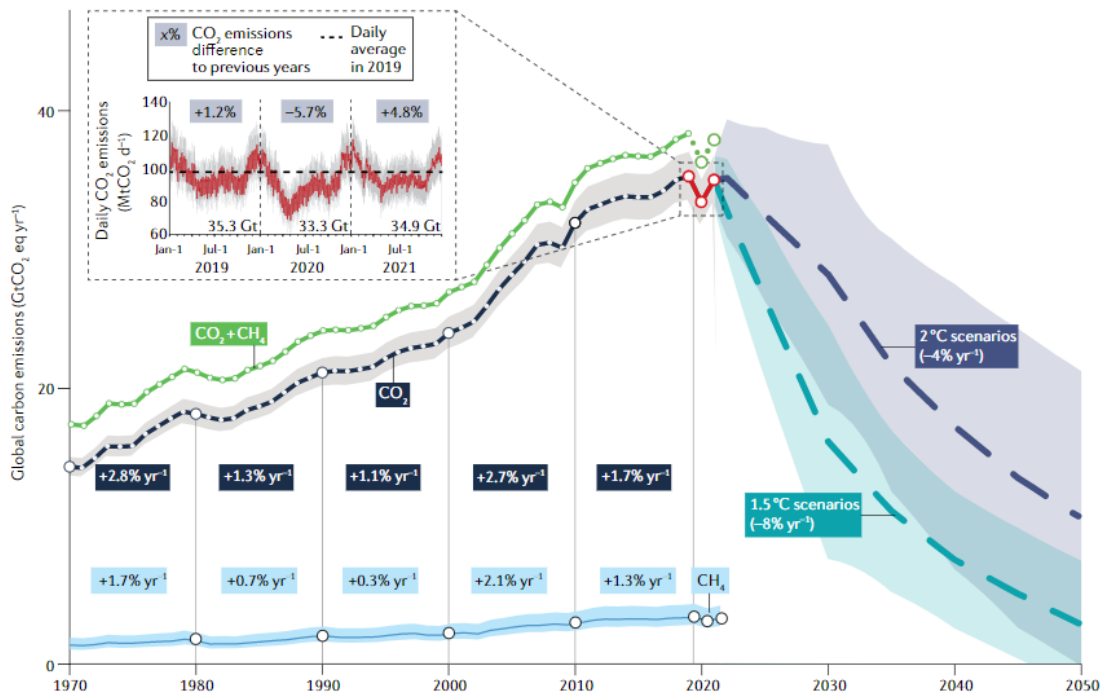
Figure 1.1: Global CO₂ and CH₄ emission trends. Temporal evolution of GHGs and possible evolution with different scenarios. [1]

The implementation of green technologies is a necessity. The main focus is to create a new possible life style able to decrease significantly the global greenhouse amount in the atmosphere, taking it to a zero emission.[3].

European Union is now moving into new forms of technologies to contrast climate change. In fact, starting from this decade, electrification is now increasing in all the countries. In fact, European Union is now moving to stop the commercialization of gasoline cars in 2035, and replace with electrical or hydrogen vehicles. Moreover, alternative forms of energy could derive from renewable fonts.

In this context, batteries are certainly useful technology for decreasing carbon dioxide and in general from greenhouse gasses in the atmosphere from transport, power and industry sectors [4]. Their large-scale use has a strong impact on a green electrification and for a climate neutral society. For these reasons, lithium ion batteries have a central role in our life, now and in the future. However, for having these results, batteries technologies need improvements. In fact, lithium ion batteries are approaching to theorical values [5]. For these reasons, batteries of the future must have ultra-high performances respect to nowadays. They must be safer,

with outstanding lifetime and reliability, and they must be sustainable and enter in a circular economy [6]. Moreover, batteries have to increase their energy and power, and must have a minor cost for a large-scale production in the factories, possibly moving to a clean and large-scale circular economy.

For this scope, the European Commission is now implementing support on new Strategic Action plans for Batteries, involving research and Factories. One of the most relevant actions made for these scopes is Battery 2030+.

BATTERY 2030+ is the European research initiative with the vision of inventing the sustainable batteries of the future. The main goal proposed is to enable Europe for large-scale and long-term vision to reach the goals recommended for the Electrification transition in European Union [7].

BATTERY 2030+ has got three main themes (accelerated discover of interfaces and materials; Integration of Smart Functionalities; Cross-cutting areas). All the main themes are divided in two areas (BIG, MAP, SENSING, SELF-HEALING, RECYCLABILTY, MANUFACTURABILITY) with a total of six research areas [8]. The areas of research involved all the fields, starting from the synthesis of new electrodes with high performances, the integration inside the cells of smart functionalities, able to increase the life of cells, and the implementation of recyclability and/ or manufacturability in the factories.
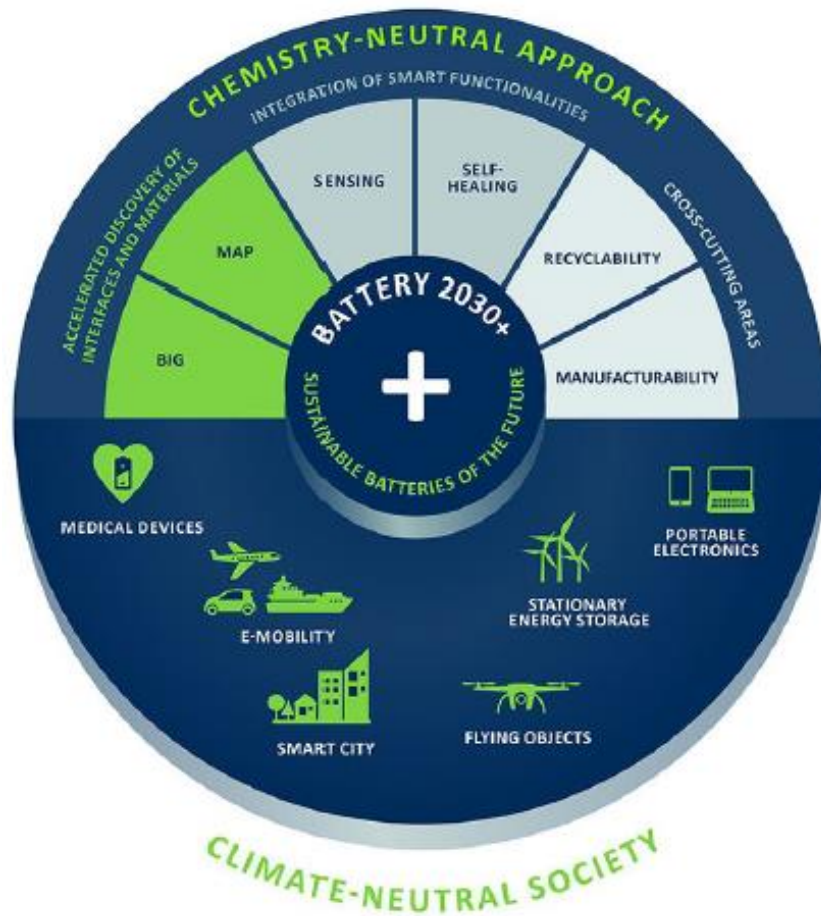
1.2 Self-healing on Lithium battery systems

Mainly focused on theme "Integration and Functionality", self-healing is one of the six aims of BATTERY 2030+. Improved batteries have to be sustainable, ensure better quality, higher reliability, prolonged lifetime and improved safety [9]. To increase the cyclability of the cell, systems require to self-repair autonomously after a damage. Consequently, systems will be able to restore their pristine conditions [10] and work for a longer time. This is a great result because a self-repairing system does not need a constant maintenance: future batteries with self-

repair capability can have lower management costs, lower environmental impact and, if well designed, higher performance.

Self-healing capability is a process directly inspired by something which already exists in nature, in fact, there are plenty different self-healing processes like the immunity system used by the organisms as a defence system. Other mechanisms are involved to restore pristine structures after being damaged. Self-healing processes on materials represent a flourishing field of research and a promising way in the developing of sustainable and long-cycle batteries.

Self-healing is intrinsically linked with sensor systems. If a battery is damaged, the sensor must be able to capture the anomaly and then transmit the information to an operator. With self-healing capability, it is possible to implement the process producing a signal able to give the self-repairing input to the cell. Vice versa, if self-healing is given without external inputs, the batteries can be able to self-repair autonomously, and the operator capture the change thanks to the information given by sensors. This input is sent by the sensor and used for monitoring the self-repaired level of the cell and the state of health of the battery pack.

Different strategies have been proposed for adding self-healing capability in LMB. Different materials used in batteries could be implemented with self-healing (cathode, anodes, separators, etc.). However, gel polymer electrolytes (GPEs) are the best options. Their use in LMBs can reduce dendrite formation, avoiding short circuits in the cells. GPEs are also able to maintain the most relevant properties of batteries, as ionic conductivity, stability of lithium on time etc. The GPEs able to self-repair represent a good option for future LMBs able to be more efficient, with a long life-cycle and with high energy density

For all these reasons, gel polymer electrolytes with self-healing capabilities have been examined in my Ph.D. work. Their synthesis, self-healing properties and performances in batteries are discussed in the following chapters.

1.3 Summary of Dissertation

In the chapter two, a brief introduction on lithium-ion batteries and lithium-metal batteries is given. To be more specific, parameters and components for LIB are described, followed by a division in class for principal gel polymer electrolytes and solid polymers, with a focus on their pros and cons.

The chapter three is focused on self-healing polymers and examples of self-healing processes are reported and at the end of the chapter and then a discussion on GPEs with self-capability properties is carried out.

In the chapter four there is a focus on the synthesis process for ureidopyrimidinone methacrylate (UpyMa), starting from an organic nucleophilic addition reaction.

The chapter five is focus on the synthesis of poly (ethylene glycol) methyl-ether-methacrylate based polymers with UpyMa as additive. Different proportion of UpyMa in the polymer has been proposed in the polymer in order to select the best GPE for LMBs. Self-healing and electrochemical measurements are carried out and discussed.

The chapter six reports the conclusions based on the study and the perspectives that can be explored more in-depth starting from the results.

Chapter 2

Lithium Ion Batteries

2.1 Introduction

During the III millennium since nowadays, energy storage has been a critical problem. On this perspective, lithium-ion batteries (LIBs) can be a solution thanks to their use in electrical vehicles as energy storage pit. Starting from 1990, LIBs have been commercialized first by Sony, and used in electronical portable devices, laptops and mobile telephones. In these last decades, LIBs use in electronics and energy storage has increased, and now, lithium batteries have now completely substituted the other batteries, in particular lead and nickel-based systems.

The success of LIBs over other battery types is clearly shown in the following Ragone plot (Figure 2.1). Lithium-ion batteries have a higher energy density (> 200 Wh kg^{-1}) if compared with other systems. In the recent years, the progress of technology allows LIBs to increase the energy density at higher values (~ 250 Wh kg^{-1}) [5]. The increase is strongly linked with the type of material inside the battery.

However, for increasing the energy density and having more efficient systems, batteries have to achieve a next-level implementation. With this scope, the solid-state lithium metal batteries represent a valid alternative, because of their high energy density, approached by lithium anode, and the safety of the polymer electrolyte. In the following paragraphs a non-exhaustive list of electrode/electrolyte of LIBs is presented and the most promising polymer families used in solid state batteries are proposed.
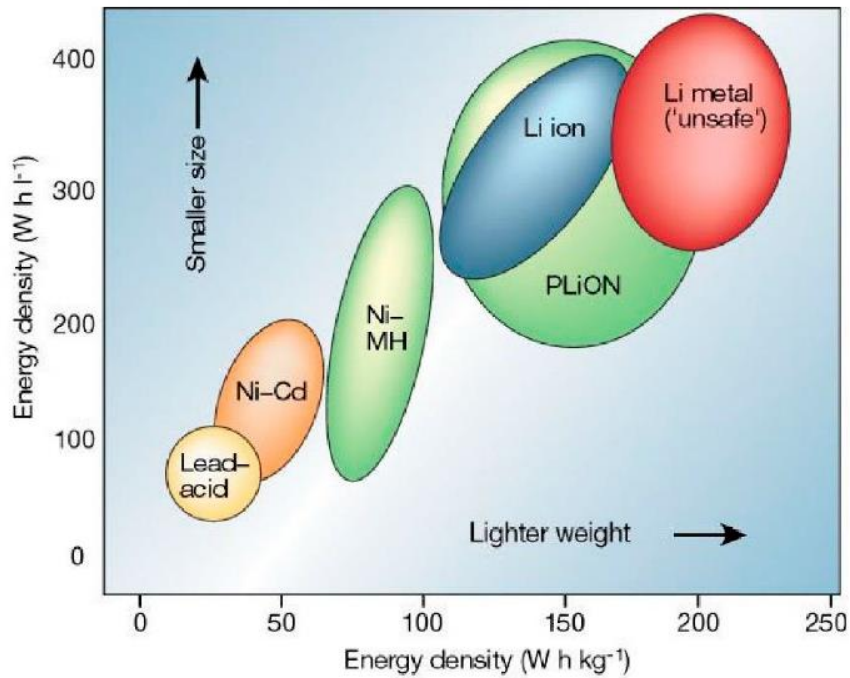
2.2 Battery Parameters

It needs several parameters to describe a single cell, each of them taken from different points of view, as for example performance, economical evaluations or environmental impact. These parameters depend on the materials involved in the cell, the reaction applied, the diffusion kinetics of the chemical species and the transport phenomena. Here a short list of the most important battery parameters is given:

Open Circuit Voltage (OCV)

The open circuit voltage is the voltage of the cell (or battery) with no load connected thus, no current is drawn or supplied. It represents the maximum Voltage available needed within the discharge, or the minimum reachable value to carry out charges from the cell. This parameter can be evaluated as the variation of Gibbs free energy level in standard conditions, due to the reactions occurring at the negative and positive electrode respectively.

$$OCV\ Cell\ =\ \Delta E^o\ =\ E^o_{cathode}\ -\ E^o_{anode}\ =\ -\frac{\Delta G^o}{n*F}$$

<div align="center">Equation 2.1</div>

Overvoltage

The overvoltage (η) is defined as the difference between the OCV and the effective voltage shown by the cell during discharge or, in other words as the difference between the potential of the cell and the OCV during the charging process.

Cell capacity

The cell capacity is the quantity of electrical charge achieved after the charge process, and can be described more specifically as the quantity of charges available during discharge process. This capacity is measured in [C] or [Ah], for example 1 Ah corresponds to 3600 C. The capacity of the cell during an interval between the time t_1 and another t_2 is measured with the following equation:

$$Q\ =\ \int_{t_1}^{t_2} I(t)\ dt\ =\ I*(t_2 - t_1)$$

<div align="center">Equation 2.2</div>

The specific capacity of the cell can be gravimetric or volumetric and is defined respectively as the amount of charge that a battery can accumulate, divided by the mass units (Ah g^{-1}) or volume units (Ah cm^{-3}).

Current density

The current density is the ratio of the total current (I) which flows to the electrodes, and the surface of the electrode (A). It is measured in [A m^{-2}]:

$$j(t)\ =\ \frac{I(t)}{A}$$

<div align="center">Equation 2.3</div>

C rate

The C rate (C) is the measure of the rate at which a battery is charged or discharged. The parameter is associated to the time required to charge and discharge the cell completely. For example, 1 C corresponds to the amount of current

necessary to charge (or discharge) the cell in a period of 1 hour. 0.1 C correspond to the current necessary to charge (or discharge) the cell in 10 hours.

Coulombic efficiency

The coulombic efficiency, Y, is the ratio between the capacity provided during the cell discharge phase ($Q_{discharge}$) and the capacity accumulated during the previous charge phase (Q_{charge}).

$$Y = \frac{Q_{discharge}}{Q_{charge}}$$

Equation 2.4

Energy

The energy of an electrochemical cell is defined as the product of the operating Voltage of the system (V) and the capacity (Q). It is measured in Joule [J], or, more commonly, in Watt-hours [Wh], which 1 Wh corresponds to 3600 J:

$$E = Q * V$$

Equation 2.5

Power

The power (P) delivered by a power source is defined as the average working voltage multiplied by the flowing current. It is related to the energy transferred per unit of time, and it is expressed in Watt [W]:

$$P = V * i = \frac{Q * V}{t} = \frac{E}{t}$$

Equation 2.6

2.3 Lithium Ion Batteries Fundamentals

A generic battery is mainly composed by using different units called cells, linked in series or in parallel.

In comparison with other typologies of batteries, lithium ion batteries are becoming most popular in the last decades, mainly because of their gravimetric and volumetric energy density.

Lithium-ion batteries are composed by four principal parts: anode, cathode, electrolyte and separator.

The anode is the electrode from which the electrons are released during oxidation reaction. On the opposite, the cathode is the electrode by which the electrons are captured because of the reduction reaction.

The electrolyte contains a solvent in addition to a dissociated salt, and it is normally added to the separator.

The separator is an electrochemically insulating material that divides the anode and the cathode. This allows the movement of the ions, but avoid the passage of the electrons. A classical model of separator is a membrane mainly made of microporous polyolefin.
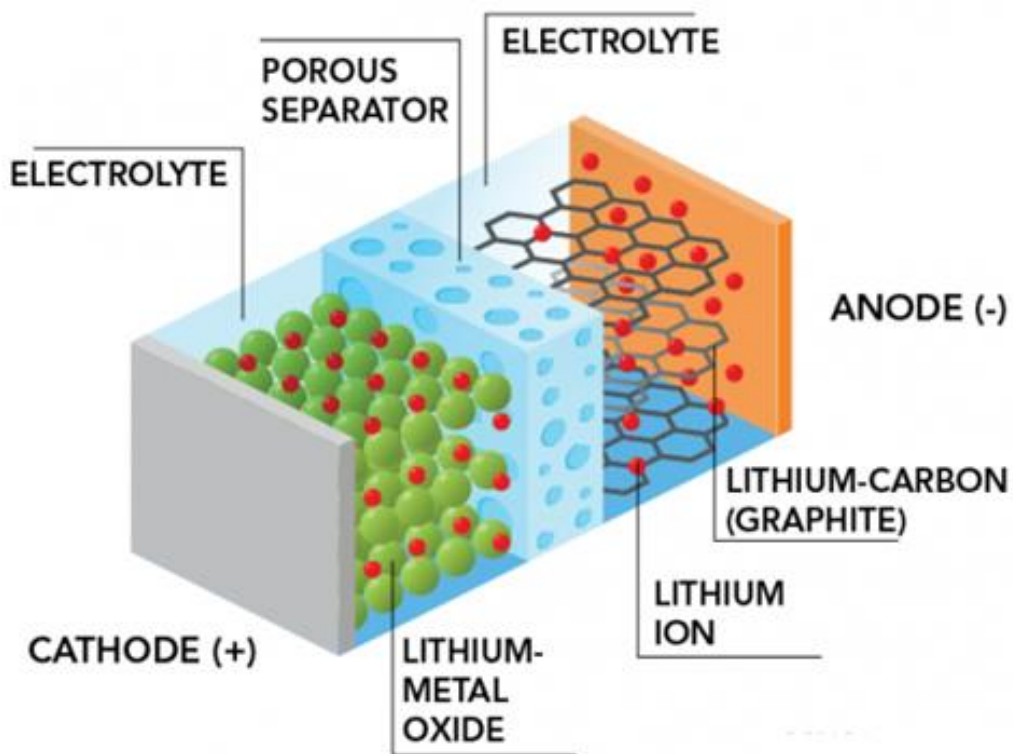
Figure 2.2: Schematic representation of components of Lithium Ion Batteries

During the processes different reactions occur at the electrolyte/electrode interfaces.

During discharge process, the negative electrode, the anode, releases electrons to the external circuit because of an oxidation reaction. On the opposite, on the cathode, electrons are accepted and reduction occurs. In the cell, a flow of anions and cations move to the corresponding electrodes, closing the electrical circuit.

In lithium-ion batteries, reversible process is available. During charge process, the flow of the electrons moves on the opposite direction, and the non-spontaneous redox reaction takes place.

Lithium-ion batteries are also known as "rocking chair batteries": at the anode starts a process often named as a "lithium sink" formation. On the opposite, the cathode is considered as a "lithium source" of Li^+.

First lithium-ion battery was produced with an anode of graphite and a $LiCoO_2$ cathode [11]. These types of cells are still the most used batteries in laptops and portables devices because of their high discharge potential (3.7 V) and for their high energy density (180 Wh Kg^{-1}).

The intercalation process takes place during the discharge/charge. During discharge process, lithium cations are de-inserted from the negative electrodes. The lithium cations migrate into the electrolytes and into the positive electrode ($LiMO_2$) [12]. As it was described before, this process is reversible and takes place on the opposite side during the charge process. [13]

. In lithium-ion batteries, the cathode is in general composed of $LiMO_2$, in which M is a transition metal [14]. On the opposite, the anode is composed of graphitic LiC_6. The reaction involved during the discharge/charge process for a generic $LiC_6/LiMO_2$ battery is the following:

$$Li_xC_6 + 2\ Li_{(1-x)}MO_2 \rightleftharpoons 6C + 2LiMO_2$$
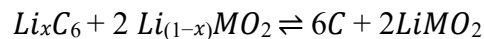
In which, the semi reactions involved at the anode and at the cathode are respectively [15]:

ANODE	$Li_xC_6 \rightleftharpoons 6C + xLi^+ + xe^-$
CATHODE	$Li_{(1-x)}MO_2 + xLi^+ + xe^- \rightleftharpoons LiMO_2$
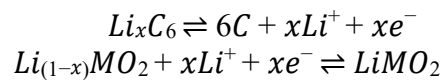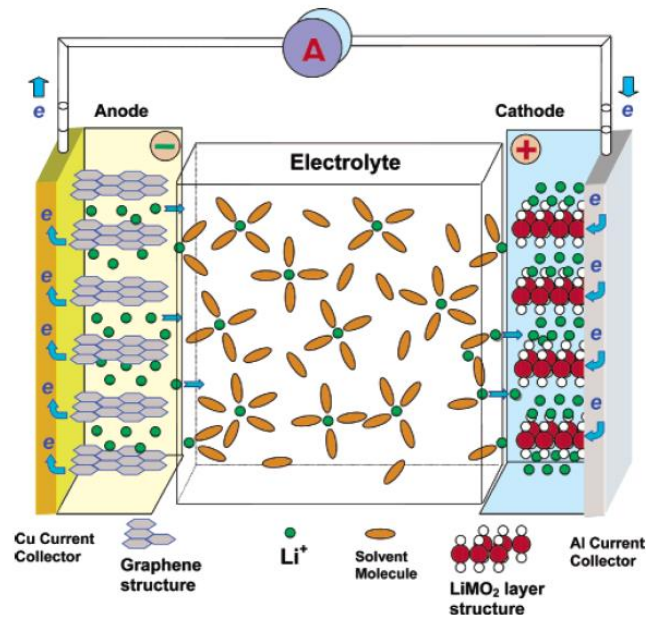
Figure 2.3: Schematic description of a lithium ion rocking-chair cell that employs graphitic carbon as anode and transition metal oxide as cathode [16].

The most common batteries are fabricated with $LiCoO_2$ as cathode and graphite as anode. The electrolyte in the separator is a mixture of organic carbonates with addition of a lithium salt. However, different other materials for LIBs are used and a short discussion is described in the following paragraphs.

2.4 Cathode materials

There are several materials that have been developed as active material for a cathode in lithium-ion batteries. The selection of the cathode depends on the type of battery and its future use. The most important features for a cathode are: low cost, easy intercalation of lithium ions in the structure, high stability. The most typical cathodes used in LIBs are LiM_xO_y or LiM_xZO_y where M is transition metal, and Z is a non-metal element. The most used cathodes in commercial LIBs are $LiCoO_2$, $LiMn_2O_4$ and $LiFePO_4$.
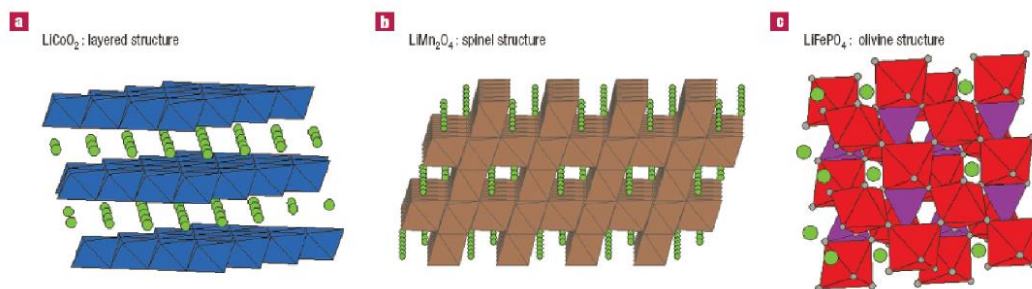
Figure 2.4: Layered, spinel and olivine structures of cathodes used in LIBs [17].

LiCoO$_2$ is the most commercial cathode used in lithium-ion batteries, because of its high stability, and good electrochemical performances (specific capacity of 140 mAh g^{-1}, operating voltage at 3.8 V vs Li/Li$^+$). This material shows a typical two-dimensional layered structure. However, LiCoO$_2$ has some issues due to the presence of cobalt metal in the structure, which is more expensive than other transition metals. Moreover, cobalt is not a "green" metal and its extraction is linked to regions with very critical exploitation issues, for example Democratic Republic of Congo, in which ethical and human rights violations still represent a huge plague. For these reasons, substitution of cobalt with other transition metal is a challenge for researchers.

LiMn$_2$O$_4$ is another cathode used in commercialized lithium-ion batteries, which presents an olivine structure with three-dimensional interdiffusion channels for Li$^+$. Moreover, manganese is less expensive and more abundant than cobalt, and its extraction does not involve any ethical issue. These reasons allow cheaper batteries can be produced than those based on LiCoO$_2$. Moreover, LiMn$_2$O$_4$ shows an operating potential of 2.2-4.2 V vs Li$^+$/Li, and specific capacity of 220 mAh g^{-1}. The most relevant problem is that manganese cathode shows high instability [12].

The complete substitution of the cobalt with other transition metals still remains difficult for commercial cathode. However, cathodes in which cobalt is partially substituted with other transition metals have been proposed by researchers in the last decades, as for example nickel, that is cheaper and greener than Co. As a consequence, LiNi$_{(1-x-y)}$Mn$_x$Co$_y$O materials have been synthesized and studied for future application in lithium ion batteries. The resulting "mixed" cathode has a controlled ratio of the three metal, depending on the features desired in the cathode. In particular, the most important are the high capacity (more nickel), better cycle stability (more cobalt) and high safety and cost (more manganese).

The most reported "mixed" cathode is $LiNi_{0.33}Mn_{0.33}Co_{0.33}O_2$, also named NMC 111. The cathode was synthesized in 2001 by Ohzuku et al., and shows a specific capacity of 200 mAh g^{-1}, and an operating potential range between 2.5 and 4.2 V vs Li/Li^+ [18]. NMC 111 could be defined as the precursor of high-energy and high voltage cathode materials. It was subjected of many systematic investigations, essential for the development of different systems, such as NMC 442 and the most popular NMC 532, characterized by good electrochemical performance and relatively low cost [19]. However, the capacity fading associated with the high-voltage operation is still a significant challenge. Other systems proposed, as NMC 622 and NMC 811, suffer of shorter life due to faster capacity fading. Figure 2.5 takes a comparison of the most reported NMC in literature [19].
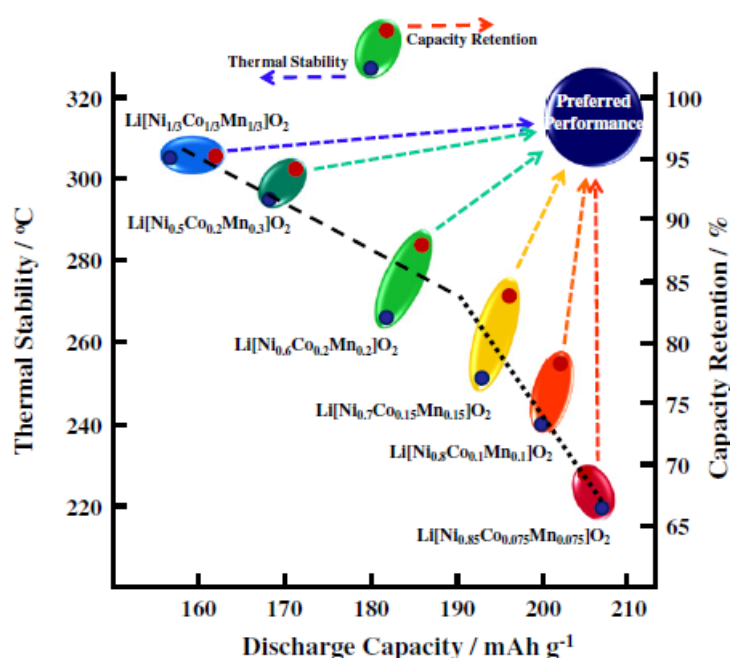
Figure 2.5: A map of relationship between discharge capacity, and thermal stability and capacity retention of Li/Li[NixCoyMnz]O2 (x = 1/3, 0.5, 0.6, 0.7, 0.8 and 0.85) [19].

$LiFePO_4$ (LFP) is another commercialized electrode material used as cathode in LIBs. Different from other transition metals, iron is an environmentally less impactful material, non-toxic and it is not expensive as other materials. [20]. In fact, Fe is one of the most abundant elements on Earth's crust, moreover, it possesses a high thermal stability (higher than 400 °C). $LiFePO_4$ has an olivine structure, in which lithium cations are intercalated into 1D linear diffusion channels [21].

Unfortunately, this means low ionic conductivity and lower density than other oxides, and poor volumetric energy density. However, LFP has good electrochemical features. In fact, the operating voltage of the cathode is 3.4 V vs Li/Li$^+$, and its specific capacity is 170 mAh g^{-1} [22]. Thanks to its long cycle life, low environmental impact, high thermal stability, LFP is a good candidate for wide range of battery applications, in particular for stationary applications where long cycle life is a key aspect [23].

Eventually, Table 2.1 summaries the most relevant features of the most common cathodes used in literature for lithium ion batteries [21].

Crystal structure	Compound	Specific capacity (mAh g^{-1}) (theoretical/experimental/typical in commercial cells)	Volumetric capacity (mAh cm^{-3}) (theoretical/ typical in commercial cells)	Average voltage (V)	Level of development
Layered	LiTiS$_2$	225/210	697	1.9	Commercialized
	LiCoO$_2$	274/148	1363/550	3.8	Commercialized
	LiNiO$_2$	275/150	1280	3.8	Research
	LiMnO$_2$	285/140	1148	3.3	Research
	LiNi$_{0.33}$Mn$_{0.33}$Co$_{0.33}$O$_2$	280/160	1333/600	3.7	Commercialized
	LiNi$_{0.8}$Co$_{0.15}$Al$_{0.05}$O$_2$	279/199	1284/700	3.7	Commercialized
	Li$_2$MnO$_3$	458/180	1708	3.8	Research
Spinel	LiMn$_2$O$_4$	148/120	596	4.1	Commercialized
	LiCo$_2$O$_4$	142/84	704	4.0	Research
Olivine	LiFePO$_4$	170/165	589	3.4	Commercialized
	LiMnPO$_4$	171/168	567	3.8	Research
	LiCoPO$_4$	167/125	510	4.2	Research

Table 2.1: Comparison of main cathode electrode materials in relation to their main characteristics: crystal structure, theoretical/experimental/commercial gravimetric and volumetric capacities, average potentials, and level of development [21]

Binders

In the cathode preparation, a specific non-reactive component called binder is used. An ideal binder is able to preserve the structure of the electrode during operation, avoiding any active material detachment from the current collector and limit problems of safety. Moreover, it must have a good stability, both physical (in particular thermal) and chemical (it must not show side reactions with the other cell components). Eventually, it has to be eco-friendly and cheap.

The most used binder in LIBs is polyvinylidene difluoride (PVDF) for its good electrochemical stability. However, its use is strongly dependent of N-methyl pyrrolidone (NMP), which is the most used solvent for the preparation of the electrode with PVDF as a binder. NMP heterocyclic compound is dangerous for the environment and toxic for human, so its application has to be limited.

2.5 Anodes Materials for LIBs

A good anode has to be a safe material for humans, able to avoid secondary reactions between lithium cations and the electrolyte, must be cheap and eco-friendly and in the end, its specific capacity must be relevant.

Graphite is the most used anode in commercialized lithium-ion batteries because it possesses a planar structure in which layers are linked by Van der Waals forces. The intercalation of lithium cations inside the graphite occurs in between planar graphitic sheets [24]. This anode shows an operating potential of 0.2 V vs Li/Li$^+$ and it is thermally stable, moreover, it is cheap and the theoretical gravimetric capacity is 372 mAh g^{-1} and the volumetric capacity is ~735 mAh cm^{-3}. However, compared to other anodes such silicon and lithium, it has low specific capacity. During the battery operation, the so-called solid electrolyte interface (SEI) is formed at the anode surface during the first cycles, and generally it consists of decomposition products, mainly from the electrolyte [25]. Nevertheless, SEI is also an insulator, in fact it avoids other decomposition reactions between the anode interface and the electrolyte. A controlled SEI formation is necessary to avoid safety issues such as loss of specific capacity and short circuits in lithium-ion batteries.
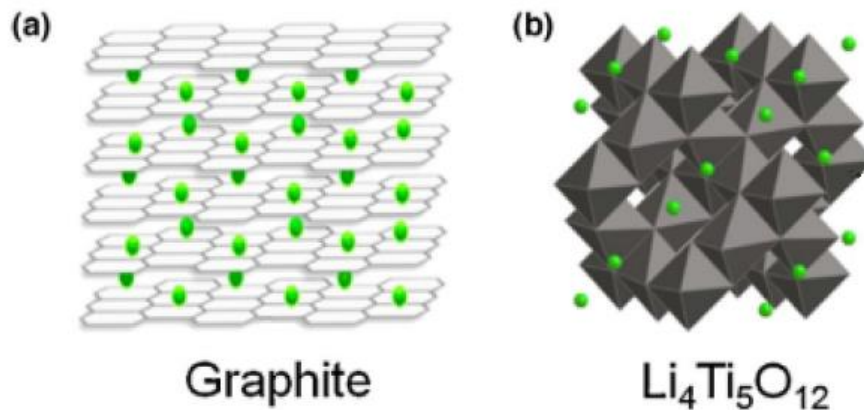
Figure 2.6: Crystal Structures of (a) lithiated graphite, (b) lithium titanate (LTO) [21]

The addition of silicon into graphite to form Si/C anode is a valid strategy to obtain LIBs with high energy density and specific capacity. Silicon is one of the most abundant elements in the earth crust, so it is economical and green. Moreover, it can be easily drugged via a low-cost mechanism, to form $Li_{22}Si_5$ with a theoretical

capacity of 4200 mAh g^{-1} [26]. Indeed, the anode possesses a low de-lithiation potential (0.4 V vs. Li$^+$/Li), this limits the lithium precipitation on the surface and, consequently, increases the safety of the devices. However, the main drawback of Si/C anode is the volume change during the charge/discharge process (the volumetric expansion is around 300%). The main consequence is a dramatic impact on the life cycle of the cell due to the volume expansion, fractures and pulverization of the structure in the electrode, which brings to the loss of the electrical contact between the active material and the current collector. For limiting the volume expansion, different solutions, as the insertion of suitable binders, or SEI film-forming ability of electrolyte, are under investigation by researchers.

Lithium titanate Li$_4$Ti$_5$O$_{12}$ (LTO) is a valid alternative anode in respect of graphite. Discovered by Ohzuku in the middle of 1990, LTO has a cubic spinel structure (Figure 2.6b). With a theoretical capacity of 175 mAh g^{-1} and a typical flat charge and discharge potential of approximately 1.55 V, LTO could be valid anodic material. Even if it possesses a lower specific capacity than graphite anode, its high compatibility with non-aqueous electrolyte systems, mixed with high stability and non-toxic properties, makes it a good candidate for negative electrodes.

Another widely studied negative electrode material is tin. Tin shows a great interest because of its high theoretical specific capacity (990 Ah g^{-1}) and, consequently, the possibility of obtaining battery with high energy density and power [27]. However, tin based electrodes show fast capacity fading upon cycling as well, generally ascribed to the large volume expansion associated to the alloying reaction with Li.

Titanium oxide TiO$_2$ presents high interest research because of its high potential for lithium intercalation (about 1.75 V), and theoretical capacity around 330 mAh g^{-1}. Moreover, it has a high chemical stability and negligible volume change during charge/discharge (< 4%) which means good cycling and lifetime [28].

However, the metallic lithium still remains the most interesting material for anode in batteries. Pure metallic lithium presents the lowest standard electrode potential (-3.04 V vs SHE) and it is the lightest metallic element [29]. With higher gravimetric capacity (3861 mAh g^{-1}), metallic lithium is now the best candidate for anode material in future next-generation batteries. However, its high reactivity with electrolytes, and lithium dendrite growth during charging/discharging process, limit its applications. The disadvantages of lithium metal anode, and the main solutions for its application are better described in following paragraph.

In the following table a short list of the advantages and disadvantages of the most common anodes for LIBs are shown [30]:

Active anode material	Theoretical capacity (mAh g^{-1})	Advantages	Common issues
Insertion/de-insertion materials			
A. Carbonaceous	200-600	➢ Good working potential	❖ Low coulombic efficiency
a. Hard carbons	1116	➢ Low cost	❖ High voltage hysteresis
b. CNTS	780/1116	➢ Good safety	❖ High irreversible capacity
c. Graphene			
B. Titanium oxides	175	➢ Extreme safety	❖ Very low capacity
a. LiTi$_4$O$_5$	330	➢ Good cycle life	❖ Low energy density
b. TiO$_2$		➢ Low cost	
		➢ High power capability	
Alloy/de-alloy materials			
a. Silicon	4212	➢ Higher specific capacities	❖ Large irreversible capacity
b. Germanium	1624	➢ High energy density	❖ Huge capacity fading
c. Tin	993	➢ Good safety	❖ Poor cycling
d. Antimony	660		
e. Tin oxide	790		
f. SiO	1600		
Conversion materials			
a. Metal oxides(Fe$_2$O$_3$, Fe$_3$O$_4$, CoO ,	500−1200	➢ High capacity	❖ Low coulombic efficiency
Co$_3$O$_4$, Mn$_x$O$_y$, Cu$_2$O/CuO, NiO, Cr$_2$O$_3$,		➢ High energy	❖ Unstable SEI formation
RuO$_2$, MoO$_2$/MoO$_3$ etc.)		➢ Low cost	❖ Large potential hysteresis
		➢ Environmentally compatibility	❖ Poor cycle life
b. Metal phoshides/sulfides/nitrides	500−1800	➢ High specific capacity	❖ Poor capacity retention
(MXy; M = Fe, Mn, Ni, Cu,		➢ Low operation potential and Low	❖ Short cycle life
Co etc. and X = P, S, N)		polarization than counter oxides	❖ High cost of production

Table 2.2: Most common anode materials used for lithium ion batteries [30]

2.6 Electrolyte Solution for LIBs

A good electrolyte solution requires a stable SEI formation, low viscosity, with a high wettability of the separator. Typically, the electrolyte is a mixture of linear or non-linear carbonates and a salt. Common organic solvents that can be chosen for lithium batteries are carbonate esters and ethers, in cyclic or a-cyclic structures [16]. Carbonyl oxygen in carbonate electrolytes is the binding site for Li$^+$ cation. As a consequence, the solvent molecules with C=O groups have a relevant role in the mobility of the cations [31]. A list of organic solvents mainly used in LIBs is given in Table 2.2 [16]. However, carbonate electrolytes suffer of high flammability. In fact, their flash point is around 30 °C. Moreover, starting from 5.0 V (vs Li$^+$/Li), carbonates degrade. As a consequence, liquid electrolytes can cause problems of safety, consumption of materials, and decline of electrochemical properties in the cells. For these reasons, replacing liquid electrolytes (LE) are now under investigation by researchers.

The most common salts used in literature are shown in Table 2.3. Salts in the electrolytes in LIBs are often fluorinated, because of their excellent resistance to the anodic decomposition. In particular, LiPF$_6$ (lithium hexafluorophosphate) is the most common salt, for its excellent electrochemical properties and good anionic mobility [32].

Lithium bis(trifluoromethanesulfonyl)imide, also known as LiTFSI, is a good candidate to replace LiPF$_6$. LiTFSI has a good ionic conductivity and high good thermal stability However, the main problem of LITFSI is the corrosion of the Al current collector, especially when the battery is in full state of charge[33].

Lithium boxaloborate (LiBOB) possesses an electrochemical stability window over than 4.5 V, consequently is one of the most common salt for high voltage cathodes for LIBs [34]. On the opposite, the solubility of LiBOB is a lower than LiPF$_6$, thus means a minor ionic conductivity when LiBOB salts is used.

Solvent	Structure	M. Wt	T_m/°C	T_b/°C	η/cP 25°C	ε 25°C	Dipole Moment/debye	T_f/°C	d/gcm^{-3}, 25°C
EC		88	36.4	248	1.90, (40 °C)	89.78	4.61	160	1.321
PC		102	-48.8	242	2.53	64.92	4.81	132	1.200
BC		116	-53	240	3.2	53			
γBL		86	-43.5	204	1.73	39	4.23	97	1.199
γVL		100	-31	208	2.0	34	4.29	81	1.057
NMO		101	15	270	2.5	78	4.52	110	1.17
DMC		90	4.6	91	0.59 (20 °C)	3.107	0.76	18	1.063
DEC		118	-74.3 [a]	126	0.75	2.805	0.96	31	0.969
EMC		104	-53	110	0.65	2.958	0.89		1.006
EA		88	-84	77	0.45	6.02		-3	0.902
MB		102	-84	102	0.6			11	0.898
EB		116	-93	120	0.71			19	0.878

Table 2.3: Lists of organic solvents for lithium battery electrolytes[16]

Salt	Structure	Al corrosion	σ, mS cm^{-1} 1 M in PC (25°C)	σ, mS cm^{-1} 1 M in EC−DMC (25°C)
LiPF$_6$	Li$^+$[PF$_6$]$^-$	No	5.8	10.7
LiClO$_4$	Li$^+$[ClO$_4$]$^-$	No	5.6	8.4
LiAsF$_6$	Li$^+$[AsF$_6$]$^-$	No	5.7	11.1
LiBOB		No	~5.0*	~11.0*
LiTFSI	Li$^+$[N(SO$_2$CF$_3$)$_2$]$^-$	Yes	5.1	9.0

Table 2.4: Lists of organic solvents for lithium battery electrolytes [33]

Room-temperature ionic liquids (ILs) represent an interesting category of electrolytes for the scientific community to produce supplant liquid electrolytes in

LMBs [35]. ILs are organic salts that have the main properties to be liquid at room temperature. They have been considered by researchers as systems with properties of salts and liquids solvents. Differently from liquids, they have a high boiling points, high viscosity and low volatility. Moreover, as they are salts, it is possible to combine different cations and anions for obtaining different ILs with different properties. However, as they are liquids, they possess high Li-salt solubility, and considerable ionic conductivity [36]. The most known ILs used in LIBs are imidazolium, pyrrolidinium and piperidinium cations with the combination of classical anions used in commercial salts (PF_6^- is the most used) [37]. Thanks to high boiling temperature and non-volatility properties, they have been used in new safer LIBs [38], [39]. Moreover, their use is preferred because of their high oxidation potential (~5 V vs Li^+/Li), non-flammability, their low vapour pressure, elevated thermal stability, low toxicity. Eventually, they can act as ionic liquid-derived polymers, as wetting agents' systems able to form films on the electrode surface for the protection of lithium metal anode in LMBs [40].

Unfortunately, ILs present low ion-conductivity in respect to liquid electrolytes. For this reason, the mixtures of IL and liquid carbonates-based electrolyte, must be well investigated to achieve the safety characteristic and preserve high ionic conductivity. Even the combination of ionic liquids with lithium salts is a valid option for increasing the conductivity. Nyholm et al. fabricated an ionic liquid containing LiTFSI, and 1-butyl-1-methylpiperidinium bis(trifluoromethanesulfonyl)imide. The liquid electrolyte exhibits a conductivity of 1.3×10^{-3} S cm^{-1} at room temperature and the cell assembled with SnO_2 as electrode has a discharge capacity of 486 $mAhg^{-1}$ when it cycles 80 °C [41].
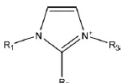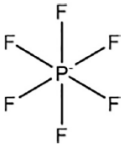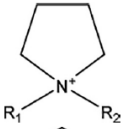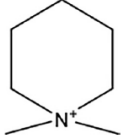
Cations	Structure	Anions	Structure
Imidazolium		Hexafluorophosphate	
Pyrrolidinium			
Piperidinium			

Table 2.5: Structures of some commonly used cations and anions in ionic liquid electrolytes [37]

2.7 Lithium metal as anode for next generation batteries: perspectives and main challenges

Lithium-ion batteries are now the main power sources for electronics, as mobile devices, tablets, smartphones, etc. However, the continuous expanding market of electronics, mixed to the increase of full-electric vehicles and stationary storage system, has brought to light the need of battery systems with higher performance standard. Despite their constant improvements, and their commercial success during the last decades, in different fields the performing duties are not adequate. The more typical example is electrical vehicle, in which it is required batteries with performances and fast charges [42]. It is imperative to develop new alternative battery chemistries with lower costs and higher energy density for both these applications and the emerging technologies. The substitution of graphite anode with pure lithium metal can represent the most valid solution for more performant batteries. In fact, the gravimetric capacity of lithium is 3861 mAh g^{-1}, which is ten times higher than graphite (372 mAh g^{-1}) [43]. Moreover, this means that the energy density of LMBs are 400 Wh Kg^{-1} and 1500 Wh L^{-1} [44].
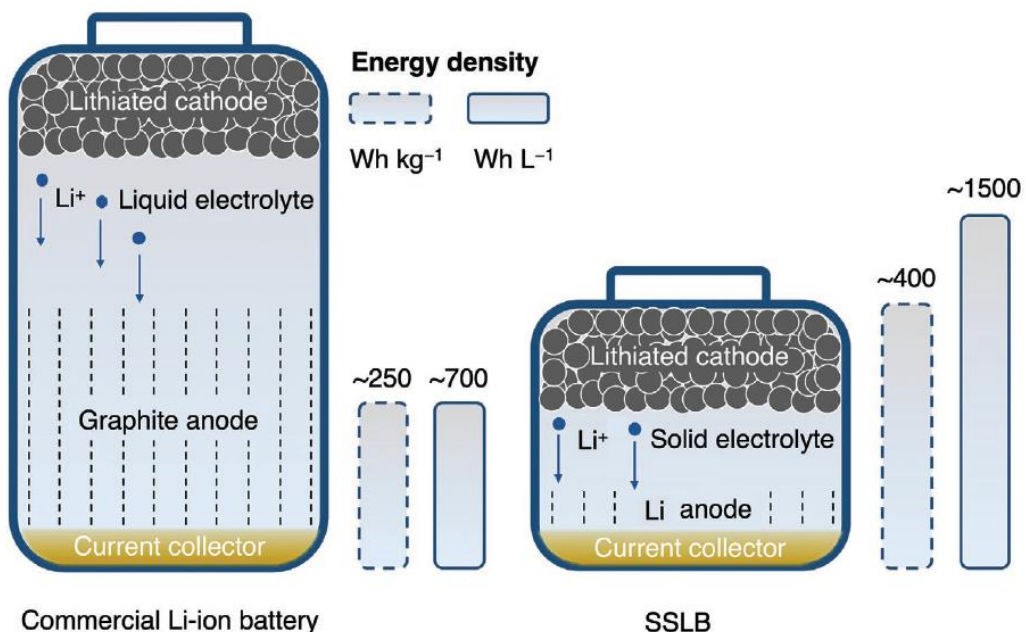
Figure 2.7: Schematic representation and comparison of solid-state lithium metal batteries and commercial Li-ion batteries [45]

22

The simple substitution of the graphite with lithium can provide a battery with high gravimetric energy density and a minor volume [46][47]. This is a great advantage for electrical vehicles.

Actually, substantial efforts are made to finally benefit from the advantages of Li metal anodes in commercial rechargeable cells, and most research programs are now launched for accelerate this transition. The Figure 2.8 takes a short comparison of recent roadmaps in the world. In particular, Europe is now moving for become competitive with the other continents, planning the transition to LMBs starting from 2025 with solid state lithium metal batteries.
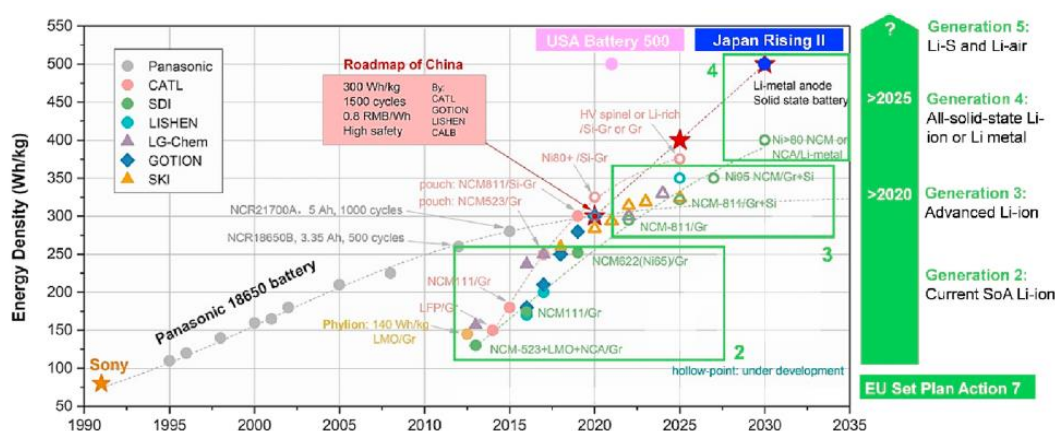
Figure 2.8: Comparison of roadmaps and targets of different R&D programs worldwide. Evolution of battery chemistry is also depicted. Plot modified from the Battery 2030+ Roadmap [29]

However, different challenges are now limiting the application and the commercialization of LMBs, first of all the high reactivity of lithium. In fact, its low standard reduction potential is also the root of its high reactivity [29]. Metallic lithium is chemically unstable with many electrolytes, polymers and ceramics. Even when stored under inert conditions, i.e., under argon, lithium readily reacts with trace residual atmospheric gases, resulting in a surface passivating layer. The most common products of these secondary reactions consist of Li_2O, $LiOH$ and Li_2CO_3 [48]. The so obtained inorganic compounds are called "solid electrolyte interface (SEI) and affect the coulombic efficiency and long-term cycling of LMBs [49].

However, the most relevant issue related to lithium anode is the dendrite growth. Lithium dendrite is an uneven deposition of lithium on the surface of the anode [50]. This phenomenon of dendrite growing, have been studied by different scientists, the first one was Wranglen in 1960 [51].

Lithium dendrites appears during charging process at very low overpotentials (0.1 V/Li) and can be observed as a regular deposition of Li-metal on the surface of

the lithium anode [52]. However, when the overpotential is increased, (0.5-3.5 V/Li), the lithium deposition starts going irregular, and the reaction is followed by the formation of whisker dendrites. The continuous plating/stripping process brings to a continuous dendrite growing with mossy (bush like) and shape forms. Dendrite formation goes on, appearing as a fractal structure until it erupts on the surface of the separator, causing short circuits of the cells [53] .
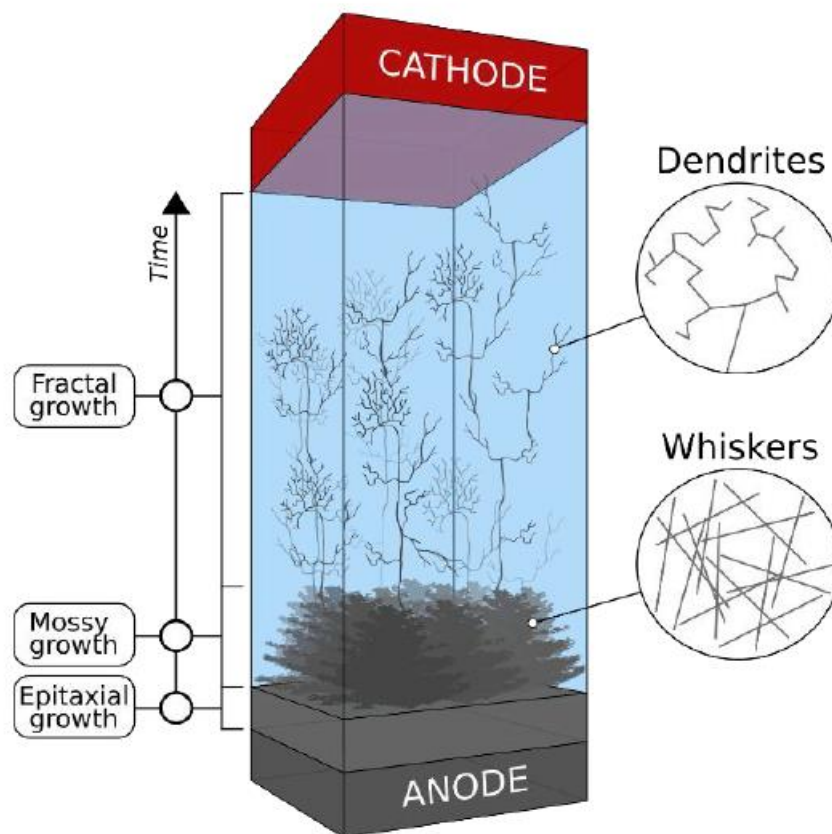
Figure 2.9: Schematic representation of lithium growth as observed experimentally under battery operating conditions [54].

In general, dendrites develop in different morphologies. The most common are epitaxial, mossy granular, whiskers and fractal. Some morphologies are unstable and can convert into each other's or coexist in different types simultaneously. Dendrites can grow in all directions, but generally they evolve in a single specific branch.

The main problems caused by the dendrite growth are described as follows:

- Short circuits of the cells. The growth of the dendrites causes the pierce of the separator. As a consequence, the negative anode will be in contact to the cathode, short-circuiting the cells. The short circuiting of the cell may cause electrolyte ignition and battery explosion. This means low cell stability and short cycle life.
- Side reactions. Dendrite formation is linked to electrolyte depletion. Lithium can react with commercial electrolytes. These reactions irreversibly consume lithium and electrolyte, and, consequently reduce the specific capacity of the cell.
- Increase of polarization. Side reactions may cause a formation of a film which is not ionically conductive. As a consequence, polarization increases, causing malfunction of the cell.
- Volume expansion. With the dendrite growth, the lithium becomes more porous, occupying a major volume and as a result, there is a fatal loss of coulombic efficiency and relatively safety issues.
- Formation of "dead lithium". Dendrites are also able to diverge from the anode. As a consequence, the detached lithium is able to move easily into the electrolyte. The main consequence is the loss of lithium during the charge/discharge process, so it is "dead". Moreover, this movement causes loss of coulombic efficiency and safety issues, causing problems of SEI formation.
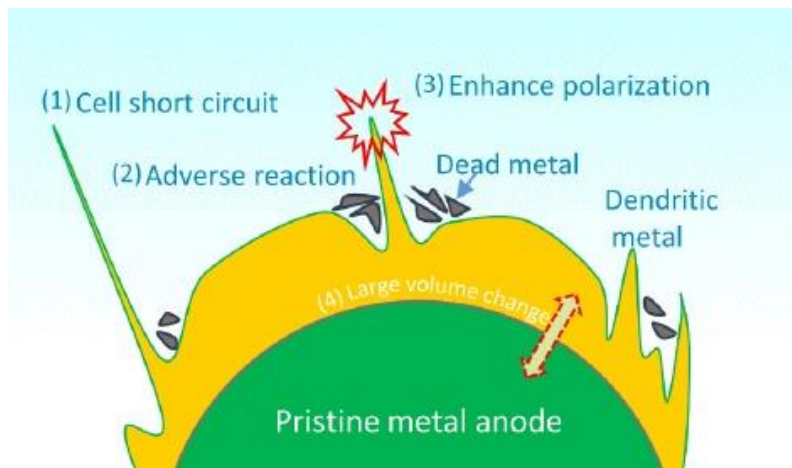
Figure 2.10: Schematic illustration of problems caused by lithium dendrite formations [55].

Different strategies have been proposed since 1960s to limit dendrite growth in LMBs. First of all, alloying structures have been proposed, as Si, Al, C, to reduce significantly the dendrite formation [56]. However, the alloy anodes do not solve the problem of volume changing inside the electrode. For these reasons, it is critical for alloying anodes to have long cycles life and safe operation [57].

Another strategy is the organic interface design. In this case, a mask is created between the anode and the liquid electrolyte in order to protect lithium against the side reactions with the electrolyte. Moreover, the mechanical strength of mask is also responsible in blocking the dendrite formation [58].

2.8 Polymer Lithium Metal Batteries

Suppression of lithium dendrites during charge/discharge process is the main solution to solve hazards and unsafety problems in LMBs. For this reason, the introduction of a solid polymer electrolyte inside the battery system could be a relevant solution [59]. Polymer electrolytes (PEs) are membranes with similar ion transport properties of common liquid electrolytes. Since 70's, researchers have focused on solid polymer in LMBs to decrease side reactions at the lithium anodes and the advantages have soon appeared clear. Polymer are able to limit or even avoid dendrite growth and short circuiting. For these reasons, lithium metal solid state batteries (LSSBs) are innovative solutions for safer batteries with high energy density [60]. A good PE must have some features, described in Figure 2.11. The most relevant are [61]:

- high ionic conductivity. Liquid electrolyte possesses a conductivity at room temperature of 10^{-3} to 10^{-2} S cm^{-1}. Polymer electrolytes are approaching 10^{-3} S cm^{-1} at ambient temperature.
- High transference number. A large transference number can reduce the polarization during charge–discharge processes, and thus increasing the power density.
- Chemical, thermal and electrochemical stability.
- Mechanical Strength. The mechanical strength is important for limiting the dendrite growth and avoid the short-circuits.
- High boiling point (>180 °C).
- High level of purity.
- Safer, fire retardants, low cost and eco-friendly.
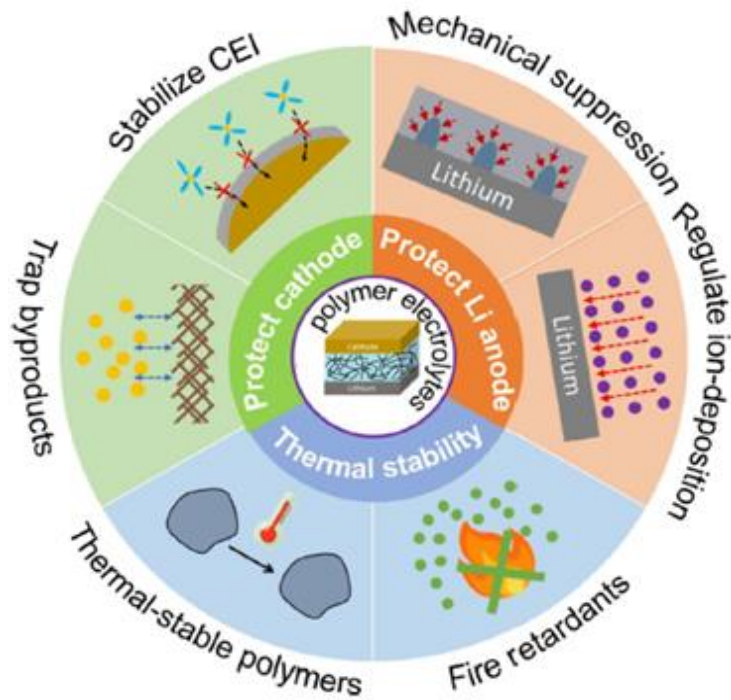
The features of a polymer are strictly dependent on its chemical bonds and its architecture design.

Polymers have different structures. The most relevant in solid state batteries are linear, comb-like, hyperbranched and crosslinked [62].
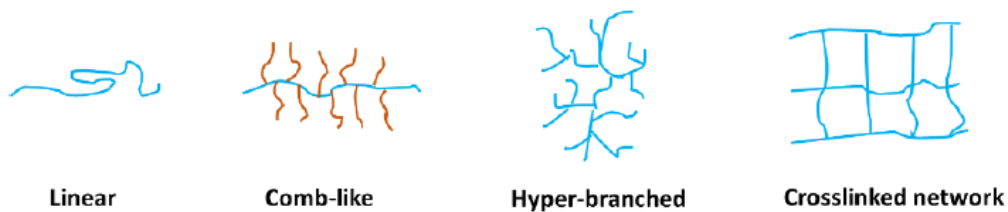
A linear architecture is the simplest structure that can be found in polymer morphology. In this form, the polymer chains are not linked by chemical bonds or lateral chains, but only via secondary interaction, as Van der Waals forces. Because of these weak interactions between the chains, the chains possess a high mobility;

this often brings to an increased ionic conductivity and high transference number. Linear polyethylene oxide (PEO) is one of the first polymer studied for application in lithium metal battery [62]. PEO is a poly-ether with the following chemical structure: $H\text{-}(O\text{-}CH_2\text{-}CH_2)_n\text{-}OH$ [63]. Its use in different fields has increased in the last years (as in different fields for example biological and medical science), mainly because of its low cost and low toxicity.
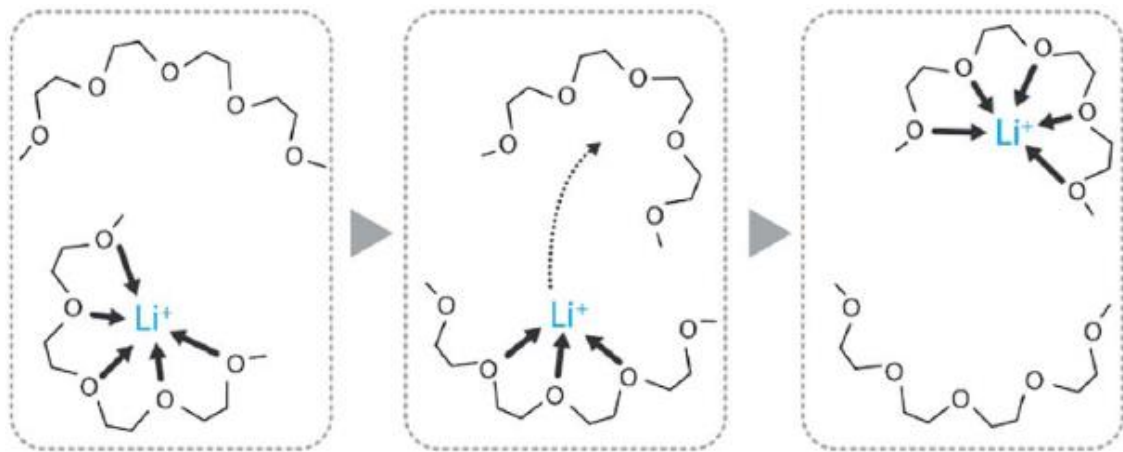
Figure 2.13: Schematic drawing of Li+ transport in a PEO matrix, assisted by the segmental motion of the polymeric chains [64]

The ethoxy group is able to complex the Li^+, as reported in the scheme of Figure 2.12. Moreover, repeated ethylene oxides in linear structure are also responsible of the transport of lithium ion. The main consequence is a good ionic conductivity and ion transference number. However, the linear morphology is also responsible to high level of crystallinity inside the polymeric structure [65]. Because of the increasing of the amorphous phase, PEO are often use in LMBs at temperature conditions higher than room temperature (generally 50 °C – 60 °C) [66]. Although batteries for EVs usually work at high temperature, a solid-state system requires operation in a wider range, which includes lower temperature ranges.

Linear structure is also responsible to low mechanical strength, because is not able to contrast dendrites growth. Moreover, the terminal -OH group confers at polymer hygroscopic features.

Polycarbonates (PCs) have been investigated as an alternative for polymer electrolytes. In fact, their chemical structure is similar to the cyclic and linear carbonates used as liquid electrolytes. As a consequence, polycarbonates are high-molecular weight analogues of the linear alkyl carbonates and they demonstrates reasonable performances in LMBs. Polycarbonates can coordinate easily the Li^+

with the carbonyl group oxygen, and, as a consequence, the movement of the lithium inside the polymer is enhanced. Polymer with aromatic structures in the side chain possess a more rigid structure than the aliphatic ones. Those restrict the movements of the chains and increase their crystallinity. The more preferred are polytrimethylene carbonate (PTMC), poly(ethylene carbonate) (PEC) and poly(propylene carbonate) (PPC) because of their amorphous structure, flexible chain segments and high dielectric constant.

In different cases, the copolymerization of different polymers is a technique used to obtain new polymers with more performant properties.

Poly (vinylidene fluoride) (PVDF) is used as polymer electrolyte because of its peculiar properties. Thanks to its polar C-F bond, it possesses a high dielectric constant and a good capability in the dissolution of lithium salts [67]. Moreover, the electrochemical stability of PVDF is high (> 5.0 V vs Li/Li$^+$) [68], [69]. However, its application as linear polymer has been limited in LMBs because of its poor interfacial properties. The C-F bonds are able to create a polymer with a semi-crystalline nature. As a consequence, the ionic conductivity is lower compared to other PEs [70]. The copolymerisation of PVDF with hexafluoro propylene (HFP), shown in Figure 2.14, is a smart solution for increasing its properties. In fact, the new polymer (PVDF-HFP) has an improved ionic conductivity, because of the presence of the HFP, that has an amorphous structure, in contrast with the semi crystalline of vinylene fluoride [71]. Recently, Wang et al. fabricated a PVDF-HFP based polymer electrolyte for application in LMBs. The polymer exhibits an ionic conductivity of 9.4×10^{-4} S cm^{-1} at room temperature and an electrochemical stability window wider than 5.2 V [72].
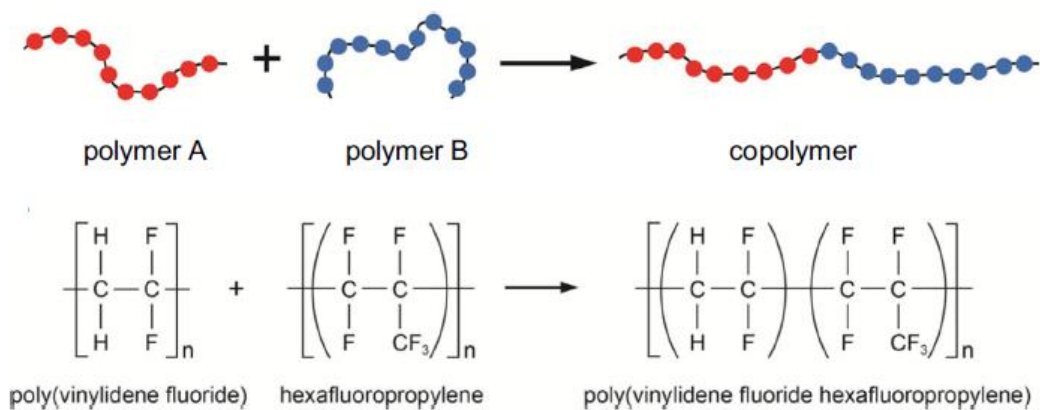
Figure 2.14 Pictorial model of the preparation of a copolymer and an example of copolymer formed by PVDF and HFP [73]

29

To decrease the crystalline structure of polymers, other different architectures have been proposed.

Architectures with side chains have been explored by researchers for applications in LMBs. In that case, the side chain of polymer possesses a higher level of disorder due to the presence of "branches" inside their structure. Depending on the length of the side chains, it is possible to have different morphologies as comb-like, and hyper-branched, which are architectures that present incorporated side chains. The presence of side chains is responsible of the increase of the amorphous phase. In the case of comb-like and hyperbranched, the mobility of the side chains could also give high transport of lithium ions.

Polyacrylonitriles (PANs) are one of the classes of polymers major used for the synthesis of PEs. In fact, their structure has a -CN group as side chains. The presence of ciano group allows a high interaction with the carbonyl -C=O groups of the carbonate liquid electrolytes and Li^+ ions [44]. This is possible without losing any mechanical properties of polymer [45]. Moreover, PAN is thermal and electrochemical stable. It possesses flame resistance and capability to contrast oxidative degradation [46]. The high ion-solvating ability allows PANs to be good candidates for GPEs [47].

However, some issues are related to the CN group, which is responsible of high crystallinity, causing low ionic conductivity. The crystallinity is due to the polar interactions between adjacent ciano groups in the polymer side chains. For these reasons, the copolymerization of PAN with different polymers, as poly(vinyl acetate) (PVAc) in PAN to form poly-(acrylonitrile-vinyl acetate) (PVA), or PMMA-incorporated PAV is a solution for enhancing the ionic conductivity and the mechanical stability [78].

Yang et al. fabricated a polymer electrolyte PAN/PVA based for application in solid state systems. The polymer exhibits an ionic conductivity of 1.13×10^{-4} S cm^{-1} at room temperature, a lithium ion transference number of 0.5, and a discharge capacity of 159.6 mA h g^{-1} at 0.1 C when a Li/PE/LFP cell is assembled [79].

On the opposite, crosslinked polymers possess higher strength and stability, because of their reticulate architecture in which all the chains are interconnected.

Polymethyl methacrylates (PMMA) and polyethyl methacrylates (PEMA) are classes of thermoplastic polymer studied for possible use in PEs [48]. Differently from other polymers, they have a completely amorphous structure. Moreover, the polymer chain with ether group is good to increase the movement of the lithium ions inside the polymeric structure. The ionic conductivity at room temperature is in the range $5 \times 10^{-3} - 5 \times 10^{-5}$ S cm^{-1}, higher than other polymers used in PEs[81]. Their chemical structure is quite similar to PEO, except for the methacrylate group.

Poly (ethylene glycol) methyl ether methacrylates (PEGMEM) are a class of PEMA in which the terminal -OH group is substituted by a -OCH$_3$. As a consequence, PEGMEMs are less hygroscopic and have a high compatibility with carbonates solvents. Moreover, from other polymers used in GPEs, PEGEMEM is economical, and possesses good interfacial stability with lithium [82].

PEGMEM has the advantages of wide availability, good electrochemical stability and low toxicity [83]. Moreover, mechanical and thermal properties of PEGMEM could be increased with by a copolymerization. In fact, methacrylate can be easily modified by reacting with other polymers, forming co-polymers with different architecture.

The polymerization with polyethylene glycole diacrylate (PEGDA) allows crosslinked polymer electrolyte with high thermal stability [84]. Xu et al fabricated a reticulate polymer electrolyte by using PEGDA as crosslinker. The obtained PE exhibits good ionic conductivity (1.29×10^{-4} S cm^{-1}) and a discharge capacity of 113.3 mAh g^{-1} after 100th cycle at 0.1 C and 60 °C in a Li/PE/LFP full cell [85]. Moreover, it is relatively easy to introduce side chains for giving the polymer peculiar characteristics. This is easily due to the methacrylate group, that allows polymerization by thermal or UV polymerization [86]. These methods are relatively easy, and cheap.

PEGMEM is expected to be beneficial for Li$^+$ transport and have the ability to solvate the Li$^+$ or the liquid electrolyte inside of the polymer matrix by the C=O polar group [87]. As a consequence, PEGMEM systems show good ionic conductivity, and high electrochemical stability.

Polymer matrix	Molecular formula	Glass transition temperature T_g/°C	Melting point T_m/°C
PEO		−64	65
PC		5	Amorphous
PAN		125	317
PMMA		105	Amorphous
PVDF		−40	171
PVDF-HFP		−90	135

Table 2.6: Polymer matrix, with chemical formula and min characteristics [88].

The main problems related to the use of polymer electrolyte in LMBs is the ionic conductivity. For increasing the ionic conductivity, three are the main strategies used in literature: the addition of solid salt in polymer structure, the addition of an inorganic filler to decrease the crystallinity of the polymer, the addition of liquid electrolyte to swell in polymeric electrolyte. For these reasons, PEs have been classified in three families: solid polymer electrolytes, composite polymer electrolytes (CPEs) and gel polymer electrolytes (GPEs).

Solid polymer electrolyte is a class in which liquid electrolytes are completely substituted by solid structure able to move cation ions and stop dendrite growth. Starting from studies of 1970s, SPEs could be a promising solution for the battery of the future [89].

There are different subcategories of this huge family: conventional salt-in-polymer or solid polymer electrolyte, and single ion conducting polymer electrolytes (SICPEs) are the most important [90]. All solid polymers have mixed with different lithium salts for increasing the mobility of lithium ions. In general, salts are lithium bis(trifluoromethanesulfonyl)imide (LiTFSI) or bis(fluoromethanesulfonyl)imide (LiFSI). SPEs have excellent flexibility, safety performance, good contact with electrodes. The absence of any liquid electrolytes allows SPEs being safer. In fact, the full elimination of liquid electrolytes reduces secondary reactions at the lithium anode. The presence of a solid structure allows to contrast dendrite formation with a mechanical resistance. However, the main problem of SPEs is the low conductivity at room temperature (in general lower than 10^{-4} S cm^{-1}) and inferior thermal and electrochemical stability [91].

In order to increase the ionic conductivity at room temperature, different choices have been proposed. The most promising is the single ion polymer conducting (SICPEs), which is mainly characterized by the presence of anchored anionic species into the polymer chain. The presence of negative charges affects the Li$^+$ ion and increases the ionic conductivity. However, the conductivity of SPEs is far below the classical liquid electrolytes.

Composite polymer electrolytes (CPEs) are a class of materials in which inorganic particles are inserted into a polymer structure. Oxide nanoparticles are incorporated into the solid phase of the polymer [91]. The most typical oxides used are SiO_2 and Al_2O_3 and TiO_2, that are environmentally friendly and cheap [73]. First studies of CPEs have been reported by Weston and Steel in 1982 [92], by using alumina and PEO. Insertion of the particles in the polymer structure has the main rule to decrease the crystallinity of the polymer electrolyte. As a consequence, the ionic conductivity at room temperature is increased. Moreover, for the presence of

ceramics inside the polymer, CPEs possess high thermal stability and the high capability of suppression of the dendrites [93].

However, the main disadvantage of CPE is the poor contact between the electrodes. This restricts their direct use in LMBs.

Gel polymers electrolytes are a class of polymer electrolytes in which a polymer structure is swelled in liquid electrolytes, forming a gel structure [94] [81]. GPEs are mainly based of a polymer, in which liquid electrolytes have the rule of plasticizer. Different from SPEs, GPEs present higher ionic conductivity (more than 100 folds of improvements over the SPEs), particularly at room temperature. GPEs possesses a high interfacial contact with electrodes and improved mechanical flexibility [40] Liquid electrolytes used in LMBs are incorporated inside the polymer structure, empowering the amorphous structure of the polymer [95]. For these reasons, GPEs are improved thermal and electrochemical properties. As a combination of solid and liquid electrolytes, their features are a good compromise for their use in solid state lithium metal batteries. Gel polymer electrolytes have been studied since 1975, when Feuillade and Perche introduced them in lithium batteries [42]. Then, Tarascon et al. reported their GPE with PVDF-HFP in 1 M $LiPF_6$ in ethylene carbonate (EC): dimethyl carbonate (DMC) (1:1 v/v) solution in $LiMn_2O_4$/C battery with a rate capability of 115 mAh g^{-1} [97]. The properties of the GPEs are determined by the correct choice of liquid electrolyte and polymers. Liquid component is crucial to increase interfacial stability and ionic conductivity [43]. Typically, for the preparation of GPEs, commercial carbonates have been proposed, as, for example 1 M $LiPF_6$ in ethylene carbonate (EC): diethyl carbonate (EDC) (1:1 v/v) solution. The correct choice of polymer structure plays a relevant role on shape flexibility and mechanical strength [99].

GPEs could be a promising solution for solid state batteries. The main reasons are summarised in Figure 2.15. However, nowadays there is not a GPE able to be commercialized in LMBs. For this reason, researchers are still working for finding gel system able to have the performances for their commercialisation. Even if GPEs are not commercialized, different systems have properties consistent to the standard liquid electrolytes for LIBs. As reported in literature, Kuo et al. [100] fabricated a PVDF-PAN gel polymer electrolyte that showed high thermal stability up to 400 °C and good electrochemical stability up to 5.0 V (vs. Li/Li$^+$). A flexible PVDF-co-HFP gel polymer was fabricated by Kang et al. [101]. The membrane showed a high conductivity of 2.3 x 10^{-3} S cm^{-1} at room temperature. The results proposed shows the importance of GPEs family to increase long-term stability of Li metal cells for future and more performant batteries.
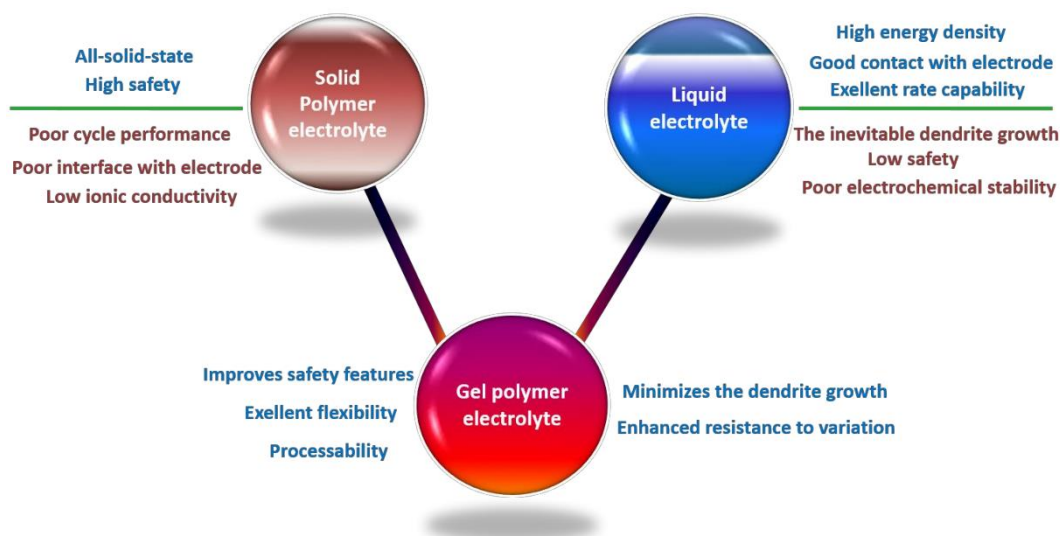
Figure 2.15: Advantages and disadvantages of solid polymer electrolytes (SPEs), liquid electrolytes (LEs), and gel polymer electrolytes (GPEs) [102]

2.9 Conclusions

LMBs suffer of safety problems due to high reactivity of lithium metal, and for dendrite growth during plating/stripping processes. One of the possibilities is the introduction of solid-state electrolytes. Different options have been discussed, however, for their versatility, dendrite suppression and high ionic conductivity, GPEs remain one of the best solutions for more performant lithium metal systems. For its low toxicity and low cost, amorphous state at room temperature, and electrochemical properties, PEGMEM based polymers systems have been investigated for GPE preparation. The architecture selected was crosslinked, because it is the most interesting for limiting the dendrite growth in solid state batteries.

One possibility for more attractive PEGMEM polymers for LMBs is giving them self-healing properties. Even if the solid polymeric structure allows to limit dendrites, PEs have a degradation process during its use. If the polymer allows self-repair when works, it can have high electrochemical performances and long cyclability. Function of self-repair is a priority for more performant and safer batteries. This self-healing feature can be obtained by introducing an additive in GPEs. The introduction of self-healing capability in polymers for lithium metal batteries have been discussed in next chapters.

Chapter 3

Self-healing Polymers

3.1 Introduction

During its timeline, materials are subjected at external forces. Degradation of the materials could be physical, or chemical. The main examples are corrosion, thermal degradation, oxidation or other secondary chemical reactions, UV radiation or a combination of these factors [103]. As a consequence, the life of materials, and also their performances, are decreased. Moreover, a ruined material needs to be replaced, increasing costs and material consumption. The ability of a material to contrast autonomously degradation is defined self-healing [104].

Self-healing is the ability of the material to self-repair itself after being cracking by an external force or after secondary reactions. It could be generated by external (as for example the introduction of an initiator that will create a reaction), or internal stimuli (as, for example, the use of chemical secondary bond, that are present in the material). It can also be created by changing the temperature or the pressure conditions of the materials [105].

Self-healing materials have certain features that allow them to be more attractive than others. First of all, self-healing materials are able to rebuild the initial mechanical properties of the cracked parts [106]. Moreover, their life cycles are longer. Their capability of self-repair allows them to contrast deterioration, and can overcome the costs derived from repairing and substituting pieces or components due to continuous damages [107].

Self-healing features are inspired by nature ability of certain systems to self-repair [108]. The most common are for example, skin and bones in human body. But self-healing capability is also present in plants systems. In nature, self-repair is also important for preventing water losses and is even a system of protection of external attacks or pathogens invasion [109]. Nature self-healing systems have been studied by scientists for understanding how they can do this function. Moreover, in the last decade research has empowered its studies for repeating self-healing effect in different materials. As a consequence, there is a strong increase of the articles published in the world, in particular after 2000.
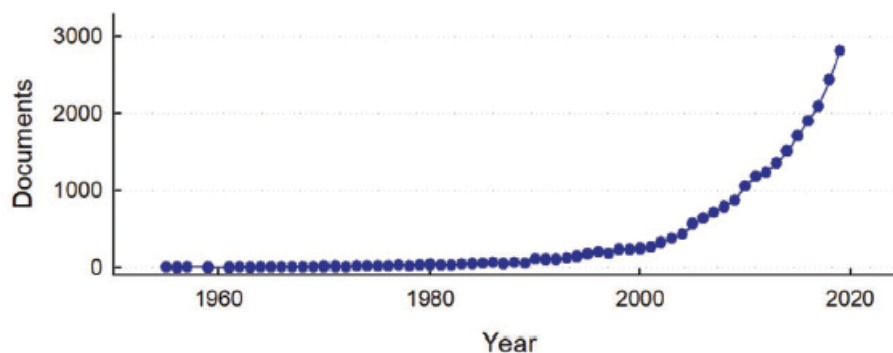
Figure 3.1: Scientific documents sorted by subject area considering a total of 27 383 documents (source: Scopus. Search term: self-healing. Query date: September 26, 2020) [110]

Self-healing materials could be divided in two different families, depending on the self-healing mechanism is produced. Extrinsic self-healing materials are obtained through the use of a healing agent introduced in the material during the fabrication. On the opposite, intrinsic self-healing depends on autonomous chemical or supramolecular bonds, that can be activated spontaneously during the formation of the crack [110].

In the last decades, researchers have been focusing on the self-healing capability in all the materials families: metals, ceramics, polymers [111]. Even if there are some cases of metals [112] and ceramics [113] systems able to heal themselves after damages, the most interesting studies have been carried out on polymers. Polymers can be easily modified during synthesis for introduce additives able to give self-healing capability. Moreover, metals and ceramics could self-repair at high temperatures, polymers could give self-repair even at room temperature [114]. For these reasons, SH polymers have been interested scientists for their synthesis and for their future application. As for example, in lithium metal batteries, self-healing capability could be easily inserted in polymers separators. In

this chapter, Self-healing polymers are discussed. Firstly, a brief introduction of self-healing processes in nature is given. Then, different self-healing mechanisms are reported. The materials have been divided by physical or chemical self-healing effects. A list of self-healing polymers for metal battery applications is also reported.

3.2 Self-healing process in Nature

For the synthesis of different self-healing polymers, scientists take inspiration of nature and how some natural systems are able to self-repair themselves [115]. Even in plants and animal systems, self-healing features have been found in tissues and organs. Interestingly, in plants and other living systems, self-healing is divided in two different steps. The first phase is characterized by a fast sealing of the injury. This prevents any other biosystem propagations, water loss and protects the body from external attack [116]. Depending on the systems, the first step, called self-sealing, required from hours to days. In the second phase self-healing is strongly remarkable, and the system heals damaged tissues removing the unuseful parts and restoring them with new ones. On this step, cell division takes place. The second step generally restores the physical and mechanical properties of the injured tissue and requires from days to weeks.
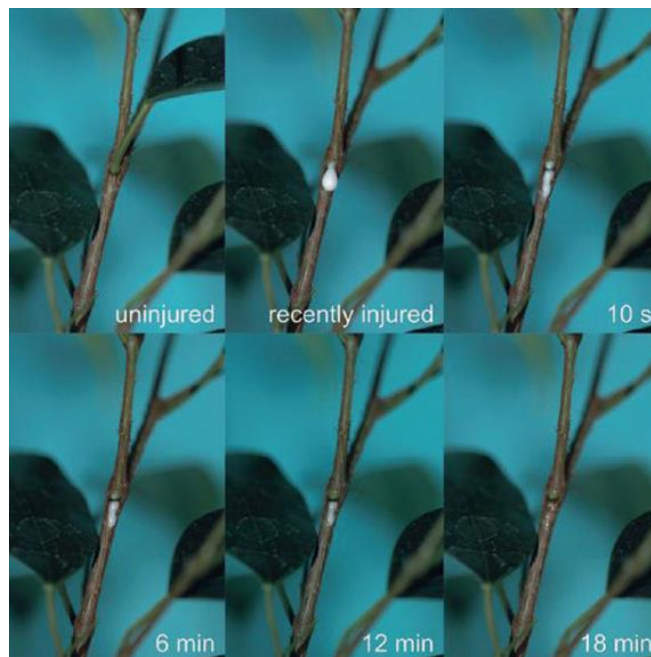
Figure 3.2: Observation of latex coagulation after injuring the bark [117]

Latex plants as Ficus have the capability to self-repair thanks to the latex emulsions. Latex is a milky plant exudate, collocated in specific plant elongated cellular micro-tubes called laticifers. When the plant is damaged, the cracked micro-tubes release the latex. The emulsion is able not only for the role of the plant defense, but also for coagulating the scar without external stimuli [109], [117].

One of the main human tissues able to self-repair autonomously is the skin. When the skin is cut, an inflammatory process is activated for cleanse the wound from foreign cells. In humans, it consists on formation of a fibrin clot and secretion of chemotactic agents. After that, the wound is repaired by a second phase, in which the tissue is made. Last, the process is the remodelling phase, in which all the functional processes of the skin have been turned on, and the self-healing process gradually stops its function [118].

A vascular self-healing in nature is the homeostasis involved by blood circulation. When there is an injury on the site of the blood system, immediately white globules release the transmembrane receptor tissue factor, able to create a coagulation cascade event in which platelets are involved. Platelets collocate themselves inside the injury, and triggered a crosslink mechanism for the synthesis a first thrombus. After that, platelet-platelet interaction stabilizes the loss of blood into the tissue and the restoration of the initial tube even because of the help of the fibrin deposition.
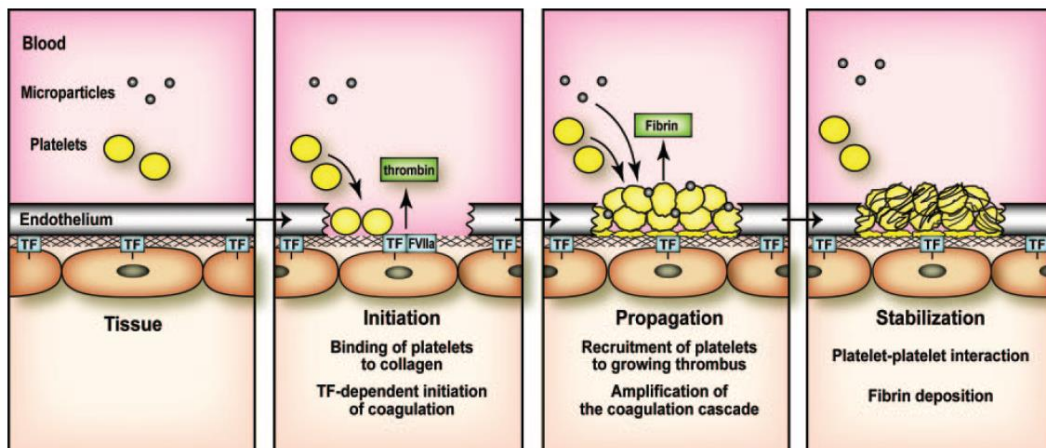
Figure 3.3: Formation of a clot at the site of blood vessel injury[119]

38

Secondary and tertiary structures of proteins are made of supramolecular interactions between amino acids constituted the proteins themselves. Typically, hydrogen and S-S bond are involved by using carboxylate and amino groups of the amino acids, or the -SH group of cysteine. In some cases, the π-π interactions, involved by aromatic structure of cysteine and tyrosine are also relevant for self-repair. When a protein is damaged, it partially loses its structure and, as a consequence, its mechanical properties and functions. However, the protein is able to create a mechanism in which secondary interactions, cracked during the damage, are restored. As a consequence, the structure of the protein is replaced and, self-repaired. Titin is a functional structural human protein which is present in the linear filaments of muscles. When the protein is stressed by a mechanical force, it loses its structure. However, when the stress is released, titin is able to restore its virgin structure thanks to the internal H-bond interactions of the amino acids.
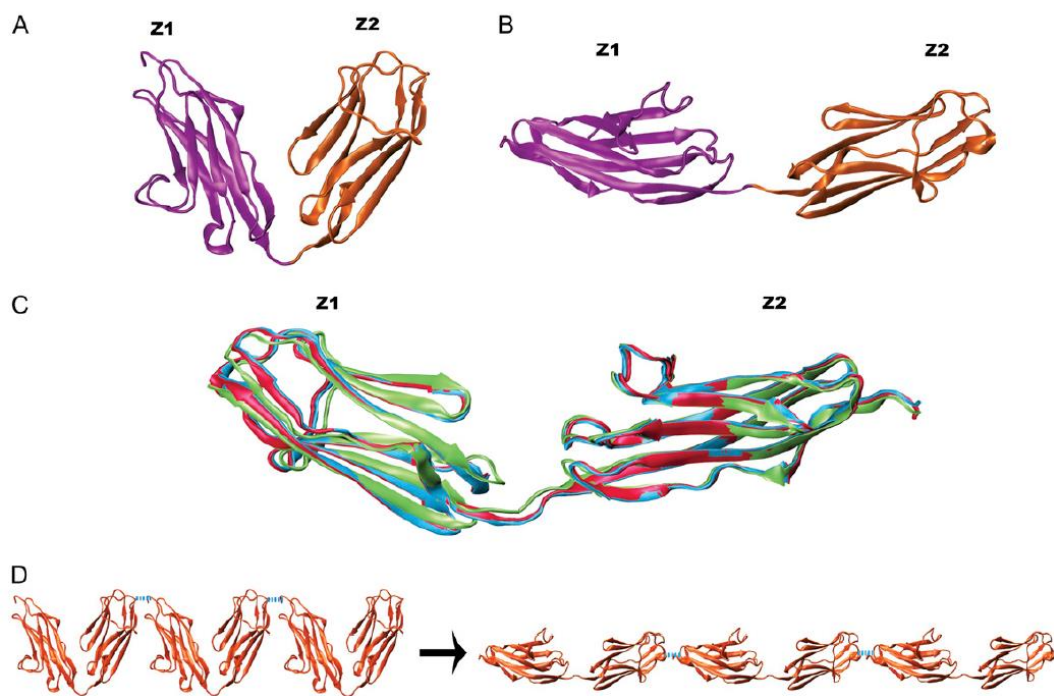
Figure 3.4: Experimentally derived conformers for titin and the restoration of its structure after being stressed [120]

3.3 Physical Self-healing by Physical O' Connor model
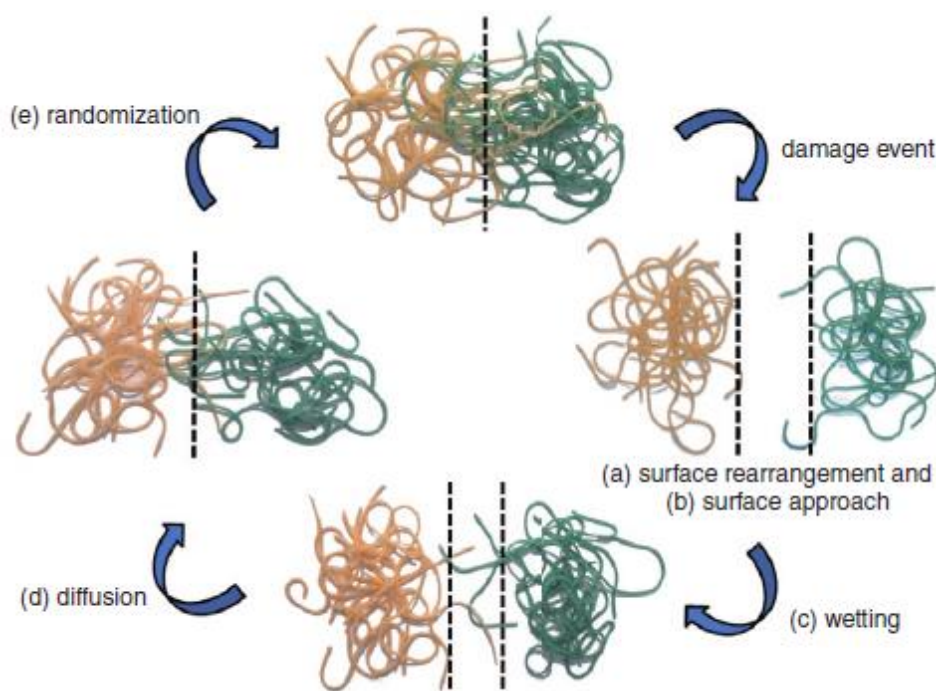
Figure 3.5: Stages of self-healing mechanism for polymeric segments [64]

The first example of self-healing mechanisms in polymers are based on physics principles and have been studied by O'Connor [122]. It is quickly described on Figure 3.5, and it is based on Brownian effects and/or molecular diffusions of polymer chains in the matrix when damaged.

The polymer is cracked and divided in two parts. After placing the two parts one near each other, and after an external stimulus (as for example, a wetting procedure), the polymer chains of the first cracked part move into the opposite part and vice versa. The diffusion process of the chains destroys the damage thanks to randomization process, restoring the pristine structure of the polymer.

The main determining step of physical self-healing procedure is the movement of the chain into the polymer. Diffusion depends on the nature of the chain polymers and on its reticulation [123]. Moreover, even external condition can increase (or decrease) the ability of the polymer to restore itself. In fact, diffusion is favored by high temperature and pression. Even the presence of a solvent can help the polymer movement. For these reasons, physic O' Connor model is famous in SH studies, but rarely used in self-healing polymers. In fact, self-repair is often given by a chemical

interaction inside the polymer structure. In this case, chemical reactions involved for self-healing applicability [124], and basically they are divided in two families, depending on SH is trigger by formation of new covalent or non-covalent bond [125]. Depending on the strategy used for the chemical self-healing mechanism, self-healing could be divided in nanoparticles, vascular or intrinsic polymers.

3.4 Self-healing mechanisms: encapsulated, vascular, Autonomous chemical self-healing

Self-healing polymers can be divided in three main families, shown on the Figure 3.6: encapsulated (or nanoparticles), vascular or intrinsic [126]. The three typologies are different because of the different strategy used for releasing self-healing capability [127].
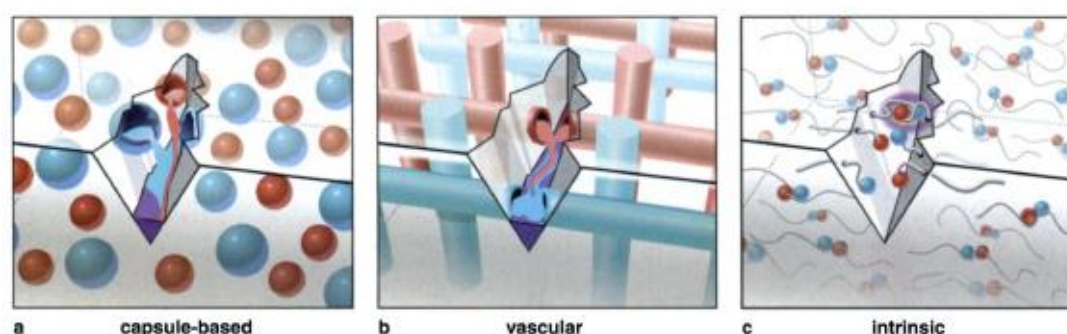
Figure 3.6: Self-healing systems divided into encapsulated, vascular, autonomous categories [67]

Capsule-based systems consist on a matrix in which there are molecules entrapped on nanoparticles in the polymer structure [128]. When the polymer is damaged, capsules release the molecule, which are able to create a healing reaction, Capsule-based mechanism is used when there is a reaction in which a catalyst is necessary. If the catalyst is not encapsulated, it can act even when not necessary. With capsule-based system, the catalyst will only react when released, because it is entrapped into a shell structure. So, it is possible to activate self-healing effect only when necessary [129].

One of the most relevant self-healing reaction given by nanoparticles is the ring opening metathesis polymerization (ROMP). Cyclopentadiene monomers and ruthenium based catalyst are inserted into different epoxy capsules in a polymer

matrix. When there is a damage, the capsules are broken, from now on the monomers and catalyst are free to move inside the scar and begin the polymerization process. Once they are in contact, the catalyst begins ROMP reaction, changing cyclopentadiene into polyclopentadiene recovering the material for damage, and, hence the scar.
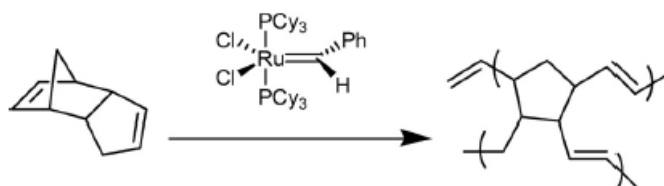
Figure 3.7: ROMP Grubb's Reaction

Tolentino Chivite et al. synthesized a Grubb's self-healing polymer in which the materials for the reaction are entrapped into commercial epoxy resins. Self-healing capability is tested and confirmed at -20 °C [130]. Nevertheless, the high cost of the ruthenium limited its application. Moreover, the insertion of new polymer (like polyciclopentadiene), inside the polymer matrix can decrease the peculiar properties of the pristine polymer.

In vascular systems, catalysts or healing agents are inserted into vascular structures. These could be single tubes, or could be planes three dimensional channels. When there is a damage, even vascular systems are broken. The damaged structure releases the catalyst or the liquid reactant. A self-healing reaction between reactants takes place, which is able the recover the broken structure. Even if there are similarities, the vascular system is preferred than the capsule-based if one or more reactants are liquid.

Autonomous self-healing is an intrinsic capability of the polymer, given by chemical structure of the main or the side chain of the polymers. When the matrix is damaged, the polymer is able to self-repair thanks to its capability to create these interactions without any external stimuli. The mechanism of autonomous self-healing depends on the chemical bond in the polymer [131].

3.5 Challenges between vascular autonomous and intrinsic in LMBs

Unfortunately, extrinsic self-healing requires two conditions necessary for restoring the initial conditions. Firstly, the two chemicals need to be separated by different strategies, as vascular and microcapsules. Moreover, the chemicals have to be in contact for giving their specific reaction only when the system needs a heal. This mechanism is quite challenging and needs several improvements in complex systems. Moreover, the healing process is strongly dependent on the microcapsule (or vascular systems) involved during the crack. In the polymer there could be lots of vasculars or microcapsules, but only the damaged ones are able to give the peculiar reaction able to restore the injury. If the polymer is damaged in an area in which microcapsules or vascular systems are not involved, the polymer is not able to contrast the injury [132]. Moreover, once the reactants are exposed, and are free to move into the polymer system, they cannot be replaced. If another crack happens in the same material, and all the reactants are lost or used during previously self-repair, the heal procedure cannot be activated. Different strategies have been studied for empowering microcapsule extrinsic self-healing, such as dispersion of one reactant in polymer matrix, or use of gases derived from the environment. However, even in these cases, the application of these strategies in LMBs remains a big challenge, because of the high reactivity of lithium and the side reaction presented in battery systems [133].

As a consequence, even if extrinsic approaches are interesting for different typologies of materials, no relevant applications have been reported in literature in case of lithium metal batteries [134]. Lithium metal batteries are systems with high reactivity. The insertion of materials able to create a self-healing reaction inside the battery and, at the same time, to avoid side reaction is still an issue because the activation by an external stimulus is a further challenge in a closed system, such as the electrochemical cell.

On the opposite, autonomous self-healing is related to chemical interactions able to be activated without an external stimulus. The most used in different fields are hydrogen bonds, and ionic interactions. Differently from vascular or microcapsules, autonomous self-healing has significant advantage [135]. In fact, it benefits of different healing processes, that could be repeated several times without any dispersion of materials. On the opposite, the mechanism of vascular and microcapsules self-healing is strongly dependent on the reactant that is inside the structure, and the reactant that is free when the crack is given. For these reasons,

the mechanism of autonomous self-healing is favour on systems which are highly reactive and closed as lithium metal batteries.

3.6 Application of self-healing in LMBs

Lithium metal batteries are systems subjected to physical and chemicals deterioration [136]. With the insertion of smart materials able to recover some functions and contrast mechanical damage, durability and functions of the cells will last for a long time. Self-healing ability can not only prolong the reliability of the cells, but avoid the replacement of the materials, reducing the waste of materials and resources. For these reasons, self-healing capability is considered as one of the most important smart functionalities (with sensing) to adopt in new batteries [137]. However, different approaches have been discussed by scientists for the insertion of self-healing inside LMBs. In fact, LMBs are composed of different materials (electrodes, electrolytes, binders, etc.). Moreover, cells suffer of different problems (lithium dendrites, formation of SEI, etc.). The insertion of a material able to self-repair limiting all the problems of the cell is quite challenging. However, self-healing capability adopted on a single material (as for example, polymer electrolytes) must solve the problems related to that part of the batteries, in order to diminish side effect and empower the life of systems.

As described before, several electrodes suffer of volume change due to the intercalation process of the lithium inside the structure. For these reasons, binder is used for contrast the problem of volume change as, for example, in silicon anodes. A binder able to self-repair could be a smart option for empowering the life of electrode and block volume change of electrodes [138].

Recently, Coskun et al fabricated a self-healing binder for the silicon anode. The material is composed of hyperbranched β-cyclodextrins, able to easily anchor silicon and avoid their volume change [139]. Moreover, their good interaction with adamantane (high association constant of $K_m = 5.29 \times 10^4$ M^{-1}) can create a high host-guest interaction. In fact, the typical configuration of cyclodextrins let molecule host easily hydrophobic structure. For these reasons, when the binder is cracked, the binder is able to self-repair because cyclodextrins and adamantane restore easily their primitive structure, in which adamantane is host inside cyclodextrins [140]. The improved capacities of cells have been obtained, with good capacity retention after 150 cycles.
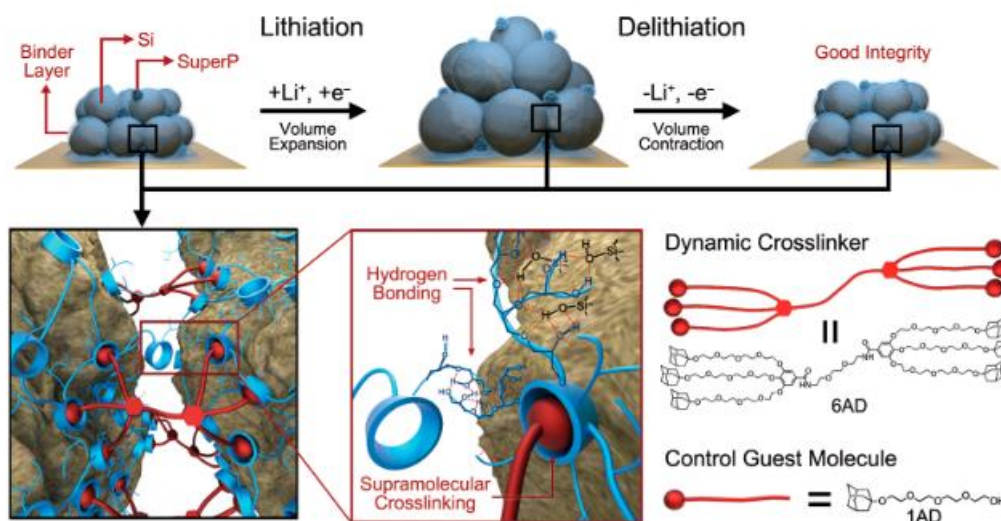
Figure 3.8: Host-guest interaction between Adamantane and cyclodextrin in Silicon anode [139]

Zheng et al. investigated a new binder for silicon anode able to self-repair based on the metal complex interactions. They fabricated a new alginate polymer able to interact with Ca^{2+} cations. The structure is able to stabilize silicon change of volumes. Moreover, when the binder is cracked, the polymer is able to reassemble itself because of the restoration of the chemical bond between hydroxide and/or carboxylate group of alginate and positive charge of calcium [141]. The choice of a good binder is essential for the mechanical stability of both cathode and anode, and for diminishing the volume change of the electrodes. However, the successful of self-healing binder are still in progress.

In any cases, for lithium metal batteries, the high reactivity of lithium with liquid electrolytes remains the main problem to solve. As a consequence, new polymer electrolytes able to "trap" in their structure carbonates and able to self-repair are a valid option for stabilizing metal anode and avoid the side reactions involved between lithium and electrolytes. New PEs able to self-repair when a dendrite grows is also a valid option for empowering the life of the cells. Nevertheless, the applicability of self-healing in lithium metal batteries is not so simple. New SH materials, able to be used in batteries, are able to self-repair because of chemical reactions or interactions. This means to add another chemical reaction into system with a lot of chemical and electrochemical interactions. As a consequence, the self-healing capability must be inert to all the systems involved in LMBs, as for example, the metals of the electrodes. Moreover, their SH capability has to be selectively activated when necessary [142]. Last, the molecules

45

responsible of SH effect do not have to react with any battery components, giving side reactions. In brief, any molecule with SH effect included in a polymer electrolyte should not affect its main properties that are: high ion conductivity, high ion transference number, high thermal, chemical and electrochemical stability [143]. The problem is quite challenging for all researchers.

As described in last chapter, several opposite reactions are involved in LMBs. One of the most relevant is the SEI formation, due to reactions between the liquid electrolyte and lithium [144]. Nevertheless, SEI could have a role in protection of lithium metal, SEI formation mainly caused loss of material, low electrochemical performances and problems of unsafety [145].
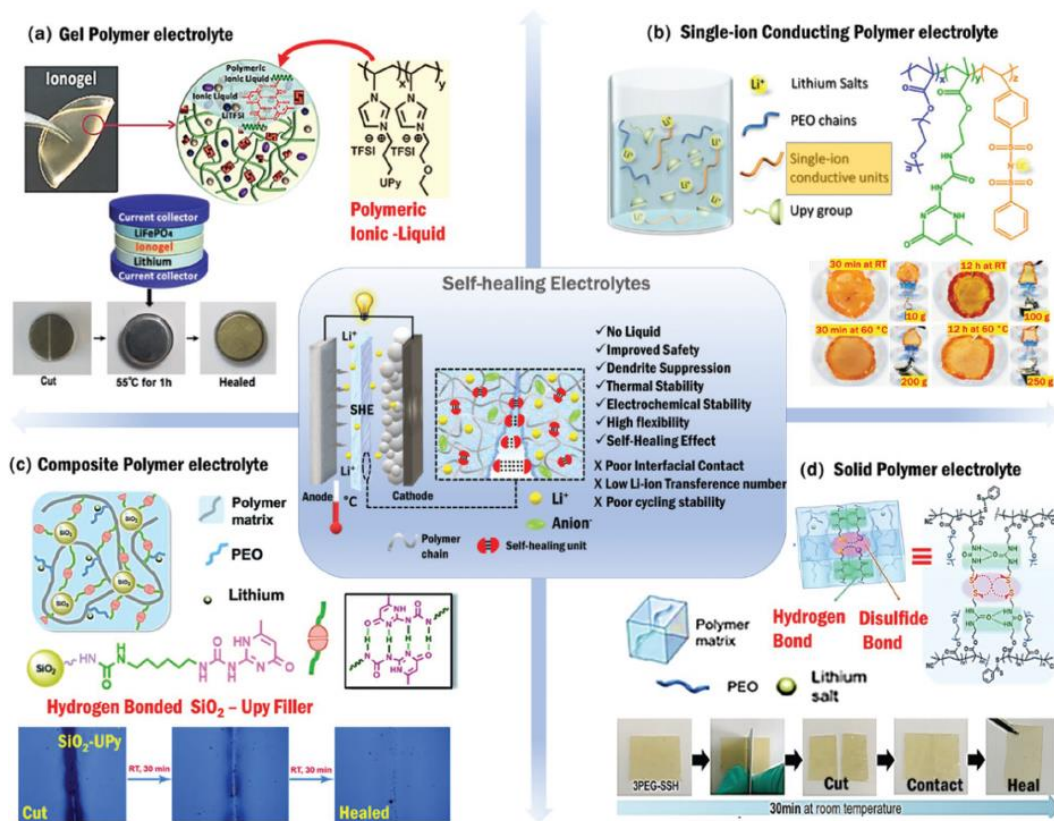
Figure 3.9: Self-healing polymer electrolytes for safer Li-ion batteries: examples of different categories explored [145]

Moreover, the insertion of a self-healing polymer inside the battery could solve not only problems of safety, but also could empower life of the cells and the reliability of batteries. Moreover, the mechanical strength given by PEs into the lithium metal is a significant response against the dendrites, main cause of short

circuits and loss of batteries materials in lithium metal systems. Different polymers structures have been proposed for synthesis of solid states electrolytes. However, PEOs and PEGMEMs remain the most promising in literature with the most applicability. The addition of chemical interactions, given by different additive added into the side chain of the polymer structure, are the base for give at PEs self-healing interactions.

Different chemical bonds have been used for giving self-healing capability in methacrylates. One of the most interesting is the C-C bonds given by spontaneous Diels-Alder reaction (D-A).

D-A reaction involves two unsatured reactants, a diene and a dienophile, for the synthesis of a cycloalkene [146]. It is one of organic reactions able to give new C-C bonds [147]. For these reasons, it is remarkable used in organic chemistry for synthesis of new compounds. Diels-Alder reactions is quickly described in the Figure 3.11: when dienophile and diene are one near each other are able to react, giving rise of two new C-C bonds, a new double bond and the elimination of two double bonds.

diene   dieneophile
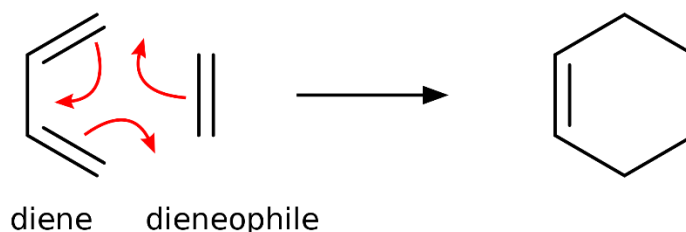
Figure 3.10: Mechanism of Diels Alder Reaction

Thanks to its capability of giving new C-C in certain conditions, Diels-Alder is commonly used in different applications, one is the self-healing capability [148]. In fact, at high temperatures, it is possible to spontaneously activate it, resulting new C-C bonds and restoring the pristine conditions of the polymer [149]. Under UV-irradiation conditions, spontaneous Diels Alder could be activated even with the presence of two alkenes, with the synthesis of new C-C bonds. By using this mechanism, Chung et al. described a self-healing process on PMMA modified with photo-cross-linkable cinnamate monomer, 1,1,1-tris-(cinnamoyloxymethyl)ethane, which involved Diels-Alder reaction under UV treatment [150] .
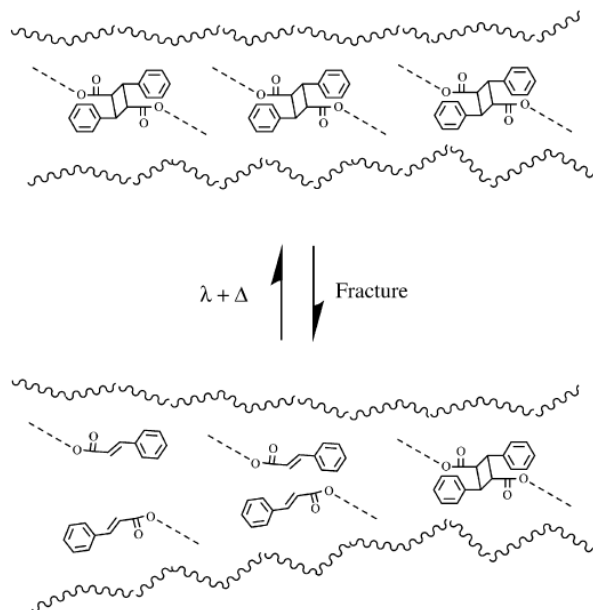
Figure 3.11: Mechanism of fracture and repair of thermo and photo-induced healing in PMMA[150]

However, reversible self-healing mechanism has got several challenges in lithium metal batteries. In fact, the specific conditions required for giving self-healing are not directly applicable in commercial smart batteries [151]. In fact, it is difficult to heat or using a UV irradiation mechanism on batteries for giving self-healing capability [152]. Moreover, in normal conditions, the system could not be able to contrast dendrite growth, because only under treatment the SH properties are activated. Furthermore, a high number of double bonds inside a polymer electrolyte could be dangerous for the batteries because they could react with lithium metal. For these reasons, Diels Alder reaction is difficult to apply in self-healing polymer electrolytes for LMBs.

Even reactions involving chemical bonds (as ROMP) are excluded [153]. In fact, the mechanism involves an external stimulus, difficult to operate in the case of a "close-box" as batteries. For these reasons, scientists have been focused on autonomous intrinsic self-healing, able to induce a healing procedure without any external interactions.

As a consequence, the most chemical bond used for self-healing application is autonomous hydrogen bond interaction [154].

3.7 Hydrogen bond on Self-healing polymers

A hydrogen bond is an electrostatic interaction made by a hydrogen bond with a high electronegative atom [155]. Generally, the atom is often oxygen (O), nitrogen (N) or fluorine (F). In these conditions, the hydrogen is poor of electrons because of the high electronegativity of the elements to which is bound. The hydrogen is able to interact easily with another molecule in which there is a donor element with a pair of electrons. H-bond interaction is weaker than covalent bonds. However, it is stronger than other secondary interactions, as for example van der Waals [156].

One of the most typical examples of hydrogen bond is the molecule of water. A single water molecule is able to create four hydrogen bonds because of the interaction between the oxygen lone-pairs and the hydrogen of a second molecule (and vice versa). The main consequence of hydrogen bond in water is the high melting and boiling point in comparison with other molecules with the same molecular weight [157].

However, not only water, or other aqueous ones, are able to give hydrogen bonds. Different organic species, as biomolecules of polymer or biomolecules, are able to give strong hydrogen bond interactions [158].

A typical example of molecule is DNA. DNA is made of different polynucleotides, able to form double helix form. The structure of DNA is given because of the hydrogen bonds, mainly given by coupling of the nucleobases composing the nucleotides (the "monomers" that compose the DNA structure). When DNA is damaged, it is able to self-repair because of the strong interaction given by the hydrogen bond into the different nucleobases that compose the double helix. For these reasons, nucleobasis are studied for self-healing capability in polymers structure.

The applicability of hydrogen bond interaction in self-healing polymers is mainly studied by different researchers [159]. Hydrogen bond is an autonomous bond, so it does not need a stimulus for its synthesis, even if its formation is favourite at high temperature. Its appearance is given automatically when the hydrogen is close to electronegative elements with a couple of electrons of another molecule. As a consequence, there is not a chemical reaction involving reactants, products and by-products, that often are able to react with other chemical species, which are part of the material. In the case of lithium metal batteries, this is a great advantage: the presence of high reactive anode as metal lithium imposes a self-assembly able to be inert with the metal. Moreover, the insertion of species able to give hydrogen bond interactions in the classical polymers used for the synthesis of PEs is not an obstacle, in presence of PEGMEM substrates. The presence of an

additive able to give strong H-bond interaction in PEs could be an interesting solution for solid state electrolytes in lithium metal batteries. However, the strong interaction between H-bonding molecules and water could be an obstacle [160]. In fact, water-based structures cannot be used in LMBs because of the strong reactivity between water and lithium. For these reasons, H-bonds apolar molecules are the main choice for the construction of strong H-bond self-healing polymers for application in LMBs.

Different strategies have been considered to insert self-healing functionality with hydrogen bonds interactions [161]. Typically, the introduction of a single H-bond interaction for molecules could not be sufficient for application of self-healing in polymers systems. For these reasons, single molecule able to determine multiple hydrogen bond systems are often favourable because of its capability of empowering self-capability in polymer systems [130].

In last years, ureidopyrimidinone (Upy) is a molecule that captured the attention of researchers [96]. The typical structure of the molecule is able to give four hydrogen bonds with another Upy molecule. Dimerization of Upy in chloroform is spontaneous, and has got a ΔG°_{dim} of -35 kJ/mol. Their force is intermediate of typical covalent bonds and weak interactions [163].

Ureidopyrimidinone has got great attention for giving self-healing capacity to classical polymer used for solid state electrolyte. The main reason is their applicability in self-healing is the multiple H-bonding interactions. Moreover, with organic synthesis or with classical polymerization processes, Upy group can be easily inserted into the polymeric structure, because it can easily enter into the polymerization process by its double methacrylate bond.
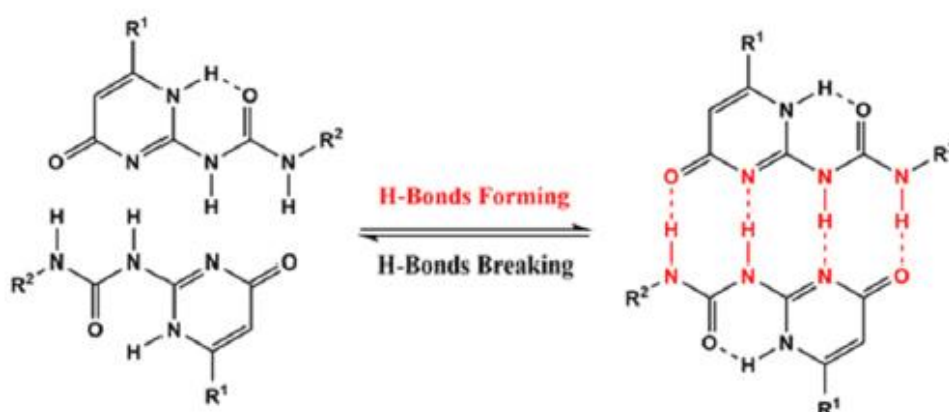
Figure 3.12: Upy quadruple H-bond interaction [82]

50

The insertion of a Upy with methyl methacrylate gives ureidopyrimidinone methacrylate (UpyMa), which is a good option for the synthesis of an additive with SH properties. Methacrylate group is useful for the insertion of the molecule inside the polymeric structure of the polymer. Upy group is the part of the molecule able to give self-healing capability. On the opposite, the double bond of the methacrylate could be used for the insertion of Upy group inside the polymer structure. Different types of polymerisation processes, as reversible addition−fragmentation chain-transfer (RAFT), UV induced or thermopolymerization have been interestingly used for giving easy polymers with Upy groups in lithium metal batteries [164].

SiO$_2$-Upy additive is used by Xue et al. for the preparation of a PEO composite polymer electrolyte able to self-repair it in one hour. The polymer is tested in Li/PEO/LFP cell, showing a discharge capacity of 139 mAh g^{-1} for 60 cycles at 60 °C [165].

Xue et al. designed a self-healing solid polymer electrolyte UpyMa based to be used in LMBs. Their synthesis is made by using UV-polymerization with PMMA as main oligomer and LiTFSI is used as a salt for increasing the conductivity of the material. The polymer is able to self-repair itself after being cracked in 2 hours at 60 °C. Moreover, it showed a discharge capacity of 130 mAh g^{-1} at 0.1 C rate at 60 °C in Li/polymer/LFP cell assembling [166].

Xue et al. fabricated a single ion electrolyte for solid state batteries. The SPE is synthesized by using RAFT polymerization. SICP is able to self-repair in 30 minutes at 60 °C. Moreover, its capacity in Li/SPE/LFP cell is 129.3 mAh g^{-1} and the cell is tested for 60 cycles at 0.1 C rate at 60 °C.[167].

Xue et al. polymerized a self-healing polymer electrolyte able to self-repair itself in 2 hours at 60°C. RAFT polymerization was the strategy for the insertion of ureidopyrimidone methacrylate into the PEGMA polymer structure. The polymer is tested in Li/polymer/LFP cycling at 0.1 C rate for 120 cycles at 60 °C [168].

There are many other examples of UpyMa used in PEs in LMBs [169]. However, there are different challenges to solve for their application in commercial systems. Firstly, the conductivity of the system has to be enhanced. PEs in which UpyMa is inserted possess high conductivity at 60 °C. However, lithium batteries work mainly at room temperature, conditions in which the conductivity of polymers are low. Temperature condition is also limiting for cycling cells and for SH features. A good SH polymer is interesting if it could work at RT with considerably high cycles and high cell capacity. Eventually, the synthesis conditions of the polymer are relevant. The high quantity of solvent used in the polymerization is not environmentally friendly. A direct synthesis of the polymer without the help of the solvent is considered green and reduce the cost of the final materials.

3.8 Conclusions

Even if UpyMa is introduced in PEs for giving self-healing features, many parameters have to better for their future use in LMBs

In conclusion, different are the features for a good self-healing polymer. Moreover, their applicability depends on the material in which it will be used. For lithium metal batteries, the main property is the absolutely non-reactivity with lithium metal. Moreover, a good SH polymer has to be high ionic conductivity, high electrochemical and thermal stability, high capacity of reduce dendrite growth, environmental friendly with a low cost. UpyMa as addictive in polymeric structures as PMMA or PEO is a preliminary additive to be used for synthesis of new smart materials [170].

For these reasons, different kind of polymer with PEGMEM as oligomer and UpyMa as self-healing additive have been investigated. Different experiments have been described for understanding their properties in future self-healing gel polymer electrolytes. Synthesis of UpyMa and its application in PEGMEM gel polymer electrolyte have been described in the following paragraphs.

Chapter 4

Synthesis of Ureidopyrimidinone Methacrylate

4.1 Introduction

In the last decades, the application of self-healing is remarkable in lithium-metal batteries production. The self-healing process is a mechanism able to create spontaneous bonds inside the polymeric structure, and, as a consequence repair a damaged area. This type of structure has been investigated in this dissertation with the H-bond interaction, with a focus on ureidopyrimidinone methacrylate, because of its ability to create multiple hydrogen bonds via dimerization process. For all these reasons, the application of this molecule as an additive in gel polymer electrolyte, based on polyethylene glycol methyl ether methacrylate is now explained. However, UpyMa is not available on the market, so it is necessary to synthetize it for its use as an additive for GPEs.

4.2 Reaction of the synthesis of UpyMa

The synthesis process of UpyMa is achieved using a coupling reaction between two commercial reactants, 2-isocyanatoethyl methacrylate (ICEMA) and methyl

isocytosine (MIS). These two reactants are available on the market (for example Sigma Aldrich) and are relatively cheap materials. The synthesis is obtained mixing reactants within an organic solvent, without using any catalysts. The reaction is described in Figure 4.1. It is obtained by the nucleophilic nitrogen of MIS, which can attack the carbon of isocyano-group of ICEMA. The result is the synthesis of the typical ureidic group, and, as a consequence, the UpyMa.
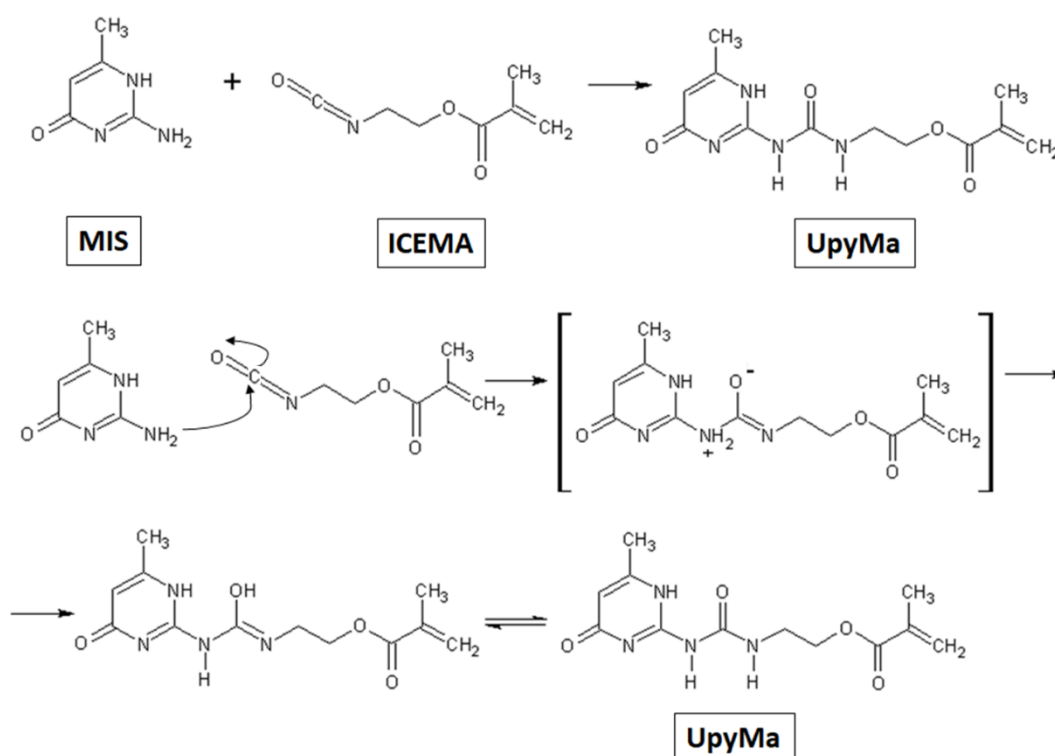
Figure 4.1: Representative Mechanism of the synthesis of UpyMa by Coupling reaction of ICEMA and MIS

Amino group of MIS is a typical nucleophilic group with a strong capability to attack electrophilic species. On the opposite side, the carbonyl group of isocyano presents one carbon molecule that loses its electron bonds, because of the strong electronegativity of the closer nitrogen and oxygen. For these reasons, the nitrogen atom of the amino group of MIS reacts selectively with the carbonyl group of ICEMA; this leads to the formation of an unstable mid-reaction. The molecule has a new C-N bond and shows two more charges, positive on the amino group of MIS and the negative on the oxygen atom within the carbonyl group of ICEMA. During

this transition a spontaneous transposition happens within the process, in which the solvent acts as a helper to the reaction. A proton H^+ is moved from the positive nitrogen of MIS to the negative oxygen. The product formed is an enol balanced by a chetonic form, much more stable. This final step brings to the final product of the coupling reaction, UpyMa.

Thanks to ICEMA and MIS processes, it is easy to synthesize the ureidic group of the UpyMa, without any losses of product of the reaction. Moreover, double bond of methacrylate remains untouched during the adding reaction. For these reasons, the coupling reaction is a good compromise for the synthesis of UpyMa.

4.3 Synthesis of UpyMa

The entire production process of UpyMa could be divided in two parts: the synthesis process, and the extraction process from the solvents.

First, MIS is added into a dimethyl sulfoxide (DMSO) solvent in a flask. The solution is then placed into an oil bath at the temperature of 170 °C for ten minutes with a molar concentration of 1.6 mol/L. Then the second reactant, ICEMA, is added into the solution. The ratio between MIS and ICEMA is 1.0:1.1. MIS and UpyMa possess similar solving properties and because of that their separation could be difficult. On the other hand, ICEMA can be easily removed from solution by washing the product with organic solvents. Using this proportion, it is possible to obtain a completely balanced reaction useful to remove easily the reactants not involved in the reaction.

After adding the ICEMA in the flask, the solution is immediately removed from the oil bath and located in a water bath at room temperature. The insertion of the second reactant activates the coupling reaction. In fact, the product starts to get visible as a white compound. Moreover, the water bath is also useful for preventing side reactions, such as polymerization of UpyMa, that occurs at high temperature. In the water bath, the process of UpyMa precipitation continues for two hours at room temperature. Finally, the UpyMa is entirely visible as a white product, wet by DMSO solvent. The excess of ICEMA and DMSO is removed by washing the sample with distilled water and hexane. The product is stored at room temperature waiting for the evaporation of the residual hexane solvent. However, after the cleaning process, the compound remains wet and swelled with DMSO and because of its presence, is necessary to extract the residual solvent for further removing in the UpyMa.

The product is placed in CHCl$_3$ solution, then to obtain homogeneous solution an over-satured NaCl water solution is added and mixed. This process leads to the formation of two-phases, from which the organic phase is removed; the procedure of extraction is repeated twice. After this step, sodium sulphate is added inside chloroform solution to absorb the water excess in the product.
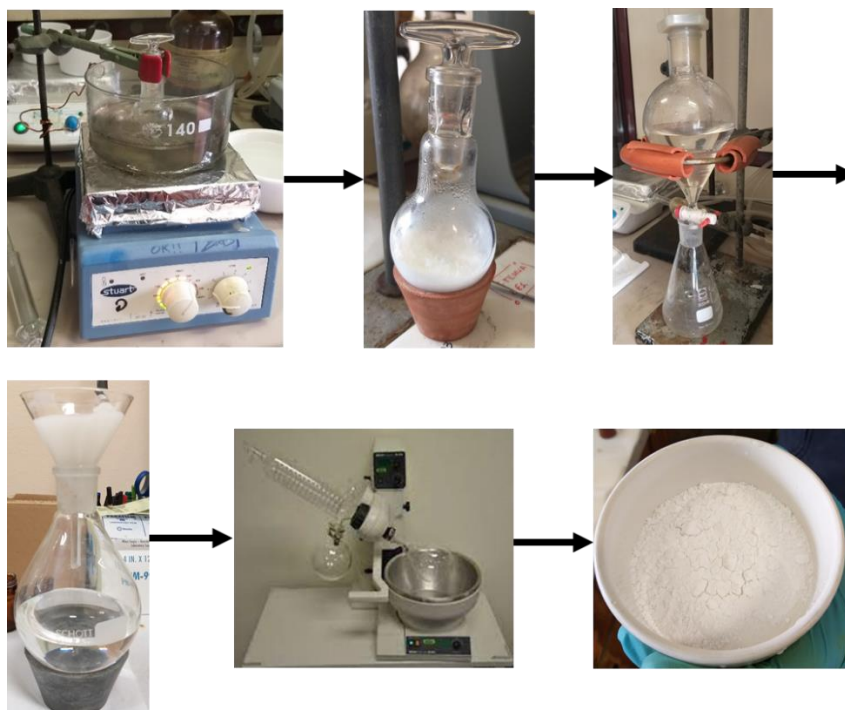
Figure 4.2: Schematic representation of the synthesis procedure of UpyMa, followed by the extraction process.

4.4 Characterization of UpyMa by NMR and FTIR

The product of the reaction is then analysed by ^{1}H nuclear magnetic resonance (NMR). NMR spectra were recorded by the Bruker 200 MHz NMR analysis is carried out at room temperature using deuterated chloroform as solvent, which was dried using a 4 Å molecular sieves.
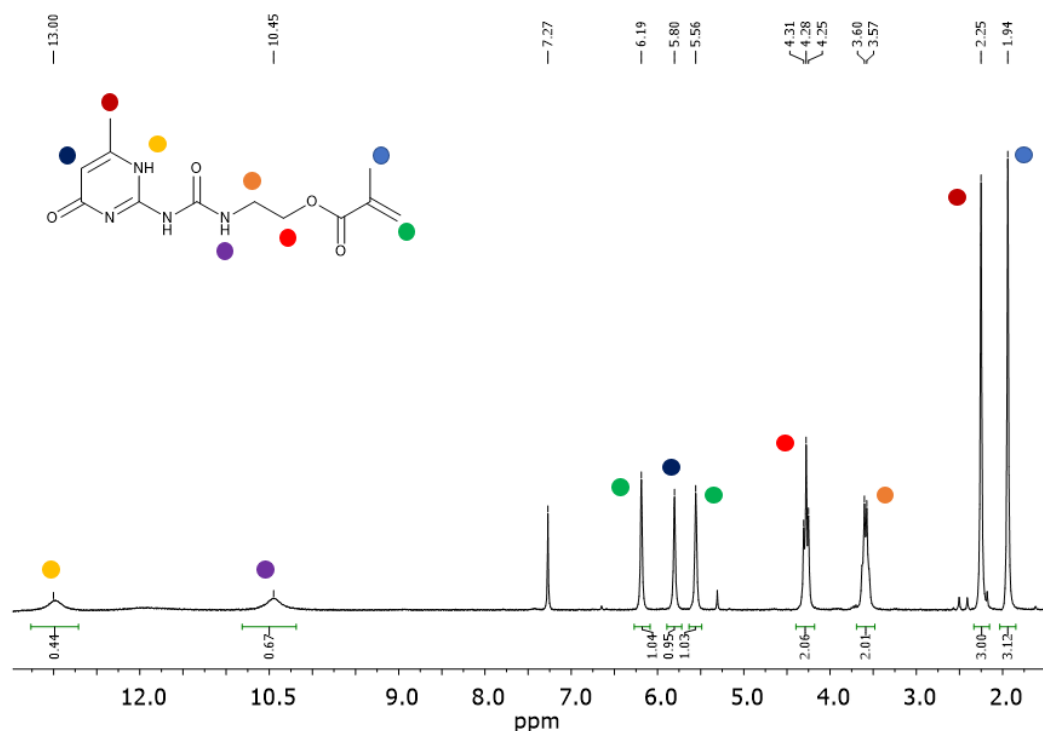
Figure 4.3: ¹H NMR spectrum of UpyMa

As can be seen in Figure 4.3, the peaks represent the hydrogen in the UpyMa and all protons represent a typical hydrogen in UpyMa, except for the peak at 7.26 ppm, which is of the solvent used for the NMR analysis. The results appear then consistent to those reported in general literature [171]. Starting from low fields, the N-H hydrogen is seen at 12.0 ppm. The N-H hydrogen of urea group is at 10.5 ppm. The N-H direct bond in pyrimidinone group is absent because of its high mobility into the chemical structure of the molecule. The two =CH_2 hydrogens can be noted as different peaks at 6.2 ppm and 5.5 ppm. The peak assigned to the C-H of aromatic group is at 5.8 ppm. The ethoxy chain N-CH_2-CH_2-O possesses four hydrogens, that show their typical peaks on 4.3 and 3.6 ppm. Eventually, the last peaks at 2.1 and 2.0 ppm represent the methyl group inside the molecule. As a consequence, the final product of the coupling reaction is the ureidopyrimidinone methacrylate. The typical peak at 2.6 ppm, which is typical of DMSO solvent, is absent.

The correct elimination of the solvents used during the reaction and the correct synthesis of ureidopyrimidinone methacrylate are confirmed. The final yield of the reaction is 92.3 %.

Figure 4.4 shows the NMR spectra of ICEMA, MIS and UpyMa respectively. During ICEMA-MIS reaction, the conversion of isocyanate into urea group can be

detected. As a consequence, the typical peaks of ICEMA are visible in the NMR spectra of UpyMa. The blue, orange, red and green peaks showed in Figure 4.4 are the same in both ICEMA and UpyMa spectra. This means that no side reactions have occurred, confirming the desired mixture in the UpyMa has been obtained. In fact, the peaks of double bonds, which are labelled in green, are present in UpyMa spectra. As a consequence, polymerisation which involves the double bonds did not occur during the synthesis.
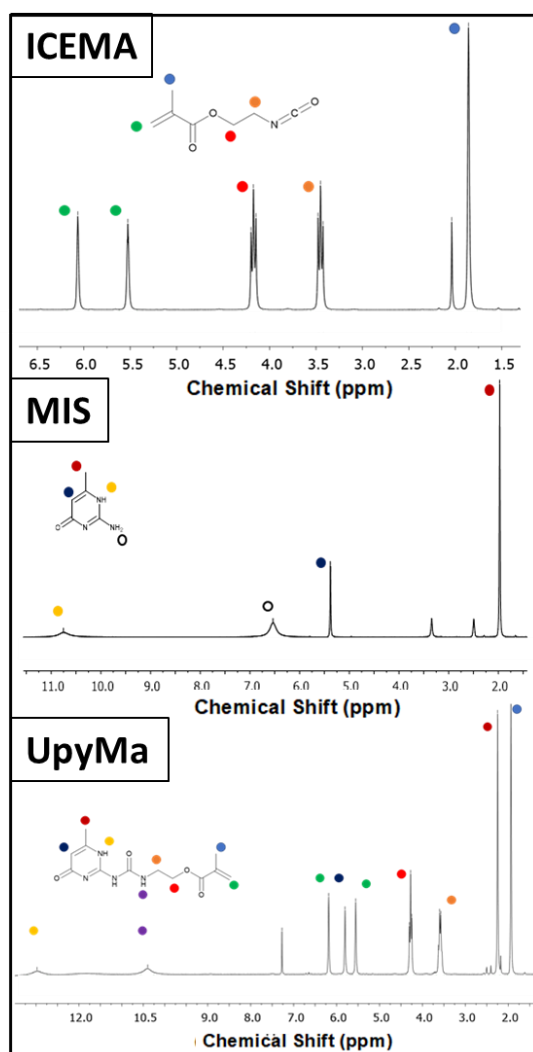
Figure 4.4: ¹H NMR spectra of ICEMA, MIS and UpyMa

The typical peaks of methyl and aromatic groups of MIS, signed in red, blue, and yellow circles, are present in the UpyMa spectra. In fact, these groups are not

58

involved in the reaction. The only difference between the two spectra correspond to the absence in UpyMa of the peak at 6.5 ppm. The relative peak corresponds to the amino group (-NH$_2$) of MIS, signed as white circle in Figure 4.4. Its absence is justified because the amino group is involved in coupling reaction with the isocyanate of ICEMA. Its absence in UpyMa spectrum confirms the complete conversion of MIS into the reaction product and as a consequence, the correct synthesis of UpyMa is achieved.

FTIR spectra of the reaction product and the ICEMA are compared in Figure 4.4. The analysis was performed by using a NicoletTM iS50 FTIR spectrometer (Thermo Scientific TM) equipped with an attenuated total reflection tool over the range 4000-400 cm^{-1} with a resolution of 4 cm^{-1} at room temperature. In the UpyMa spectra, the peaks of ureidic group are derived from the coupling reaction. The most important peaks are between 1700 cm^{-1} and 1500 cm^{-1}. In the FTIR spectrum of the product, there is a comparison of the classical peaks at 1661 cm^{-1}, 1589 cm^{-1} and 1523 cm^{-1}. It is then possible to see the respective C=O amidic group, the double bond C=C of Upy moieties, and the bending of N-H bond of amidic group respectively [166], [172]. The FTIR spectrum of the product is compared with the spectrum of the ICEMA. In Figure 4.5, the most relevant difference between the spectrum is the absence in UpyMa of the characteristic peak at 2267 cm^{-1}. The peak corresponds to the vibrational stretching of the isocyanate group of ICEMA [173], [174]. This confirms the removal of the reactant as an impurity of the reaction and the correct synthesis of the UpyMa.
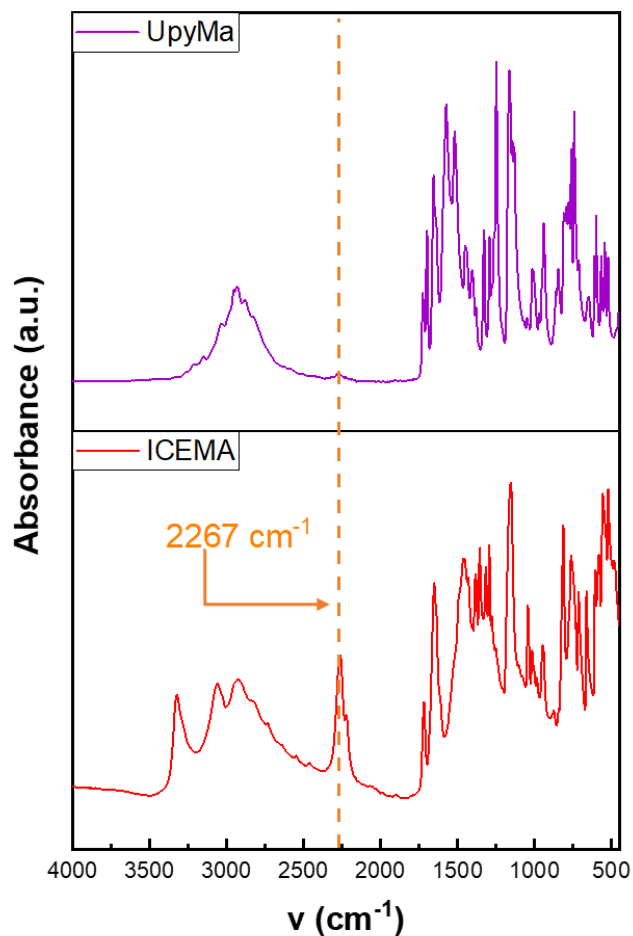
Figure 4.5: FTIR spectra of UpyMa and ICEMA.

4.5 Conclusions

In conclusion, ureidopyrimidinone methacrylate is synthesized by using a coupling reaction and characterized by NMR and FTIR analysis. The extraction process is then followed by the complete removing process of all the solvent used in the synthesis. The yield of the reaction is 92.3 %. Both NMR and FTIR analyses show the typical peaks of the urea group; this is taken as a proof of the reaction of ureidopyrimidinone methacrylate and to understand the level of purity.

Chapter 5

Synthesis of Ureidopyrimidinone Methacrylate based polymers and characterization

5.1 Introduction

Different mixtures have been studied for the synthesis of polymer electrolytes for LMBs. The oligomeric poly (ethylene glycol) methyl ether methacrylate has some interesting properties for battery application, such as low production costs, high conductivity of lithium ions, synthesis of cross-linked structure by using UV photopolymerization. Moreover, the insertion of UpyMa inside the internal structure could give the polymer self-healing effect, via multiple hydrogen bonds given by dimerization process.

Two different PEGMEM polymers with UpyMa as additive have been synthesized through UV-polymerization without the use of solvent. The membranes obtained have been characterized for understanding the correct copolymerization and the structure. Moreover, self-healing tests have been carried out to prove their self-repair properties. The electrochemical characterization of the polymers has been evaluated to discover the required features of membranes to be used as polymer electrolytes in solid state lithium metal batteries.

5.2 Synthesis of UpyMa-based polymers through UV polymerization

The polymer is produced using a matrix composed of different precursors. The oligomer is the poly (ethylene glycol) methyl ether methacrylate, with a molecular weight of 500 (PEGMEM500). As a difference to PEO's material, the substitution of -OH at the end of the chain with a methoxy group gives the structure non-polarizing properties, so that the material can solubilize easily carbonates solvents. Poly (ethylene glycol) diacrylate with a molecular weight of 575 (PEGDA575) is used as crosslinker. Due to the high number of ethoxy groups and the two double bonds, PEGDA 575 can present reticulate structure with high mobility of lithium. Since the two reactants are liquids, they can be easily mixed and used for dissolving UpyMa without the help of any solvents.

To synthesize the polymers by radical polymerization, a UV-initiator is necessary. The photo initiator chosen is 2-hydroxy-2-methyl-1-phenyl-propan-1-one (Darocur).

All the reactants are located inside a glove box in controlled argon atmosphere (MBraunLabstar, O_2 rate <0.5 ppm; H_2O <0.5 ppm) since the presence of the oxygen can inhibit the radical UV polymerization.

The formula is prepared by mixing the reactants inside a vial. First, UpyMa is weighted and mixed with the two oligomers. PEGMEM500 and PEGDA575 are added into the vial, fixed in a weight proportion 85:15. The mixing is obtained using a magnetic stirrer for 20 minutes, at different temperatures (60 °C, 50 °C, RT). However, even applying an increase in temperature levels, no difference in time to achieve the homogeneous solution is remarkable and for these reasons, the process has been developed at room temperature. At this point, the Darocur is added inside the solution, and the mixing proceeds at room temperature for other two minutes then the product is casted on a support. The thickness of the final polymer is controlled by using a Doctor Blade. The casted formulation is irradiated using a UV lamp for seven minutes with UV 365 nm wavelength.

The formula can be easily casted on glass or directly on the electrodes. The polymer is casted on a glass support to study the structure and for thermal analysis. On the other hand, for the electrochemical tests, the polymer precursor is directly casted on lithium metal anode. The synthesized membranes appear with a characteristic white colour and have a thickness of 100 μm when casted on glass

support. On the opposite, the polymer synthesized on lithium metal showed a thickness of 80 μm.

Commercial liquid electrolyte is used to swell the polymer electrolyte for electrochemical tests. In this case, the liquid electrolyte is $LiPF_6$ 1.0 M in 1:1 v/v mixture of ethylene carbonate (EC) and diethylene carbonate (DEC).

The synthesis proposed for UpyMa PEGMEM polymer electrolytes shows different advantages, and are different from other techniques, such as RAFT polymerization or condensation processes, which require organic solvents [152], [165], [167]. This synthesis process has low impact on the environment and low production costs since organic solvents are not required and the process is a quick one-shot synthesis. The possibility of casting the polymer directly on lithium is an advantage for possible scale-up production.

Two polymers have been synthesized with two weight percentage of UpyMa inside the formula, which are 5% w/w and 10% w/w respectively. These are referred as PPU5 and PPU10. Other synthesis with higher percentages of UpyMa (more than 10%) have not been considered, because of the low solubility of the UpyMa in the polymer precursor.

5.3 Characterization of the polymer electrolytes

The membranes synthesized are PEGMEM based polymer with UpyMa additive that appears as a side chain in a reticulate structure. The well-made insertion of ureidopyrimidinone inside the polymer is the fundamental to appreciate the self-healing properties of the membrane as a polymer electrolyte. Moreover, a good polymer useful in lithium batteries projecting process has to show high thermal resistance properties. To understand thermal stability process, thermogravimetric analysis (TGA) has been carried out on a single membrane. The analysis was performed between 25 °C and 800 °C in nitrogen atmosphere, by using NETZSCH TG 209F3 instrument, with the polymers casted on a glass support. The results are shown in the Figure 5.1. All the polymers have showed a degradation process that starts over 200 °C. The membranes remained stable up to 172 °C, which is the temperature at which EC:DEC liquid electrolyte begins its thermal degradation [175]. Due to their stable thermal behaviour, PPU5 and PPU10 guarantee stronger safety capabilities in lithium metal batteries range of use. PPU5 shows the best thermal stability, with a temperature in which 5% of weight is loss

of 300 °C. On the opposite, PPU10 degrades at 250 °C. The difference is probably due to the incomplete copolymerization of UpyMa in PPU10.
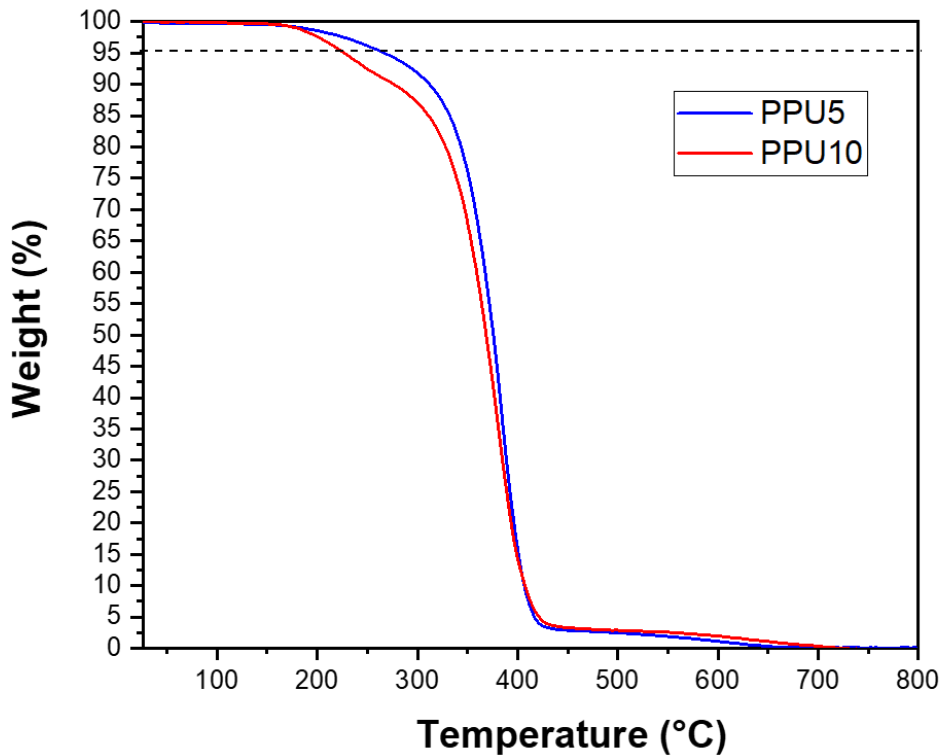
Figure 5.1: TGA curves of PPU5 and PPU10 samples.

FTIR analysis of the two membranes have been carried out to understand the copolymerization process that happens on UV irradiation and for this analysis, a NicoletTM iS50 FTIR spectrometer is used (Thermo Scientific TM). The instrument is equipped with a total reflection tool over the range 4000-400 cm^{-1}, with a resolution of 4 cm^{-1}. The results show a spectrum similar to the proposed PEGMEM polymers described in literature [166], [176]. However, two characteristic peaks at 1661 and 1589 cm^{-1} are present in the PPU5 and PPU10, respectively [166]. Such peaks, which are assigned to the group of the UpyMa, confirm the copolymerisation by the added material inside the reticulate polymer.

Moreover, there is no evidence of the characteristic peak of double bond of methacrylate at 1630 cm^{-1}, which is a sign of the success of the polymerization

[176], [177]. The double bond is in fact involved into the radical polymerization, as a result the formation of the new C-C creates the polymeric reticulate structure and the side chain with the Upy additive.
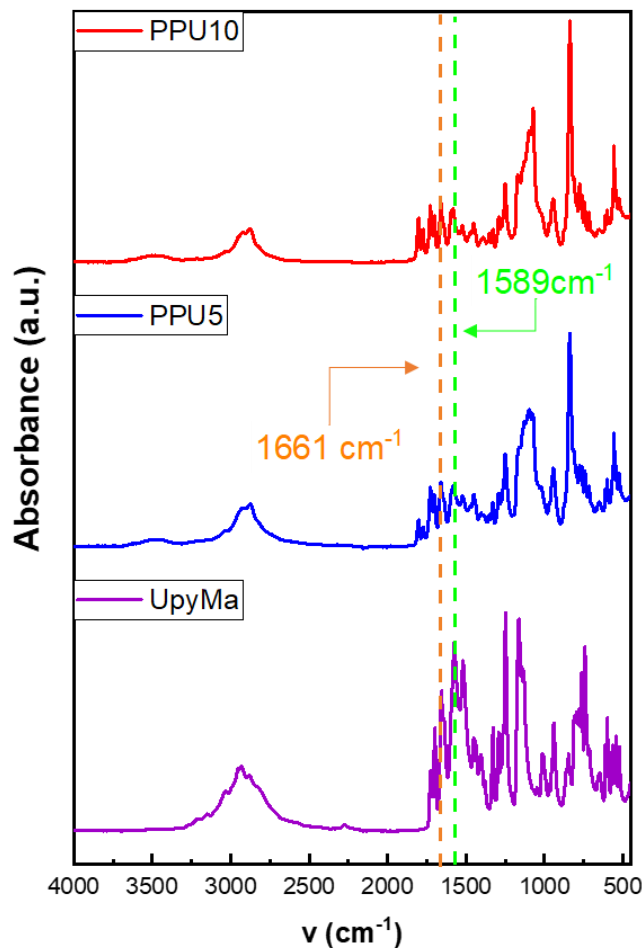
Figure 5.2: FTIR spectra of PPU10, PPU5 and UpyMa.

^{1}H-NMR analysis has been evaluated to accomplish the best synthesis process for UpyMa in PEGMEM reticulate. The spectra were recorded by using Bruker 400 MHz instrument. PPU5 and PPU10 have been analysed by using deuterated DMSO as solvent. The results have been reported on Figure 5.3. The spectra present some similarities with UpyMa spectrum and showed some characteristic peaks, as those of the Upy group labelled in violet and yellow circles. The presence of such peaks inside the NMR structure confirms that UpyMa does not degrade during UV-polymerisation [178]. Moreover, the spectrum shows a high peak on 3.5 ppm, that

is referred to all the protons of the ethoxy chain of PEGMEM500, PEGDA575 and UpyMa, and the final methoxy group of PEGMEM500. At 8.0 and 1.0 ppm phenyl and methyl group of Darocur are referred respectively.
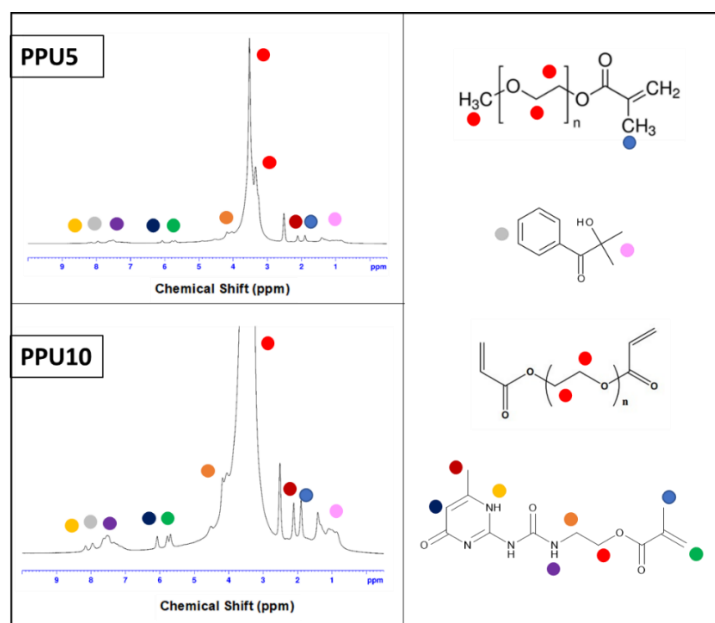
Figure 5.3: ^{1}H NMR spectra of PPU5 and PPU10 samples.

2D NMR correlation spectroscopy (COSY) is evaluated for understanding the correct assignation of the peak in ^{1}H NMR. In COSY, correlations will be observed via cross-peaks or off-diagonal peaks between two different types of protons which are bonded to adjacent carbon atoms in the structure. Correlations between the same types of protons only appear as diagonal peaks in the 2D COSY spectrum[179]. In this case, the COSY confirmed the coupling correlation of the peaks at 4.2 and 3.5 ppm, corresponding to the two -CH$_2$- groups of UpyMa, signed in orange and in red respectively.
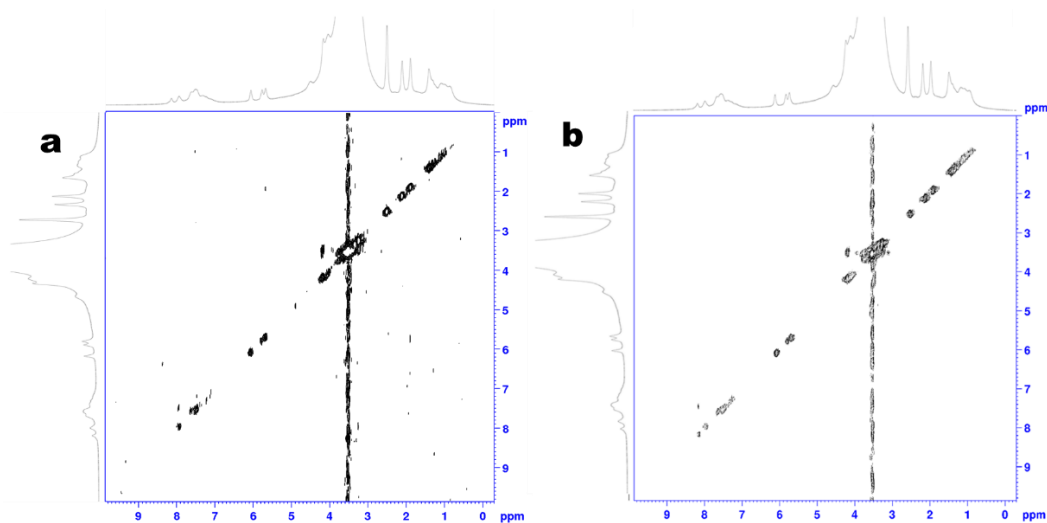
^{1}H-NMR and COSY spectra show the well-made copolymerization of UpyMa inside the polymeric structure of PEGMEM. However, in every analysis there are the typical peaks of double bonds at 6.5 ppm. However, all the molecules involved into the polymerization possess double bonds, so the identification of these peaks remains a necessity and this is why, diffusion-ordered spectroscopy (DOSY) is carried out. The DOSY is evaluated with a stimulated-echo NMR pulse sequence (Oneshot45)[40] with an implicit applied delay in gradient recovery (d16) and magnitude of the gradient purge pulse (p19) at 0.2 and 0.6 ms, respectively.

In DOSY, all the hydrogen signals are correlated to its diffusion coefficient D. The diffusion coefficient is associated to the hydrodynamic radius (R) by the following formula:

$$D = \frac{kT}{6\pi\eta R}$$

Equation 5.1

in which k is the Boltzmann constant, T is the temperature and η is the viscosity of the solvent. With DOSY, molecules with different sizes give signals with different diffusion coefficients. The results of DOSY measurements are represented in Figure 5.5.

In the case of PPU10, all the signals have different diffusion coefficient. In particular, the peaks with different diffusion coefficient correspond to the signal of the double bonds at 6.5 ppm and the UpyMa. For these reasons, in PPU10 only a part of the additive is correctly bound inside the polymeric PEGMEM chain.

In the case of PPU5, all the peaks have the same diffusion coefficient, except for the peak at 2.6, that is typical of DMSO. This corresponds to a copolymerization of the UpyMa inside the polymer structure. So, the peaks of double bonds are not linked to the UpyMa but are associated to one of the two double bond of PEGDA.
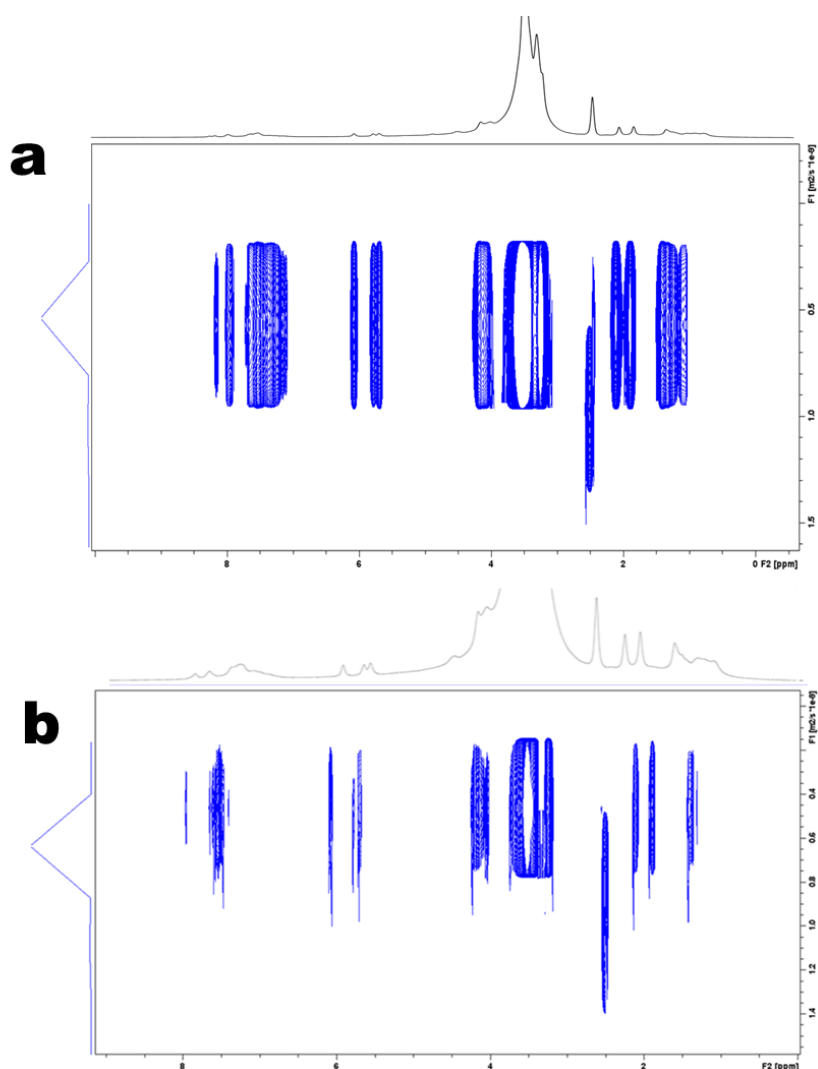
Figure 5.5: a) DOSY spectrum of PPU5 b) DOSY spectrum of PPU10

For better understanding the morphology of the polymer samples, their structure has been investigated by field emission scanning electron microscopy (FESEM). Samples morphologies were examined using a FESEM, TESCANS9000G. The FESEM analysis of the samples is depicted in Figure 5.6. First, the micrographs reveal that samples have a homogeneous surface. At high magnification, it is possible to see a wrinkled structure, which is due to the presence of H-bond of UpyMa inside the polymer reticulate. Moreover, cross-section analysis in images 5.6 c) and f) shows that PPU5 and PPU10 are characterized by a compact structure, without voids, proving the polymerization of the membranes. Moreover, the values of thickness for the membranes are 115 μm and 131 μm for PPU5 and PPU10 respectively.

Furthermore, surface energy dispersive spectroscopy (EDS) was carried out to study the correct distribution of UpyMa inside the polymer structure. In fact, UpyMa is the only precursor that possesses nitrogen inside its molecular structure. For these reasons, the nitrogen atom can be related to the content of UpyMa, demonstrating its position. The results are shown on Figure 5.6 i) and l). As expected, the nitrogen element is present in minor quantity respect to carbon and oxygen. However, EDS reveals that nitrogen is homogeneously distributed on the surface of the polymers. This demonstrates the homogeneous mix of the UpyMa inside the polymers through UV radical polymerization.
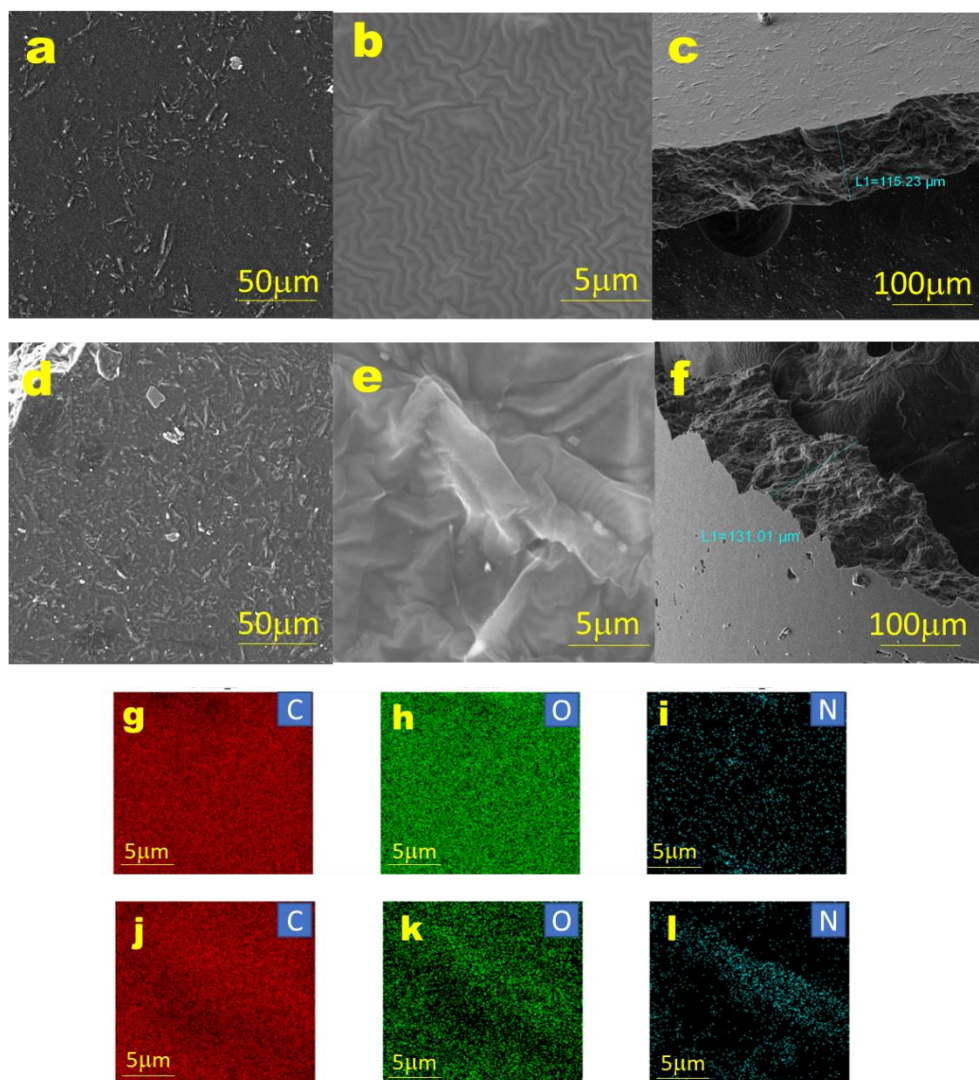
Figure 5.6: FESEM micrographs of (a) PPU5 surface at low magnification, (b) PPU5 surface at high magnification, (c) PPU5 cross-section, (d) PPU10 surface at low magnification, (e) PPU10 surface at high magnification, (f) PPU10 cross-section. EDS analysis PPU5 showing (g) carbon, (h) oxygen and (i) nitrogen elements. EDS analysis of PPU10 showing (j) carbon, (k) oxygen and (l) nitrogen elements.

In conclusion, PPU5 and PPU10 polymers have been successfully synthesized and characterized by using a solvent free UV polarization process. The polymers have been characterized by different techniques, showing the good insertion of UpyMa inside the reticulate PEGMEM structure given by PEGMEM500 and PEGDA575. Moreover, the polymers reveal high thermal stability and homogenous structure, important features for their application in lithium metal batteries.

5.4 Investigation of Self-healing properties of membranes

Self-healing tests have been carried out on membranes to study their behaviour in self-repairing after a damage. Several experiments have been proposed to understand how the membrane reacts after an external damage, and how long the membrane takes to self-heal itself. For this reason, PPU5 and PPU10 have been casted and synthesized on the glass substrate. The polymer is cut and placed between two glasses with small pressure applied by paper clips. As can be observed in current literature, the first tests were carried out at 60 °C [166], [167], [169]. In fact, the formation of hydrogen bond is kinetically favoured at higher temperature. For this reason, the damaged polymers are located into an oven. In these conditions, both polymers self-repair after two hours. The same tests were carried out bringing the temperature level at 50 °C, then 25 °C (RT). No changes in time of self-healing process were observed by decreasing the temperature. At room temperature conditions 24 hours are required to self-repair the polymer. Figures 5.7-5.8-5.9 show the obtained results, carried out by using an optical microscope and by SEM analysis on every samples.

Optical images of the polymeric samples were obtained by an optical stereo microscope Leica M80. Scanning electron microscopy (SEM) images of the polymer samples were performed by SEM Hitachi TM 3030 Plus Tabletop, operated at 15 kV.

For both samples, the mechanism involved the hydrogen bond by UpyMa dimerization, which is able to restore the damage even if a small scar is still visible.
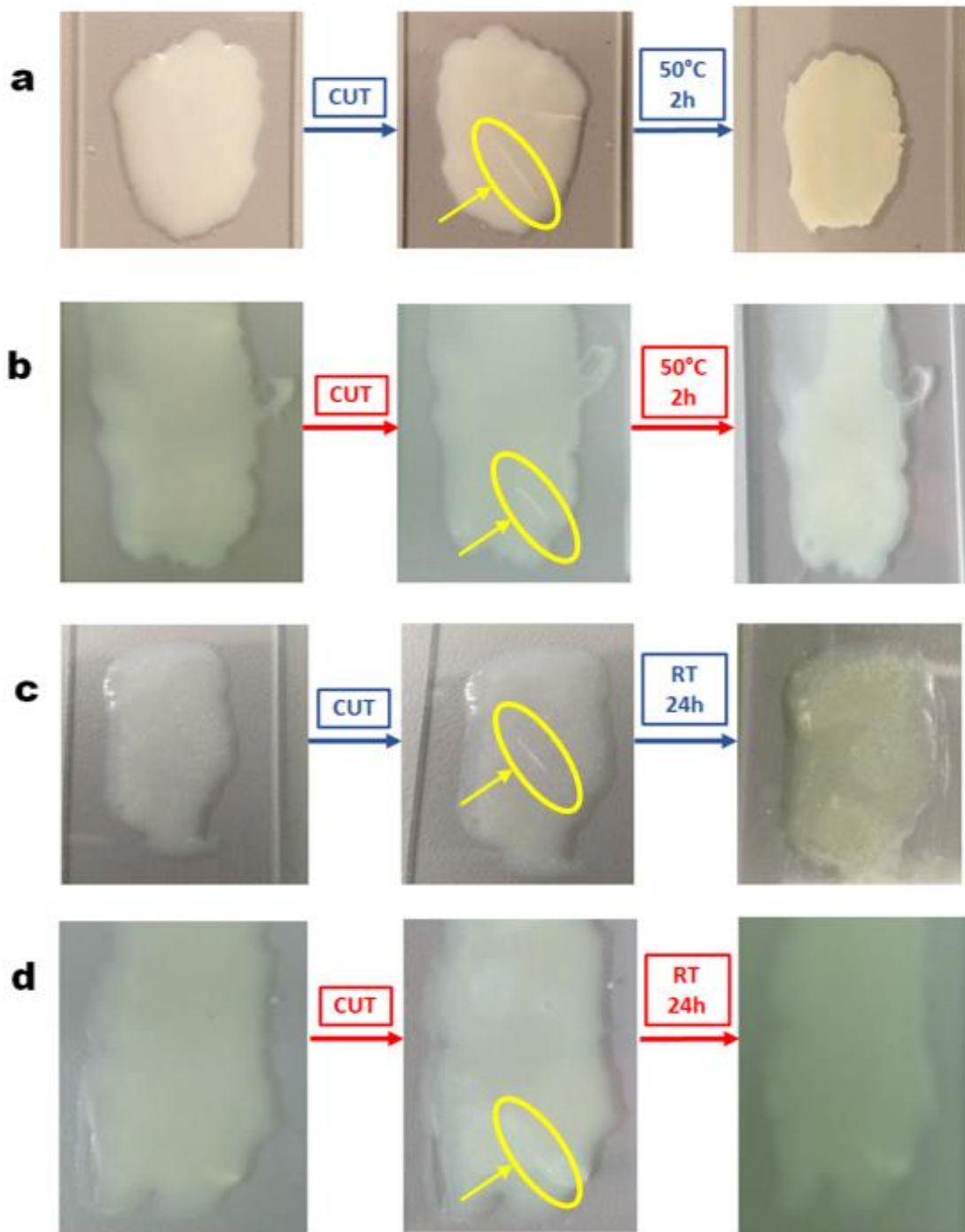
Figure 5.7: Photograph images of PPU5 and PPU10 samples between glass-slides, (left) before and (right) after self-healing process. a) PPU5 at 50 ᵒC for 2 h. b) PPU10 at 50 °C for 2h (c) PPU5 at RT for 24h (d) PPU10 at RT for 24 h.
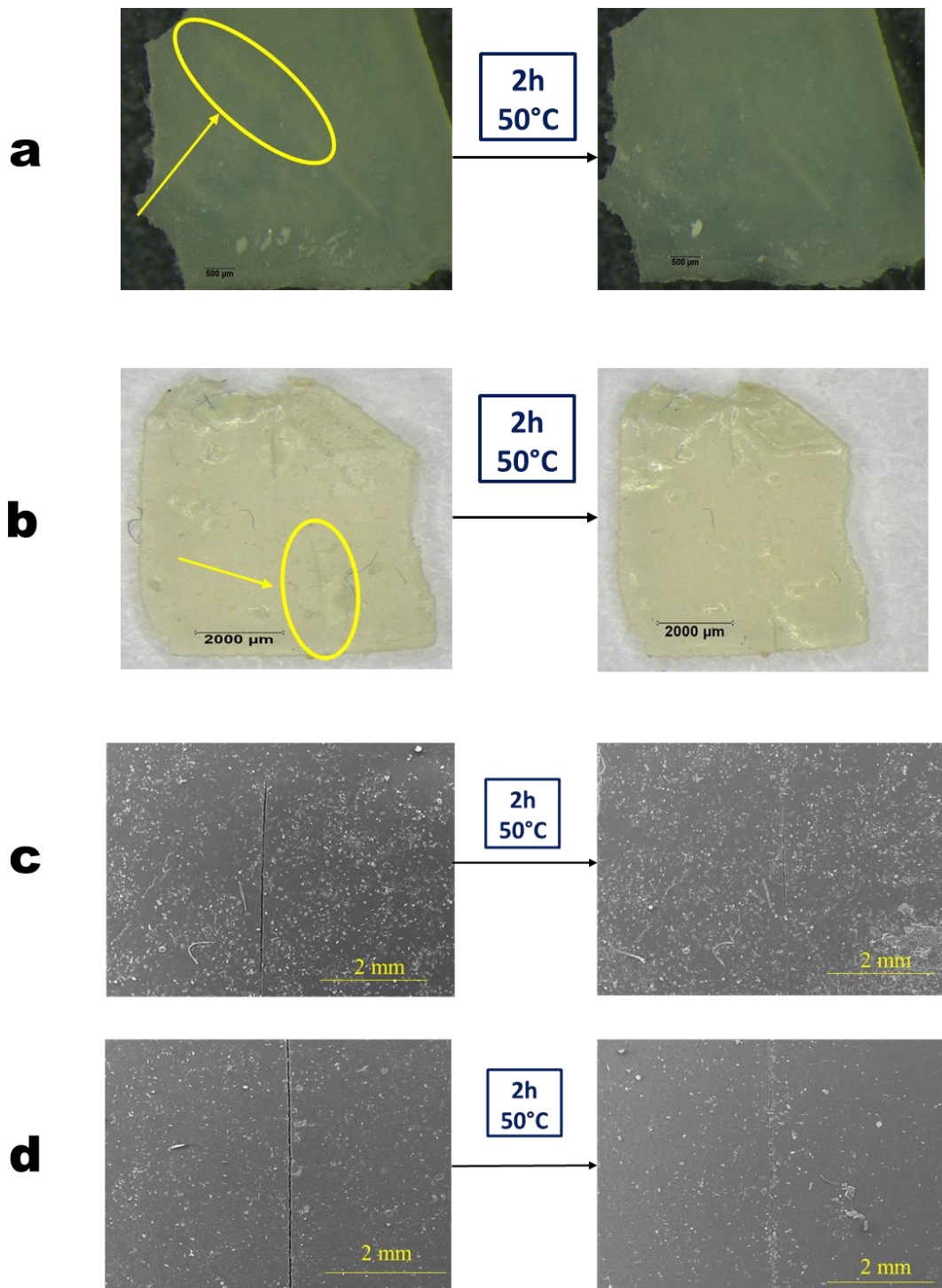
Figure 5.8: Optical images of (a) PPU5 and (b) PPU10 samples between glass-slides, (left) before and (right) after self-healing process at 50 ◦C for 2 h. SEM micrographs of (c) PPU5 and (d) PPU10 samples (left) before and (right) after self-healing process at 50 ◦C for 2 h.
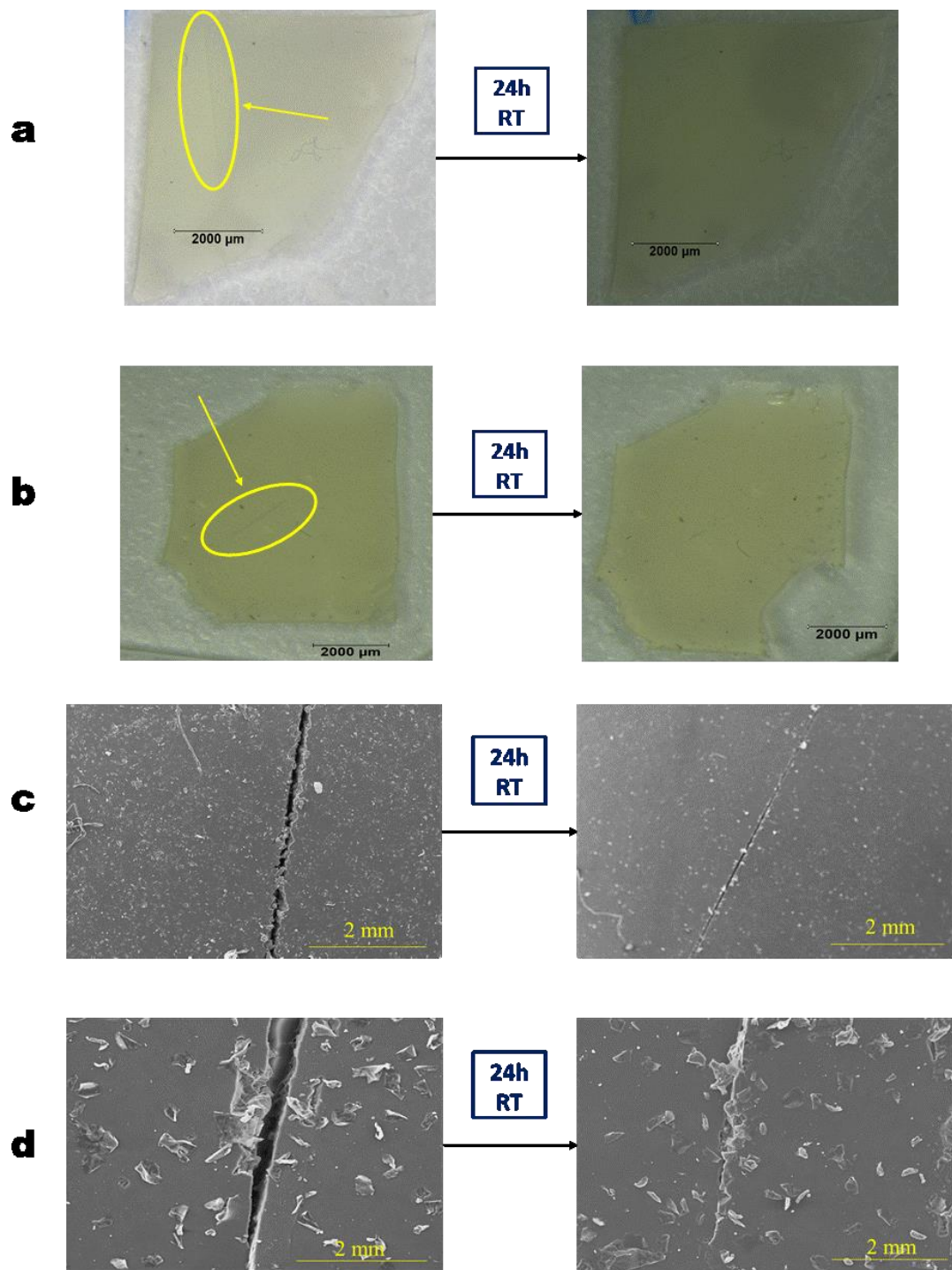
Figure 5.9: Optical images of (a) PPU5 and (b) PPU10 samples between glass-slides, (left) before and (right) after self-healing process at room temperature for 24 h. SEM micrographs of (c) PPU5 and (d) PPU10 samples (left) before and (right) after self-healing process at room temperature for 24 h.

It is very interesting to see that the two polymers show self-healing capability at the same conditions.

The difference in percentage of UpyMa does not affect the self-recover of the polymer. Polymers with limited weight percentage of UpyMa, and same self-healing conditions, can be of a great interest for a future commercialization, and that is the reason why PPU5 could be a more valid candidate instead of PPU10. Furthermore, it presents lower concentration of UpyMa in respect to other UpyMa membranes used in solid state batteries.[165]–[167]. However, its use in GPE needs more investigation.

5.5 Electrochemical performances of polymer electrolytes

The electrochemical performances of the samples have been investigated by using different analysis for understanding their potential use in LMBs.

First, the liquid electrolyte uptake (LEU) has been quantified with commercial electrolyte solution 1 M $LiPF_6$ in EC:DEC 1:1 v/v. In fact, good compatibility between the electrolyte and the polymer is relevant for gel polymer electrolyte with high performances inside the cell. LEU is a simple technique to test how the electrolyte is swelled inside the polymer for a definite time. LEU is calculated by the following equation:

$$LEU = \frac{M_e - M_0}{M_o} \times 100$$

Equation 5.2

in which M_0 and M_e are the weights of the membrane before and after immersion, respectively. Dry membranes are weighted in an inert atmosphere and then immersed in the electrolyte solution for 18 hours. The high values of electrolyte uptake results in a good interaction between electrolyte and polymer.

The liquid electrolyte uptakes are described in Table 5.1. The high LEU obtained in both polymers confirm that the presence of UpyMa inside the structure is not an obstacle for the creation of gel polymer PEGMEM based for battery systems.

LEU			
Sample	Initial weight (mg)	Final weight (mg)	LEU (%)
PPU5	82.3	332.4	304
PPU10	75.4	354.2	370

Table 5.1: LEU values for PPU5 and PPU10 samples. The electrolyte solution used consisted of LiPF$_6$ 1.0 M in 1:1 v/v EC:DEC.

Furthermore, the influence of the LEU values is verified by measuring ionic conductivity for PPU5 and PPU10 at different temperatures.

To collect ionic conductivity values (σ) of the membranes by electrochemical impedance spectroscopy (EIS) the membranes have been sandwiched between two stainless steel (SS) blocking electrodes and tested on electrochemical workstation (CHI660D). The frequency of the EIS test ranged from 1 to 10^5 Hz with an amplitude of 10 mV. The measurements were performed between 20°C and 60 °C, with a 10 °C step.

The ionic conductivities were calculated at each temperature using the equation 3:

$$\sigma = \left(\frac{l}{A}\right) \times \left(\frac{1}{R}\right)$$

Equation 5.3

in which the constants l, R and A represent the membrane thickness, the membrane resistance and surface area respectively, measured at the high-frequency intercept on EIS spectra.

The results are shown in the Figure 5.10. Ionic conductivity of the two polymers is higher than 10^{-3} S cm^{-1} for both the polymer electrolytes. PPU10 shows a slightly higher results compared to PPU5. However, the difference between the two polymers are not remarkable. The presence of higher amount of UpyMa inside the

polymeric structure does not affect the ionic conductivity of the PEGMEM samples. Moreover, in comparison which other PEGMEM polymer electrolytes, the ionic conductivity of PPU membranes are promising for their use in lithium metal systems[166], [167], [180]. Furthermore, even if the best results have been shown at 60 °C, the ionic conductivity is high even at lower temperature (PPU5 and PPU10 show a conductivity of 1.5×10^{-3} S cm^{-1} and 1.6×10^{-3} S cm^{-1} at 20°C, respectively). The results obtained show a typic T-Arrhenius plot, so the conductivity temperature-dependence data follow the Arrhenius relationship. In this case, it is interesting to calculate the activation energy (E_a) of the GPE, which is the barrier, principally Coulombic, for an ion to hop from counterion to another [181]. E_a is correlated to the conductivity by the following equation:

$$\sigma = Ae^{\frac{-E_a}{RT}}$$

<div align="center">Equation 5.4</div>

in which T is the temperature, R is the gas constant and A is the pre-exponential factor. The activation energy calculated from the slope of the fitted conductivity line is found to be 0.091 eV for PPU10 and 0.090 eV for PPU5. The difference of the activation energy appears not to be significant, with a quite high value for PPU10. The ionic conduction of PPU follows a solvent diffusion mechanism inside the polymer network with low activation energy, Moreover, the results are similar to GPEs in literature. Jung et al. [182] prepared a in gel polymer electrolyte PVC based with an E_a of 0.120 eV. Isa et al. [183] fabricated a PMMA-LiBF$_4$ gel polymer electrolyte with an E_a of 0.19 eV. The low activation energy, E_a, for the lithium is mainly caused by the amorphous nature of the polymer electrolytes that ease the fast Li$^+$ ion movement in the polymer.
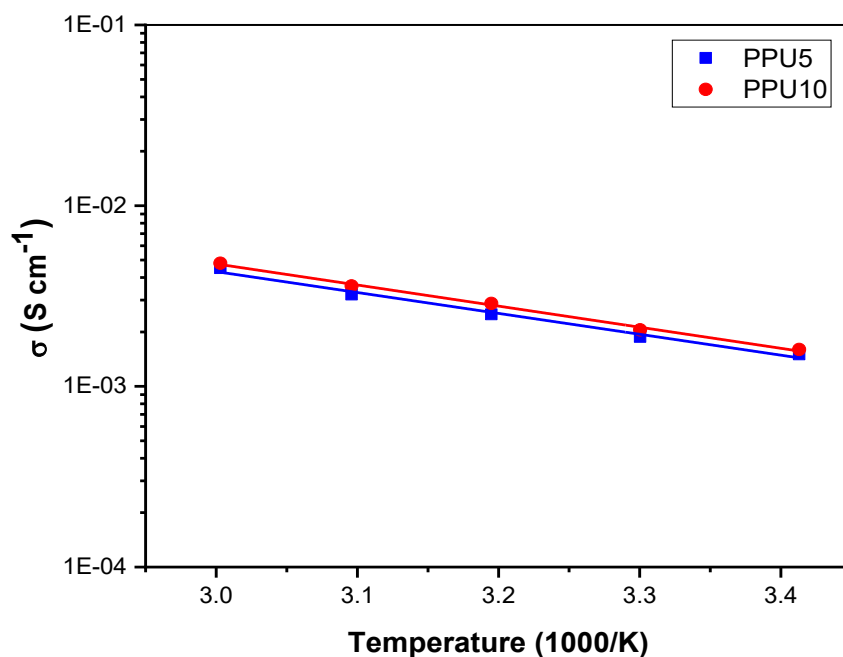
Figure 5.10: Temperature dependence of ionic conductivity for PPU5 and PPU10 samples.

Electrochemical stability, in particular at high potentials, is another crucial parameter for this application. For this reason, linear sweep voltammetry (LSV) was performed at room temperature on PPU5 and PPU10.

The tests have been performed by using an asymmetrical SS/PPU/Li cell in the potential range of 1.0 and 5.5 V vs Li^+/Li. The polymers have been synthesized directly on lithium anode.

In this case, the precursor solution containing the photo-initiator evenly covers the lithium metal, which is directly exposed to UV irradiation for seven minutes to form a well-cross-linked film with high reproducibility. This procedure is carried out in Ar-filled glove box. In situ polymerization brings back some advantages such as improved adhesion ability between the anode and the polymer[184], which decreases the interfacial resistance typical of ex-situ polymerization. The process is simple and adaptable to battery-processing methods to achieve better interfaces. Moreover, this procedure guarantees more effective mechanical integrity against dendrite growth, which in turn result in improved cell performances. In possible scale up, it reduces the amount of scrap from manufacturing and as a consequence, the cost is reduced[185].

The measurements were carried out with an electrochemical workstation (CHI660D) at a scan rate of 0.2 mV s^{-1} at room temperature. The results are shown in Figure 5.11. Basically, no evidence of side reactions has seen from 1.57 to 5.0 V vs Li$^+$/Li for PPU5, from 1.57 to 4.5 V vs Li$^+$/Li for PPU10. Up to these values, the current intensity increases because of the degradation of liquid electrolytes.
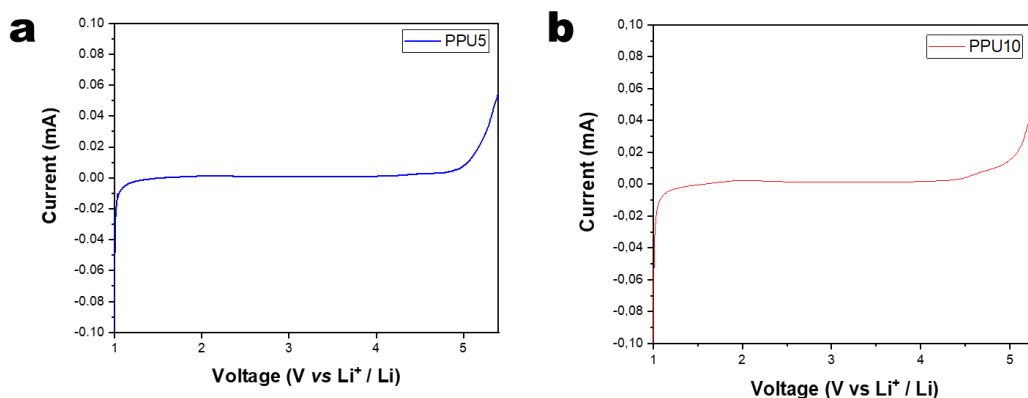
Figure 5.11 : (a) LSV plot of a Li/PPU5/SS cell at room temperature. (b) LSV plot of a Li/PPU10/SS cell at room temperature.

Despite the large electrochemical stability range of the polymer, the stability at interface with Li metal is another requirement for a GPE in lithium batteries. Therefore, interfacial stability between polymer and lithium is investigated in a period of thirty days by using EIS spectroscopy. The membranes were casted on lithium metal chips in argon atmosphere, and tested at open circuit voltage by EIS on an electrochemical workstation (CHI66OD) in Li/Membrane/Li symmetric cells. The frequency of EIS ranged from 0.01 to 10^5 Hz with am amplitude of 10 mV.

Figure 5.13 describes the results of the interfacial stability of the two polymer electrolytes. Starting from day zero, the impedance spectrum of PPU5 has a transfer resistance of 450 Ω. This high value is mainly explained by the poor initial contact between the lithium and the gel polymer electrolyte. This value increases during the first day due to the spontaneous SEI formation on lithium metal. However, from the second day, the transfer resistance decreases at 350 Ω. This may be explained by the fact that in the early stages the SEI layer has not been sufficiently developed. After two days, a more conformal SEI layer is produced, which eases more homogeneous charge transport. PPU5 maintains stable contact with lithium metal electrode, avoiding any side reactions on time. In the case of PPU10, during the first period, the sequence of events in the lithium surface is analogous to PPU5. In

fact, the contact between the surfaces and the SEI formation are the main cause of the increase in charge transfer resistance. However, the increase of resistance remains constant even in the following days. After the eighteenth day, the value of resistance was higher than 2000 Ω; this value makes the use of PPU10 in lithium cells impossible. The main reasons could be the continuous formation of SEI.

The different behaviour of the membrane could be also explained by looking at the different structures of the two polymers obtained by DOSY spectroscopy (Figure 5.5).

In PPU10, the partial copolymerization could give the increase of the resistance seen during the interfacial stability. The UpyMa not polymerized could react with lithium anode, and, consequently, make the use of PPU10 impossible in GPEs. Instead, in PPU5 all the UpyMa is successfully inserted into the polymeric structure, thus shows the stable contact with lithium seen during the interfacial stability. Moreover, interfacial stability confirms that the presence of such double bonds of PEGDA inside the polymeric structure of PPU5 does not give any side reactions with lithium.

Because of the poor interfacial stability of PPU10, PPU5 is selected as the most promising GPE in lithium metal batteries.
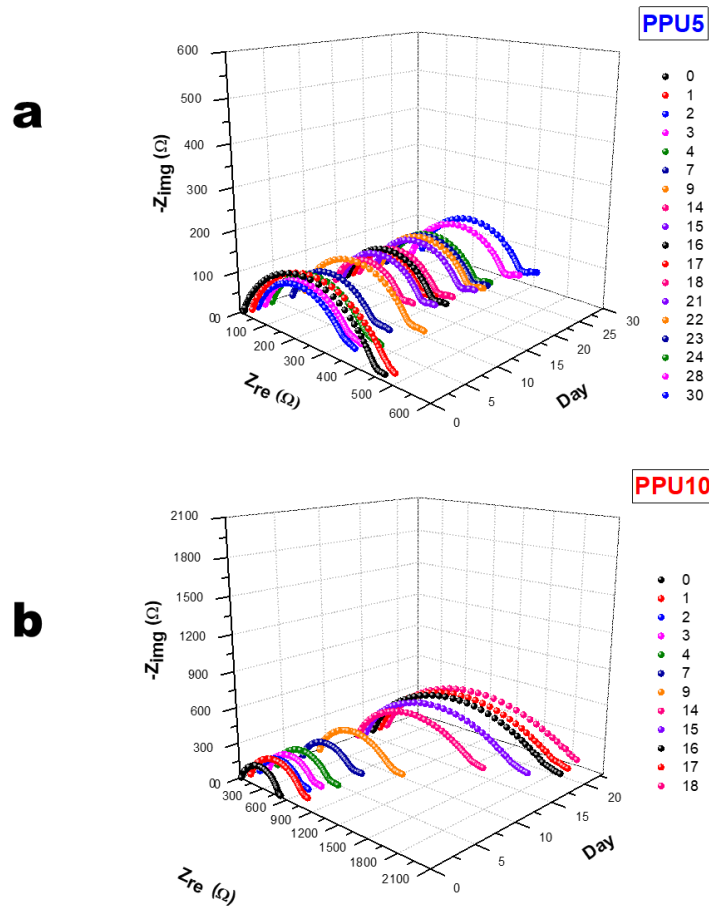
Figure 5.12: (a) Interfacial stability assessed by a Li/PPU5/Li cell at room temperature. (b) Interfacial stability assessed by a Li/PPU10/Li cell at room temperature.

Lithium ion transference number (t_{Li+}) is an important parameter related to the lithium ion batteries. It represents the ratio of the electric current carried by lithium ion to the total current carried by all the species[186], [187]. The higher value of lithium-ion transference number is a consequence of the high mobility of lithium cation inside the polymeric structure. Different investigation techniques have reported for the measurement of Lithium ion transference number, one of the most used is the developed by Abrahm [188] .

Lithium ion transference number is evaluated by performing chronoamperometry and impedance spectroscopy measurements. Such method has been developed by Bruce and Vincent [189] and is generally used to obtain the lithium transference number in polymers by using a symmetric cell, which is polarized by applying a constant potential difference (ΔV) between the electrodes. As a consequence, the monitored current initially decreases until a steady-state is

reached. Such decrease is mainly due to the establishment of a concentration gradient, which reduces the motion of the anions and increases that of the cations.

By using symmetrical Li/PPU5/Li cell at room temperature, the value of t_{Li+} is obtained by using the following equation:

$$t_{Li+} = \frac{I_s \times (\Delta V - I_o R_o)}{I_o \times (\Delta V - I_s R_s)}$$

Equation 5.5

where I_0 and I_S are the initial and steady-state current values respectively. At the same time, ΔV is the applied with DC potential (10 mV); R_0 and R_S are the interfacial impedance values at initial and steady state, respectively.

Lithium ion transference number calculated for PPU5 is 0.62. The result shows a high mobility of lithium cations inside the cell and, consequently, highly lithium ion conducting electrolyte [187].

Such high value could be explained because of the ethoxy group of the main chain of the polymer, that easily segregates the lithium cation from the anion, increasing its mobility inside the GPE. Additionally, some gel polymer electrolytes with different compositions that are reported in literature show similar lithium transference number. Yuan et al. [190] fabricated a gel polymer electrolyte with a lithium transference number of 0.72, while Schaefer et al. [191] synthesized a polyethylene glycol diacrylate GPE with a lithium transference number of 0.65. Currently, solid polymer electrolytes containing UpyMa show lithium transference number lower than 0.62. For example, Xue et al. fabricated different UpyMa SPE membranes with t_{Li+} lower than 0.30 [166]. The value calculated by Zhou et al. from a Upy-SiO$_2$ based SPE is 0.43 at 60 °C [165]. Other values of lithium-ion transference numbers in recent solid-state polymers for LMBs are shown in Table 5.2.

In summary, the high t_{Li+} value of PPU5 is very promising for the application of the GPE especially when the cell operates at higher C rates.
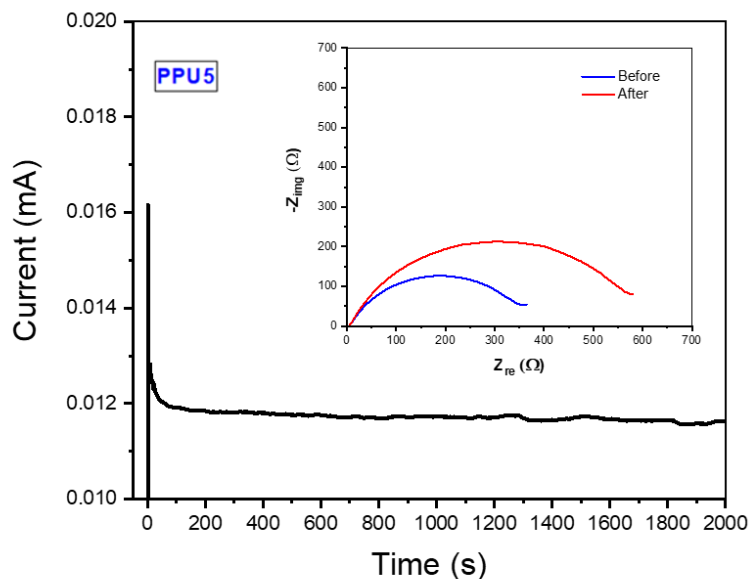
Figure 5.13: The chronoamperometry profile of a symmetric Li|PPU5|Li cell with a polarization potential of 10 mV. The inset shows the AC impedance spectra before and after polarization at room temperature.

Even if PPU5 has interesting properties for its application in lithium metal batteries, the selected GPE must possess sufficient mechanical resistance to limit or eventually suppress Li dendrites formation. Therefore, lithium plating stripping is performed on a symmetrical Li/PPU5/Li cell at room temperature at different current density values. Preliminary measurement of lithium plating stripping has been performed at a current density of 0.1 mA cm^{-2} and a fixed capacity of 0.1 mAh cm^{-2} for 75 hours. The results confirm the correct deposition of lithium during the process, therefore the absence of any lithium dendrite growth and low polarization. However, the most interesting approach is about higher current density. For these reasons, the same experiment is proposed at a current density of 1.0 mA cm^{-2} and a fixed capacity of 1.0 mAh cm^{-2}. In that case, the cell shows severe fluctuations, with a large voltage polarization. This brings lithium dendrites to grow on lithium metal surface. However, the cell keeps cycling for over 600 hours, limiting the growth of the dendrites and short-circuits.
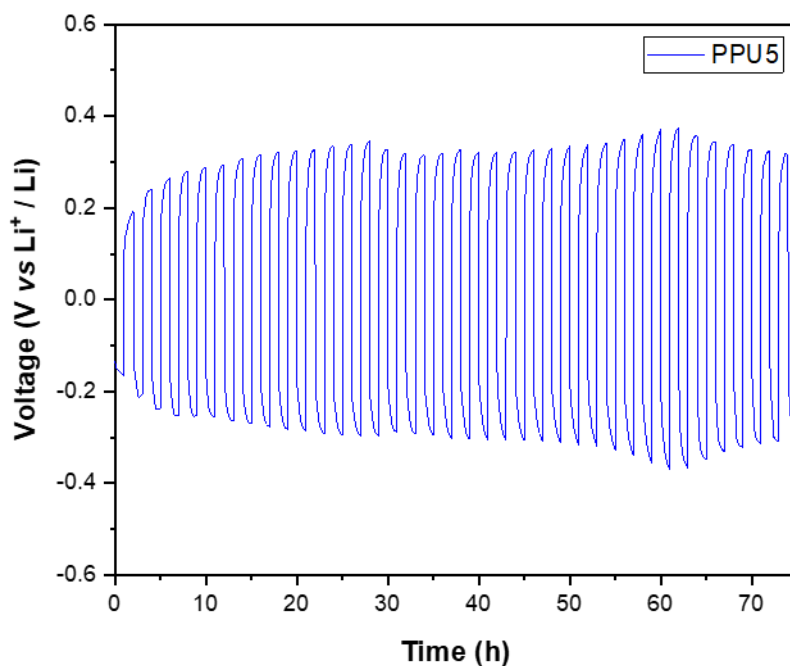
Figure 5.14: Lithium plating and stripping results of the Li/PPU5/Li symmetrical cell at a current density of 0.1 mA cm^{-2} and at a fixed capacity of 0.1 mAh cm^{-2}, at room temperature.

.

The main reason for this feature is the reticulate structure of the polymer, and the ability of self-healing induced by H-bond dimerization of UpyMa [192]. The experiment is repeated using Celgard2500 as a separator (black line in Fig. 5.15). With same conditions, the commercial separator has the same fluctuations. However, the cell loses its function after 50 hours because of the short-circuits.

The measurements demonstrate the ability of PPU5 to limit dendrite growth at drastic conditions at room temperature.
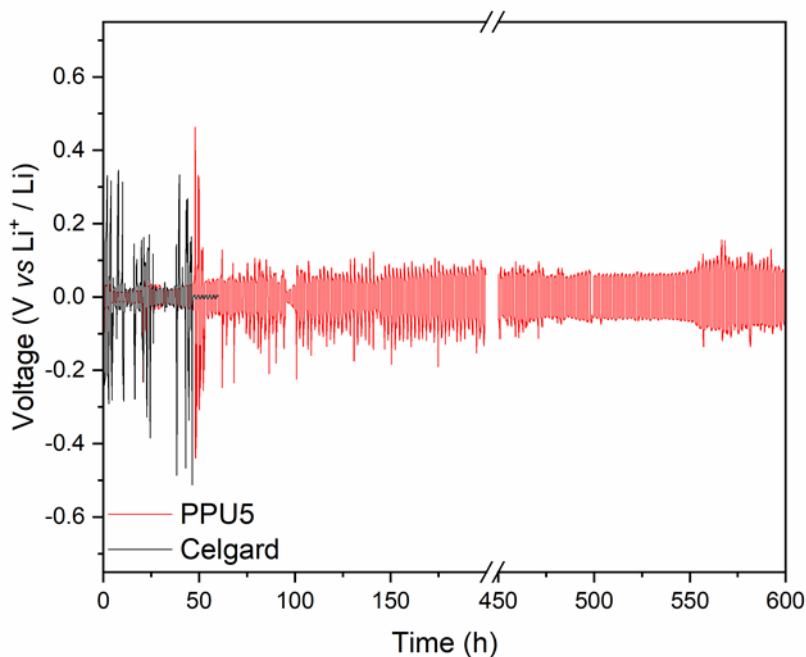
Figure 5.15: Lithium plating and stripping results of the Li/PPU5/Li (red) and Li/Celgard + LE/Li (black) symmetrical cells, at a current density of 1.0 mA cm^{-2} and a fixed capacity of 1.0 mAh cm^{-2}, at room temperature.

The rate capability of PPU5 is evaluated by using galvanostatic charge/discharge tests at different C rates. The C rates were 0.1 C, 0.2 C, 0.5 C, 1.0 C and 0.1 C. Cycling performances were investigated in a voltage range from 2.5 V to 4.2 V. Lithium iron phosphate (LFP) is chosen as cathode. LFP cathode is prepared by tape-casting a homogeneous slurry of Aleees LiFePO$_4$ with Carbon C$_{65}$ (from Imerys) and poly(viniledenfluoride) (Kynar 761 from Arkema) in NMP on aluminium foil. The weight percentage ratio was 70/20/10 of LFP, C$_{65}$ and PVDF respectively. After dried at 50 °C for one hour, the electrode rests at room temperature overnight. The cathode is then cut at 15 mm diameter disc and dried under vacuum for four hours at a temperature of 120 °C. The rate capability of the cell is tested on two different temperature: 50 °C and room temperature, in the voltage range from 2.5 V to 4.2 V. C rates are defined on the basis of LFP theoretical specific capacity (170 mAh g^{-1}). The results are reported in Figure 5.16.

In every C applied, PPU5 shows good cyclability with a relevant discharge capacity. In all the temperature conditions, the cells maintain a high discharge capacity, with a discharge capacity of 131.5 mAh g^{-1} at 1 C at 50 °C and a discharge capacity of 103.6 mAh g^{-1} at 1 C at room temperature. Moreover, the cells restore

85

the final discharge capacities of 0.1 C, that are 142 and 137 mAh g^{-1} at 50 °C and room temperature respectively, after nine cycles at higher C.
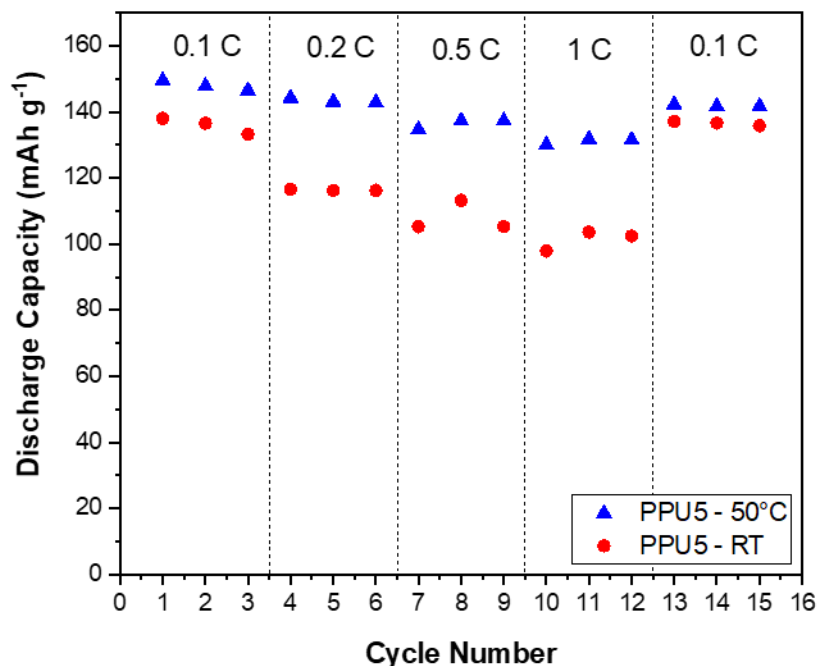
Figure 5.16: Rate capability test of a Li/PPU5/LFP cell at 50 °C and at room temperature.

The best results are detected when the cell is cycled at 50 °C, mainly due to the higher ionic conductivity that the polymer has at that temperature. However, the results obtained at room temperature are interesting. In fact, on literature basis, polymer electrolytes are currently cycled at 60 °C [165], [168] and almost never cycled at room temperature. The application of PPU5 in GPE batteries systems able to perform at room temperature is a good promising aspect for next generation solid-state batteries.

For these reasons, galvanostatic cycling performance was evaluated at 0.2 C at room temperature. The results have been shown in Figure 5.17. The cell exhibits an initial discharge capacity of 143 mAh g^{-1}, with a Coulombic Efficiency lower than 90%. This is mainly due to the SEI formation, given by the contact between lithium and PPU5.
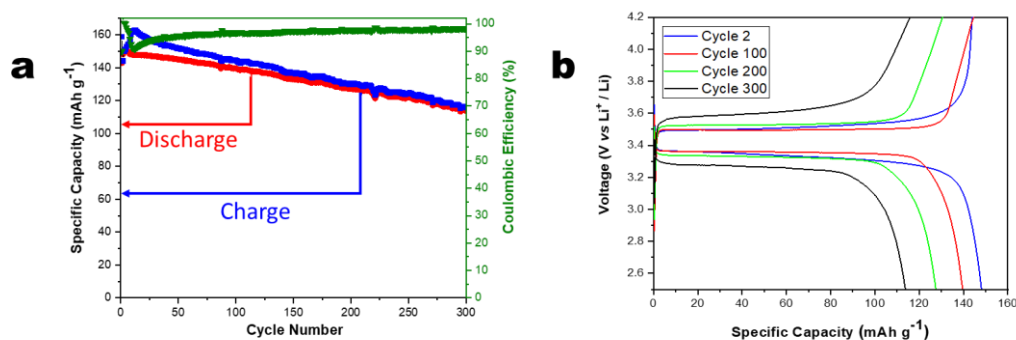
Figure 5.17: (a) Cycling performance of the Li/PPU5//LFP cell at 0.2C at room temperature. (b) Charge and discharge curves of the Li/PPU5/LFP cell at 0.2C, carried out at room temperature.

However, this phenomenon is only detected during first cycles. in fact, the coulombic efficiency increases, becoming near to 100%. The cell is able to reach 300 cycles with 98% coulombic efficiency at room temperature. The capacity retention of the cell after 300 cycles is 80%, with a specific capacity of 114 mAh g^{-1}. The cell shows a very good electrochemical performance in terms of the number of cycles obtained at 0.2 C and the temperature condition in which the test is evaluated. As described in Figure 5.17 b), a significant increase in the cell overvoltage could be noted for the first 200 cycles, preserving the typical discharge and charge voltage plateau of LFP. This is mainly due to the liquid leakage of gel polymer electrolyte during charge/discharge processes. Nevertheless, even after 200 cycles and up to the 300th, the increase resulted very limited. Even if the cell loses capacity by increasing the number of cycles, the capacity loss for cycle is only 0.07 %, and the main reason could be linked to a little decomposition of electrolyte and the SEI formation. The results are mainly an improvement of gel polymer electrolytes systems, that generally work at 60 °C at lower C rates [116], [165], [166]. Post-mortem analysis of the gel polymers electrolytes was evaluated after 300th cycle. Firstly, the cell was investigated by EIS spectroscopy and the result is compared with the impedance of the same cell before cycling. As can be seen in Figure 5.18 b), no significant signs of degradation are detected after the cycling performance. Moreover, SEM analysis of PPU5 shows no signs of deterioration. This is a further evidence of good capacity characteristics of the polymer to resist during charge/discharge processes. Moreover, the surface remains as same as the one obtained by FESEM analysis, in which fresh membranes were analysed (Figure 5.6).
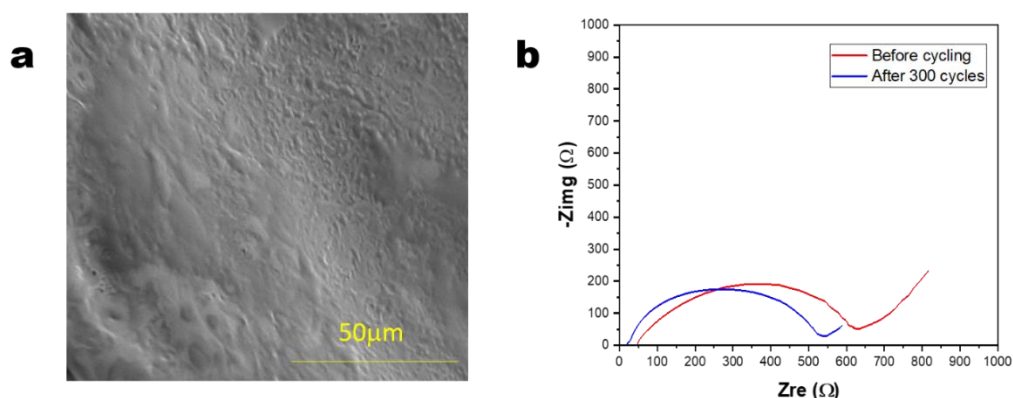
Figure 5.18: (a) SEM Analysis of PPU5 l after 300 cycles at 0.2 C rate at RT, b) Impedance of Li/PPU5/LFP cell before cycling and after 300 cycles at 0.2 C rate at RT.

To reveal self-healing properties of PPU5 inside the cell, a galvanostatic cycling test is evaluated on a complete Li/PPU5/LFP cell and compared with a cell assembled with a commercial separator (Celgard 2500).
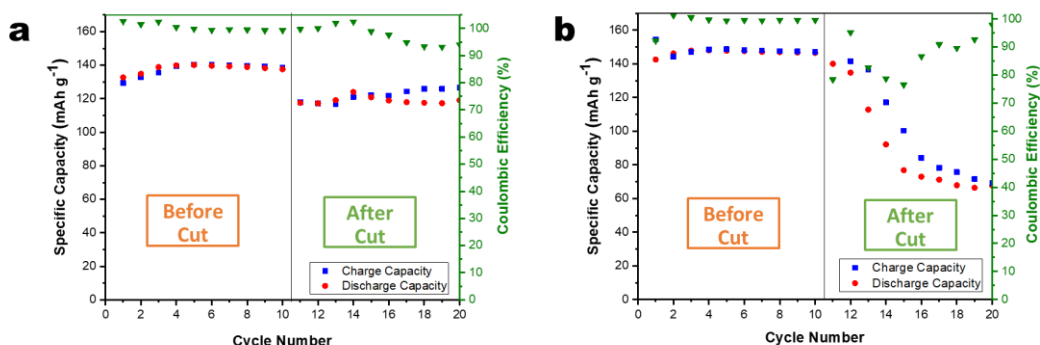
Figure 5.19: (a) Cycling performance of a Li/PPU5/LFP cell at 0.2C and room temperature before and after cutting the PPU5 membrane. (b) Cycling performance of a Li/Celgard 2500/LFP cell at 0.2C and at room temperature before and after cutting the Celgard 2500 membrane.

The cell is cycled for 10 cycles at room temperature at 0.2 C. After that, the cell is opened in inert atmosphere conditions. After damaging the polymer by a knife, the cell was re-assembled for galvanostatic cycling at 0.2 C in the same conditions (10 cycles). Before cycling, the cell was left at rest conditions in order to enable the polymer to self-repair.

During the overnight rest, the cell with GPE activates the self-healing process and restores the pristine structure. In fact, during the cycling test, the cell resumes

88

a discharge capacity of 115.0 mAh g^{-1} at the 20th cycle. Moreover, the coulombic efficiency before and after cutting is higher than 90%. FESEM analysis of the self-healed polymer has been carried out after the 20th cycle. The result is shown in Figure 5.20, in which the morphology of the membrane is quite similar to the pristine one with no signs of damages (see Figure 5.6).

On the opposite, the commercial separator loses its electrochemical performances after the damage. In fact, its specific capacity of the cell drastically collapses, with a discharge capacity of 67.0 mAh g^{-1} at 20th cycle, and the coulombic efficiency becomes unstable. The difference in the behaviour of the cells demonstrates the ability of PPU5 to self-repair even inside the cell.
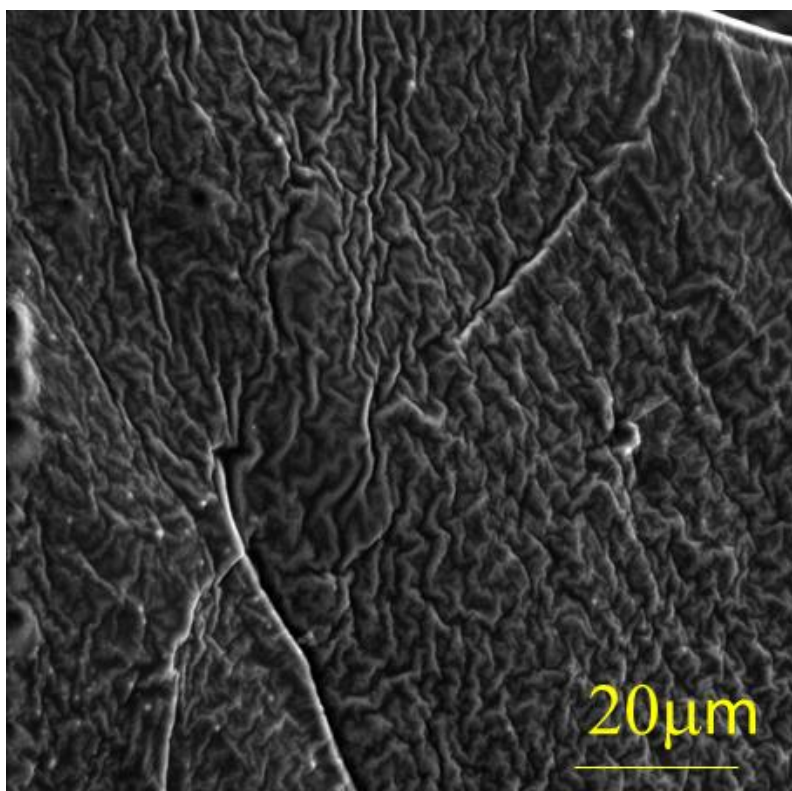
Figure 5.20: FESEM analysis of PPU5 after being cut and cycled

5.6 Conclusions

In conclusion, two different polymers have been synthesized by solvent free UV photopolymerization. The UpyMa additive is polymerized inside the PEGMEM structure, giving the PPU5 and PPU10 membranes. However, of the two membranes, PPU5 shows better interfacial stability against lithium, good electrochemical and thermal stability and electrochemical performances. Its self-healing properties have been investigated both outside and inside the electrochemical cell.

The properties of PPU5 have been compared with other self-healing GPE and/or SPE in literature for lithium metal batteries future application. The most relevant results are shown in Table 5.2.

The ionic conductivity at room temperature (1.5×10^{-3} S cm^{-1}) and lithium-ion transference number (0.62) of PPU5 are higher than other PEs proposed. Moreover, the cycling performance at room temperature, at 0.2 C for 300 cycles with a high-capacity retention of 80% is seldom reported for polymer electrolyte systems. All the tests on PPU5 showed remarkable breakthrough in the use of self-healing polymers in metal battery application.

Synthesis Conditions	GPE	Conductivity (S cm^{-1})	SH Properties	Lithium Ion transference number at RT	C rate	Number of Cycles	Capacity after cycling (mAh g^{-1})	Capacity Retention	Capacity at 1C rate in Rate Capability test (mAh g^{-1})	Refs
Photopolymerization in DMSO – 80 °C for 48 h	no (LiTFSI is added in SPE)	8.90 x 10^{-5} at RT 3.7 x 10^{-4} at 60 °C	3h at 60°C	0.22	0.1	70 at 60 °C	114	87.0% at 60°C	n.a.	[166]
RAFT polymerization in DMF for 24 h	no (LiTFSI is added in SPE)	5.62 x 10^{-6} at RT 8.07 x 10^{-5} at 60 °C	5 min at 60 °C	0.32	0.1	100 at 60 °C	138	97.5% at 60 °C	n.a.	[169]
DMF solution at 50 °C for 40 h	No (SPE without LiTFSI)	7.48 x 10^{-4} at RT 2.51 x 10^{-3} at 60 °C	24 h at RT	0.37	0.1	300 at RT	126.4	84.3% at RT	n.a.	[143]
RAFT polymerization in DMF at 70 °C for 24 h – Then at 80 °C for 24 h	yes	3.16 x 10^{-6} at RT 1.40 x 10^{-5} at 60 °C	30 min at 60 °C	0.89 (60 °C)	0.1	60 at 60 °C	129	99.7% at 60 °C	n.a.	[167]
Condensation polymerization	No (SPE without LiTFSI)	6.31 x 10^{-5} at RT 6.31 x 10^{-4} at 60 °C	60 s at ?	0.44	0.2	100 at 60 °C	120	90.0% at 60 °C	n.a. (NO Rate Capability)	[162]
Polymerization at 80 °C in ACN	no (LiTFSI is added in SPE)	1.79 x 10^{-5} at RT 1.67 x 10^{-4} at 60 °C	10 min at 60 °C 30 min at RT	0.39	0.1	50 at 60 °C	120.4	85.2% at 60 °C	n.a. (NO Rate Capability)	[152]
Polymerization in MeOH – 40 °C for 12 – Then 60°C for 24h	no (LiTFSI is added in SPE)	6.31 x 10^{-6} at RT 5.01 x 10^{-5} at 60 °C	60 min at RT	0.37 (60 °C)	0.2	100 at 60 °C	144.8	65.3% at 60 °C	40	[116]
Polymerization in EtOH – 70 °C for 24h	no (CPE)	8.01 x 10^{-5} at RT 3.98 x 10^{-4} at 60 °C	60 min at ?	0.43 (60 °C)	0.2	60 at 60 °C	139	95.9% at 60 °C	n.a. (NO Rate Capability)	[165]
RAFT polymerization in DMF at 75 °C	yes	2.93 x 10^{-5} at RT 1.78 x 10^{-4} at 60 °C	2 h at 60 °C	n.a.	0.1	120 at 60 °C	128	92.8% at 60 °C	n.a.	[168]
Without solvent UV polymerization -2h at room temperature	**yes**	**1.50 x 10^{-3} at RT 4.51 x 10^{-3} at 60 °C**	**2 h at 50° C 24 h at RT**	**0.62**	**0.2**	**300 at RT**	**113.8**	**80% at RT**	**103.6**	**Our work**

Table 5.2: Electrochemical and self-healing properties of the PPU5 membrane compared with last SH polymers in literature with the corresponding references.

Chapter 6

Conclusions and perspectives

This PhD work is based on the synthesis of gel polymer electrolytes with the capability of self-repair after being damaged. The design of different poly (ethylene glycol) methyl ether methacrylate membranes are mainly discussed and treated.

The insertion of self-healing properties inside polymeric structures is obtained using different chemical bonds. However, H-bond is the best choice for lithium metal battery, because it is considered as a closed system and H-bond interaction does not require external inputs to be activated.

Ureidopyrimidinone methacrylate (UpyMa) is an interesting molecule for self-healing task applied to gel polymer electrolyte. Its spontaneous dimerization is responsible of self-heal capability due to the formation of four hydrogen bonds. Moreover, it is easily inserted as an additive in UV polymerization through its double methacrylate bond.

Synthesis of UpyMa has been discussed in Chapter 4. UpyMa is successfully synthesized via a coupling reaction by using two low cost reactants, methyl isocytosine and 2-isocyanatoethyl methacrylate. After an extraction process, the product is characterized by using ^{1}H NMR and FTIR. The analyses demonstrate the successful synthesis of the UpyMa, with the absence of polymerization process and/or any other side reactions, and a yield of 92.3%. Moreover, the results demonstrate also the purity of the obtained product from all the reactants and the solvents used during the synthesis.

In chapter 5, UpyMa-based polymers have been synthesized and characterized. UpyMa additive is inserted inside the polymeric structure of poly (ethylene glycol)

methyl ether methacrylate through a solvent-free UV photopolymerization process. This synthesis process has low impact on environment and low production costs since organic solvents are not required. The possibility of casting the polymer directly on lithium is an advantage for possible scale-up production. Polymer with 5%w/w and 10% w/w of UpyMa are fabricated and analyzed. The insertion of UpyMa additive inside the polymeric PEGEMEM structure is confirmed by FTIR and NMR analysis.

The self-healing properties are demonstrating with SEM and optical microscope analysis. The two membranes restore their virgin conditions after being damaged in two hours at 50 °C and 24 hours at room temperature. The self-healing properties are a direct consequence of the spontaneous dimerization of UpyMa inside the polymeric structure, Interestingly, the two polymers reveal self-healing properties at the same conditions, even if the proportion of UpyMa is halved for the polymer at 5w/w%.

The aspect of UpyMa-based membranes as gel polymer electrolytes in LMBs has been evaluated. The two membranes show good results in terms of ionic conductivity and electrochemical stability. However, the poor interface stability of PPU10 avoids their applicability in future LMBs. On the other hand, PPU5 represents an ideal GPE due to its thermal and good interface stability, high lithium transference number, good rate capability at 50 °C and, more interestingly, at room temperature.

The Li/PPU5/LFP cell is able to work at 0.2 C rate at room temperature for 300 cycles, with an initial discharge capacity of 143 mAh g^{-1} and a capacity retention of 80%, and a loss of capacity of 0.07% per cycle

The self-healing properties of PPU5 inside the cell are successful demonstrated. The damaged gel polymer electrolyte is able to restore the pristine electrochemical performances of the cell at room temperature, different from commercial separator, that loses its performance after the damage. The results obtained demonstrate the successful insertion of self-healing capability inside the cell.

This work sustains the importance of self-healing gel polymer electrolytes for increasing the long-term stability in LMBs and wants to be a solid starting point for smart and safer lithium batteries use in the future.

References

[1] Z. Liu, Z. Deng, S. J. Davis, C. Giron, and P. Ciais, "Monitoring global carbon emissions in 2021," *Nature Reviews Earth and Environment*, vol. 3, no. 4. Springer Nature, pp. 217–219, Apr. 01, 2022. doi: 10.1038/s43017-022-00285-w.

[2] M. Salman, X. Long, G. Wang, and D. Zha, "Paris climate agreement and global environmental efficiency: New evidence from fuzzy regression discontinuity design," *Energy Policy*, vol. 168, Sep. 2022, doi: 10.1016/j.enpol.2022.113128.

[3] R. S. Sun, X. Gao, L. C. Deng, and C. Wang, "Is the Paris rulebook sufficient for effective implementation of Paris Agreement?," *Advances in Climate Change Research*, vol. 13, no. 4, pp. 600–611, Aug. 2022, doi: 10.1016/j.accre.2022.05.003.

[4] M. A. Hannan *et al.*, "Battery energy-storage system: A review of technologies, optimization objectives, constraints, approaches, and outstanding issues," *J Energy Storage*, vol. 42, Oct. 2021, doi: 10.1016/j.est.2021.103023.

[5] J.-M. Tarascon and M. Armand, "Issues and challenges facing rechargeable lithium batteries," 2001. [Online]. Available: www.nature.com

[6] Mauger, Julien, Paolella, Armand, and Zaghib, "Building Better Batteries in the Solid State: A Review," *Materials*, vol. 12, no. 23, p. 3892, Nov. 2019, doi: 10.3390/ma12233892.

[7]   "BATTERY-2030-Roadmap_Revision_FINAL".

[8]   J. Amici *et al.*, "A Roadmap for Transforming Research to Invent the Batteries of the Future Designed within the European Large Scale Research Initiative BATTERY 2030+," *Advanced Energy Materials*, vol. 12, no. 17. John Wiley and Sons Inc, May 01, 2022. doi: 10.1002/aenm.202102785.

[9]   R. Narayan, C. Laberty-Robert, J. Pelta, J. M. Tarascon, and R. Dominko, "Self-Healing: An Emerging Technology for Next-Generation Smart Batteries," *Advanced Energy Materials*, vol. 12, no. 17. John Wiley and Sons Inc, May 01, 2022. doi: 10.1002/aenm.202102652.

[10]   S. Wang and M. W. Urban, "Self-healing polymers," *Nature Reviews Materials*, vol. 5, no. 8. Nature Research, pp. 562–583, Aug. 01, 2020. doi: 10.1038/s41578-020-0202-4.

[11]   M. v. Reddy, A. Mauger, C. M. Julien, A. Paolella, and K. Zaghib, "Brief history of early lithium-battery development," *Materials*, vol. 13, no. 8, Apr. 2020, doi: 10.3390/MA13081884.

[12]   C. L. Heth, "Energy on demand: A brief history of the development of the battery," *An International Journal of the History of Chemistry*, vol. 3, no. 2, pp. 73–82, 2019, doi: 10.13128/Substantia-280.

[13]   M. Weiss *et al.*, "Fast Charging of Lithium-Ion Batteries: A Review of Materials Aspects," *Advanced Energy Materials*, vol. 11, no. 33. John Wiley and Sons Inc, Sep. 01, 2021. doi: 10.1002/aenm.202101126.

[14]   E. Mossali, N. Picone, L. Gentilini, O. Rodrìguez, J. M. Pérez, and M. Colledani, "Lithium-ion batteries towards circular economy: A literature review of opportunities and issues of recycling treatments," *J Environ Manage*, vol. 264, Jun. 2020, doi: 10.1016/j.jenvman.2020.110500.

[15]   Q. Wang *et al.*, "Confronting the Challenges in Lithium Anodes for Lithium Metal Batteries," *Advanced Science*, vol. 8, no. 17. John Wiley and Sons Inc, Sep. 01, 2021. doi: 10.1002/advs.202101111.

[16]   K. Xu, "Nonaqueous Liquid Electrolytes for Lithium-Based Rechargeable Batteries," *ChemInform*, vol. 35, no. 50, Dec. 2004, doi: 10.1002/chin.200450271.

[17]   F. F. C. Bazito and R. M. Torresi, "Cathodes for lithium ion batteries: The benefits of using nanostructured materials," *Journal of the Brazilian Chemical Society*, vol. 17, no. 4. Sociedade Brasileira de Quimica, pp. 627–642, 2006. doi: 10.1590/S0103-50532006000400002.

[18]   J. C. Garcia *et al.*, "Surface Structure, Morphology, and Stability of Li(Ni1/3Mn1/3Co1/3)O2 Cathode Material," *Journal of Physical Chemistry C*, vol. 121, no. 15, pp. 8290–8299, Apr. 2017, doi: 10.1021/acs.jpcc.7b00896.

[19]   H. J. Noh, S. Youn, C. S. Yoon, and Y. K. Sun, "Comparison of the structural and electrochemical properties of layered Li[NixCoyMnz]O2 (x = 1/3, 0.5, 0.6, 0.7, 0.8 and 0.85) cathode material for lithium-ion batteries," *J Power Sources*, vol. 233, pp. 121–130, 2013, doi: 10.1016/j.jpowsour.2013.01.063.

[20]   Y. Mekonnen, A. Sundararajan, and A. I. Sarwat, "A review of cathode and anode materials for lithium-ion batteries," in *Conference Proceedings - IEEE SOUTHEASTCON*, Institute of Electrical and Electronics Engineers Inc., Jul. 2016. doi: 10.1109/SECON.2016.7506639.

[21]   N. Nitta, F. Wu, J. T. Lee, and G. Yushin, "Li-ion battery materials: Present and future," *Materials Today*, vol. 18, no. 5. Elsevier B.V., pp. 252–264, Jun. 01, 2015. doi: 10.1016/j.mattod.2014.10.040.

[22]   M. Armand *et al.*, "Lithium-ion batteries – Current state of the art and anticipated developments," *J Power Sources*, vol. 479, Dec. 2020, doi: 10.1016/j.jpowsour.2020.228708.

[23]   H. Yu, Y. Jin, G. D. Zhan, and X. Liang, "Solvent-Free Solid-State Lithium Battery Based on LiFePO4and MWCNT/PEO/PVDF-HFP for High-Temperature Applications," *ACS Omega*, vol. 6, no. 43, pp. 29060–29070, Nov. 2021, doi: 10.1021/acsomega.1c04275.

[24]   H. Zhang, Y. Yang, D. Ren, L. Wang, and X. He, "Graphite as anode materials: Fundamental mechanism, recent progress and advances," *Energy Storage Materials*, vol. 36. Elsevier B.V., pp. 147–170, Apr. 01, 2021. doi: 10.1016/j.ensm.2020.12.027.

[25] S. K. Heiskanen, J. Kim, and B. L. Lucht, "Generation and Evolution of the Solid Electrolyte Interphase of Lithium-Ion Batteries," *Joule*, vol. 3, no. 10. Cell Press, pp. 2322–2333, Oct. 16, 2019. doi: 10.1016/j.joule.2019.08.018.

[26] M. T. McDowell, S. W. Lee, W. D. Nix, and Y. Cui, "25th anniversary article: Understanding the lithiation of silicon and other alloying anodes for lithium-ion batteries," *Advanced Materials*, vol. 25, no. 36. pp. 4966–4985, Sep. 2013. doi: 10.1002/adma.201301795.

[27] M. N. Obrovac and V. L. Chevrier, "Alloy negative electrodes for Li-ion batteries," *Chemical Reviews*, vol. 114, no. 23. American Chemical Society, pp. 11444–11502, Dec. 10, 2014. doi: 10.1021/cr500207g.

[28] S. Paul, M. A. Rahman, S. bin Sharif, J. H. Kim, S. E. T. Siddiqui, and M. A. M. Hossain, "TiO2 as an Anode of High-Performance Lithium-Ion Batteries: A Comprehensive Review towards Practical Application," *Nanomaterials*, vol. 12, no. 12. MDPI, Jun. 01, 2022. doi: 10.3390/nano12122034.

[29] A. Varzi *et al.*, "Current status and future perspectives of lithium metal batteries," *J Power Sources*, vol. 480, Dec. 2020, doi: 10.1016/j.jpowsour.2020.228803.

[30] S. Goriparti, E. Miele, F. de Angelis, E. di Fabrizio, R. Proietti Zaccaria, and C. Capiglia, "Review on recent progress of nanostructured anode materials for Li-ion batteries," *Journal of Power Sources*, vol. 257. Elsevier B.V., pp. 421–443, Jul. 01, 2014. doi: 10.1016/j.jpowsour.2013.11.103.

[31] K. Xu, "Electrolytes and interphases in Li-ion batteries and beyond," *Chemical Reviews*, vol. 114, no. 23. American Chemical Society, pp. 11503–11618, Dec. 10, 2014. doi: 10.1021/cr500003w.

[32] V. I. Volkov *et al.*, "Polymer Electrolytes for Lithium-Ion Batteries Studied by NMR Techniques," *Membranes*, vol. 12, no. 4. MDPI, Apr. 01, 2022. doi: 10.3390/membranes12040416.

[33] F. Schipper and D. Aurbach, "A brief review: Past, present and future of lithium ion batteries," *Russian Journal of Electrochemistry*, vol. 52, no. 12, pp. 1095–1121, Dec. 2016, doi: 10.1134/S1023193516120120.

[34] S. J. Lee *et al.*, " Effect of Lithium Bis(oxalato)borate Additive on Electrochemical Performance of Li 1.17 Ni 0.17 Mn 0.5 Co 0.17 O 2 Cathodes for Lithium-Ion Batteries ," *J Electrochem Soc*, vol. 161, no. 14, pp. A2012–A2019, 2014, doi: 10.1149/2.0211414jes.

[35] J. R. Nair *et al.*, "Room temperature ionic liquid (RTIL)-based electrolyte cocktails for safe, high working potential Li-based polymer batteries," *J Power Sources*, vol. 412, pp. 398–407, Feb. 2019, doi: 10.1016/j.jpowsour.2018.11.061.

[36] M. Armand, F. Endres, D. R. MacFarlane, H. Ohno, and B. Scrosati, "Ionic-liquid materials for the electrochemical challenges of the future," *Nature Materials*, vol. 8, no. 8. Nature Publishing Group, pp. 621–629, 2009. doi: 10.1038/nmat2448.

[37] K. Liu, Z. Wang, L. Shi, S. Jungsuttiwong, and S. Yuan, "Ionic liquids for high performance lithium metal batteries," *Journal of Energy Chemistry*, vol. 59. Elsevier B.V., pp. 320–333, Aug. 01, 2021. doi: 10.1016/j.jechem.2020.11.017.

[38] M. Armand, F. Endres, D. R. MacFarlane, H. Ohno, and B. Scrosati, "Ionic-liquid materials for the electrochemical challenges of the future," *Nature Materials*, vol. 8, no. 8. Nature Publishing Group, pp. 621–629, 2009. doi: 10.1038/nmat2448.

[39] H. Qi *et al.*, "High-Voltage Resistant Ionic Liquids for Lithium-Ion Batteries," *ACS Appl Mater Interfaces*, vol. 12, no. 1, pp. 591–600, Jan. 2020, doi: 10.1021/acsami.9b16786.

[40] M. Safa, A. Chamaani, N. Chawla, and B. El-Zahab, "Polymeric Ionic Liquid Gel Electrolyte for Room Temperature Lithium Battery Applications," *Electrochim Acta*, vol. 213, pp. 587–593, Sep. 2016, doi: 10.1016/j.electacta.2016.07.118.

[41] S. Böhme, M. Kerner, J. Scheers, P. Johansson, K. Edström, and L. Nyholm, " Elevated Temperature Lithium-Ion Batteries Containing SnO 2 Electrodes and LiTFSI-Pip 14 TFSI Ionic Liquid Electrolyte ," *J Electrochem Soc*, vol. 164, no. 4, pp. A701–A708, 2017, doi: 10.1149/2.0861704jes.

[42]   B. Scrosati, J. Hassoun, and Y. K. Sun, "Lithium-ion batteries. A look into the future," *Energy and Environmental Science*, vol. 4, no. 9. pp. 3287–3295, Sep. 2011. doi: 10.1039/c1ee01388b.

[43]   J. Lang, L. Qi, Y. Luo, and H. Wu, "High performance lithium metal anode: Progress and prospects," *Energy Storage Materials*, vol. 7. Elsevier B.V., pp. 115–129, Apr. 01, 2017. doi: 10.1016/j.ensm.2017.01.006.

[44]   T. Chen *et al.*, "Ionic liquid-immobilized polymer gel electrolyte with self-healing capability, high ionic conductivity and heat resistance for dendrite-free lithium metal batteries," *Nano Energy*, vol. 54, pp. 17–25, Dec. 2018, doi: 10.1016/j.nanoen.2018.09.059.

[45]   W. Z. Huang *et al.*, "Anode-Free Solid-State Lithium Batteries: A Review," *Advanced Energy Materials*, vol. 12, no. 26. John Wiley and Sons Inc, Jul. 01, 2022. doi: 10.1002/aenm.202201044.

[46]   S. Hein, T. Danner, and A. Latz, "An Electrochemical Model of Lithium Plating and Stripping in Lithium Ion Batteries," *ACS Appl Energy Mater*, vol. 3, no. 9, pp. 8519–8531, Sep. 2020, doi: 10.1021/acsaem.0c01155.

[47]   Q. Wang *et al.*, "Confronting the Challenges in Lithium Anodes for Lithium Metal Batteries," *Advanced Science*, vol. 8, no. 17. John Wiley and Sons Inc, Sep. 01, 2021. doi: 10.1002/advs.202101111.

[48]   M. L. Meyerson *et al.*, "The effect of local lithium surface chemistry and topography on solid electrolyte interphase composition and dendrite nucleation," *J Mater Chem A Mater*, vol. 7, no. 24, pp. 14882–14894, 2019, doi: 10.1039/c9ta03371h.

[49]   J. F. Ding *et al.*, "Review on lithium metal anodes towards high energy density batteries," *Green Energy and Environment*. KeAi Publishing Communications Ltd., 2022. doi: 10.1016/j.gee.2022.08.002.

[50]   A. Jana and R. E. García, "Lithium dendrite growth mechanisms in liquid electrolytes," *Nano Energy*, vol. 41, pp. 552–565, Nov. 2017, doi: 10.1016/j.nanoen.2017.08.056.

[51]   G. Wrang, "DENDRITES AND GROWTH LAYERS IN THE ELECTROCRYSTALLIZAT1ON OF METALS*," Pergamon Press Ltd, 1960.

[52] H. Yang *et al.*, "Recent progress and perspective on lithium metal anode protection," *Energy Storage Materials*, vol. 14. Elsevier B.V., pp. 199–221, Sep. 01, 2018. doi: 10.1016/j.ensm.2018.03.001.

[53] L. Wang *et al.*, "Engineering of lithium-metal anodes towards a safe and stable battery," *Energy Storage Materials*, vol. 14. Elsevier B.V., pp. 22–48, Sep. 01, 2018. doi: 10.1016/j.ensm.2018.02.014.

[54] A. Hagopian, M. L. Doublet, and J. S. Filhol, "Thermodynamic origin of dendrite growth in metal anode batteries," *Energy Environ Sci*, vol. 13, no. 12, pp. 5186–5197, Dec. 2020, doi: 10.1039/d0ee02665d.

[55] M. K. Aslam *et al.*, "How to avoid dendrite formation in metal batteries: Innovative strategies for dendrite suppression," *Nano Energy*, vol. 86. Elsevier Ltd, Aug. 01, 2021. doi: 10.1016/j.nanoen.2021.106142.

[56] D. Rehnlund *et al.*, "Lithium trapping in alloy forming electrodes and current collectors for lithium based batteries," *Energy Environ Sci*, vol. 10, no. 6, pp. 1350–1357, Jun. 2017, doi: 10.1039/c7ee00244k.

[57] S. Jin *et al.*, "Solid-Solution-Based Metal Alloy Phase for Highly Reversible Lithium Metal Anode," *J Am Chem Soc*, vol. 142, no. 19, pp. 8818–8826, May 2020, doi: 10.1021/jacs.0c01811.

[58] E. Paled, "The Electrochemical Behavior of Alkali and Alkaline Earth Metals in Nonaqueous Battery Systems-The Solid Electrolyte Interphase Model."

[59] X. Wu *et al.*, "Electrolyte for lithium protection: From liquid to solid," *Green Energy and Environment*, vol. 4, no. 4. KeAi Publishing Communications Ltd., pp. 360–374, Oct. 01, 2019. doi: 10.1016/j.gee.2019.05.003.

[60] C. Li *et al.*, "An advance review of solid-state battery: Challenges, progress and prospects," *Sustainable Materials and Technologies*, vol. 29. Elsevier B.V., Sep. 01, 2021. doi: 10.1016/j.susmat.2021.e00297.

[61] W. Ren, C. Ding, X. Fu, and Y. Huang, "Advanced gel polymer electrolytes for safe and durable lithium metal batteries: Challenges, strategies, and perspectives," *Energy Storage Materials*, vol. 34. Elsevier B.V., pp. 515–535, Jan. 01, 2021. doi: 10.1016/j.ensm.2020.10.018.

[62] X. Zhang, J. C. Daigle, and K. Zaghib, "Comprehensive review of polymer architecture for all-solid-state lithium rechargeable batteries," *Materials*, vol. 13, no. 11. MDPI AG, Jun. 01, 2020. doi: 10.3390/ma13112488.

[63] Z. Xue, D. He, and X. Xie, "Poly(ethylene oxide)-based electrolytes for lithium-ion batteries," *Journal of Materials Chemistry A*, vol. 3, no. 38. Royal Society of Chemistry, pp. 19218–19253, Jul. 17, 2015. doi: 10.1039/c5ta03471j.

[64] A. Varzi, R. Raccichini, S. Passerini, and B. Scrosati, "Challenges and prospects of the role of solid electrolytes in the revitalization of lithium metal batteries," *J Mater Chem A Mater*, vol. 4, no. 44, pp. 17251–17259, 2016, doi: 10.1039/c6ta07384k.

[65] M. Yang and J. Hou, "Membranes in lithium ion batterie," *Membranes*, vol. 2, no. 3. MDPI AG, pp. 367–383, 2012. doi: 10.3390/membranes2030367.

[66] K. Sashmitha and M. U. Rani, "A comprehensive review of polymer electrolyte for lithium-ion battery," *Polymer Bulletin*. Springer Science and Business Media Deutschland GmbH, 2022. doi: 10.1007/s00289-021-04008-x.

[67] J. Liu, W. Li, X. Zuo, S. Liu, and Z. Li, "Polyethylene-supported polyvinylidene fluoride-cellulose acetate butyrate blended polymer electrolyte for lithium ion battery," *J Power Sources*, vol. 226, pp. 101–106, Mar. 2013, doi: 10.1016/j.jpowsour.2012.10.078.

[68] R. Dallaev, T. Pisarenko, D. Sobola, F. Orudzhev, S. Ramazanov, and T. Trčka, "Brief Review of PVDF Properties and Applications Potential," *Polymers (Basel)*, vol. 14, no. 22, p. 4793, Nov. 2022, doi: 10.3390/polym14224793.

[69] H. Zhang, X. Ma, C. Lin, and B. Zhu, "Gel polymer electrolyte-based on PVDF/fluorinated amphiphilic copolymer blends for high performance lithium-ion batteries," *RSC Adv*, vol. 4, no. 64, pp. 33713–33719, 2014, doi: 10.1039/c4ra04443f.

[70] X. Zhang *et al.*, "Self-Suppression of Lithium Dendrite in All-Solid-State Lithium Metal Batteries with Poly(vinylidene difluoride)-Based Solid

Electrolytes," *Advanced Materials*, vol. 31, no. 11, Mar. 2019, doi: 10.1002/adma.201806082.

[71] D. Saikia and A. Kumar, "Ionic conduction in P(VDF-HFP)/PVDF-(PC + DEC)-LiClO4 polymer gel electrolytes," *Electrochim Acta*, vol. 49, no. 16, pp. 2581–2589, Jul. 2004, doi: 10.1016/j.electacta.2004.01.029.

[72] K. Luo *et al.*, "PVDF-HFP-modified gel polymer electrolyte for the stable cycling lithium metal batteries," *Journal of Electroanalytical Chemistry*, vol. 895, Aug. 2021, doi: 10.1016/j.jelechem.2021.115462.

[73] X. Yu and A. Manthiram, "A Review of Composite Polymer-Ceramic Electrolytes for Lithium Batteries," 2020.

[74] S. Li *et al.*, "Building more secure LMBs with gel polymer electrolytes based on dual matrices of PAN and HPMC by improving compatibility with anode and tuning lithium ion transference," *Electrochim Acta*, vol. 391, Sep. 2021, doi: 10.1016/j.electacta.2021.138950.

[75] L. Tan, Y. Deng, Q. Cao, B. Jing, X. Wang, and Y. Liu, "Gel electrolytes based on polyacrylonitrile/thermoplastic polyurethane/polystyrene for lithium-ion batteries," *Ionics (Kiel)*, vol. 25, no. 8, pp. 3673–3682, Aug. 2019, doi: 10.1007/s11581-019-02940-7.

[76] G. Dautzenberg, F. Croce, S. Passerini, and B. Scrosati, "Characterization of Pan-Based Gel Electrolytes. Electrochemical Stability and Lithium Cyclability," 1994. [Online]. Available: https://pubs.acs.org/sharingguidelines

[77] P. L. Kuo, C. A. Wu, C. Y. Lu, C. H. Tsao, C. H. Hsu, and S. S. Hou, "High performance of transferring lithium ion for polyacrylonitrile-interpenetrating crosslinked polyoxyethylene network as gel polymer electrolyte," *ACS Appl Mater Interfaces*, vol. 6, no. 5, pp. 3156–3162, Mar. 2014, doi: 10.1021/am404248b.

[78] S. H. Wang, P. L. Kuo, C. te Hsieh, and H. Teng, "Design of poly(acrylonitrile)-based gel electrolytes for high-performance lithium ion batteries," *ACS Appl Mater Interfaces*, vol. 6, no. 21, pp. 19360–19370, Nov. 2014, doi: 10.1021/am505448a.

[79] H. K. Tran *et al.*, "Composite polymer electrolytes based on PVA/PAN for all-solid-state lithium metal batteries operated at room temperature," *ACS Appl Energy Mater*, vol. 3, no. 11, pp. 11024–11035, Nov. 2020, doi: 10.1021/acsaem.0c02018.

[80] M. Jahn, M. Sedlaříková, J. Vondrák, and L. Pařízek, "PMMA-Based Electrolytes for Li-Ion Batteries," *ECS Trans*, vol. 74, no. 1, pp. 159–164, Dec. 2016, doi: 10.1149/07401.0159ecst.

[81] A. M. Stephan, "Review on gel polymer electrolytes for lithium batteries," *European Polymer Journal*, vol. 42, no. 1. pp. 21–42, Jan. 2006. doi: 10.1016/j.eurpolymj.2005.09.017.

[82] P. Isken, M. Winter, S. Passerini, and A. Lex-Balducci, "Methacrylate based gel polymer electrolyte for lithium-ion batteries," *J Power Sources*, vol. 225, pp. 157–162, Mar. 2013, doi: 10.1016/j.jpowsour.2012.09.098.

[83] F. A. Latif *et al.*, "Review of poly (methyl methacrylate) based polymer electrolytes in solid-state supercapacitors," *Int J Electrochem Sci*, vol. 17, 2022, doi: 10.20964/2022.01.44.

[84] M. Liu *et al.*, "A new composite gel polymer electrolyte based on matrix of PEGDA with high ionic conductivity for lithium-ion batteries," *Electrochim Acta*, vol. 354, Sep. 2020, doi: 10.1016/j.electacta.2020.136622.

[85] Z. Wei *et al.*, "A large-size, bipolar-stacked and high-safety solid-state lithium battery with integrated electrolyte and cathode," *J Power Sources*, vol. 394, pp. 57–66, Aug. 2018, doi: 10.1016/j.jpowsour.2018.05.044.

[86] J. R. M. Giles, F. M. Gray, J. R. Maccallum, and C. A. Vincent, "Synthesis and characterization of ABA block copolymer-based polymer electrolytes," 1987.

[87] X. Liu, X. Xin, L. Shen, Z. Gu, J. Wu, and X. Yao, "Poly(methyl methacrylate)-Based Gel Polymer Electrolyte for High-Performance Solid State Li-O2Battery with Enhanced Cycling Stability," *ACS Appl Energy Mater*, vol. 4, no. 4, pp. 3975–3982, Apr. 2021, doi: 10.1021/acsaem.1c00344.

[88] P. Yao *et al.*, "Review on Polymer-Based Composite Electrolytes for Lithium Batteries," *Frontiers in Chemistry*, vol. 7. Frontiers Media S.A., Aug. 08, 2019. doi: 10.3389/fchem.2019.00522.

[89] J. C. Barbosa, R. Gonçalves, C. M. Costa, and S. Lanceros-Méndez, "Toward Sustainable Solid Polymer Electrolytes for Lithium-Ion Batteries," *ACS Omega*, vol. 7, no. 17. American Chemical Society, pp. 14457–14464, May 03, 2022. doi: 10.1021/acsomega.2c01926.

[90] S. Li *et al.*, "Progress and Perspective of Ceramic/Polymer Composite Solid Electrolytes for Lithium Batteries," *Advanced Science*, vol. 7, no. 5. John Wiley and Sons Inc., Mar. 01, 2020. doi: 10.1002/advs.201903088.

[91] A. Varzi, R. Raccichini, S. Passerini, and B. Scrosati, "Challenges and prospects of the role of solid electrolytes in the revitalization of lithium metal batteries," *J Mater Chem A Mater*, vol. 4, no. 44, pp. 17251–17259, 2016, doi: 10.1039/c6ta07384k.

[92] J. E. Weston and B. C. H. Steele, "EFFECTS OF INERT FILLERS ON THE MECHANICAL AND ELECTROCHEMICAL PROPERTIES OF LITHIUM SALT-POLY (ETHYLENE OXIDE) POLYMER ELECTROLYTES," 1982.

[93] P. Yao *et al.*, "Review on Polymer-Based Composite Electrolytes for Lithium Batteries," *Frontiers in Chemistry*, vol. 7. Frontiers Media S.A., Aug. 08, 2019. doi: 10.3389/fchem.2019.00522.

[94] Y. G. Cho, C. Hwang, D. S. Cheong, Y. S. Kim, and H. K. Song, "Gel/Solid Polymer Electrolytes Characterized by In Situ Gelation or Polymerization for Electrochemical Energy Systems," *Advanced Materials*, vol. 31, no. 20. Wiley-VCH Verlag, May 17, 2019. doi: 10.1002/adma.201804909.

[95] A. Arya and A. L. Sharma, "Insights into the use of polyethylene oxide in energy storage/conversion devices: A critical review."

[96] M. S. M. Misenan, A. S. A. Khiar, and T. Eren, "Polyurethane-based polymer electrolyte for lithium ion batteries: a review," *Polymer International*, vol. 71, no. 7. John Wiley and Sons Ltd, pp. 751–769, Jul. 01, 2022. doi: 10.1002/pi.6395.

[97] A. du Pasquier, P. C. Warren, D. Culver, A. S. Gozdz, G. G. Amatucci, and J.-M. Tarascon, "Plastic PVDF-HFP electrolyte laminates prepared by a phase-inversion process," 2000. [Online]. Available: www.elsevier.com/locate/ssi

[98] K. S. Ngai, S. Ramesh, K. Ramesh, and J. C. Juan, "A review of polymer electrolytes: fundamental, approaches and applications," *Ionics*, vol. 22, no. 8. Institute for Ionics, pp. 1259–1279, Aug. 01, 2016. doi: 10.1007/s11581-016-1756-4.

[99] F. Baskoro, H. Q. Wong, and H. J. Yen, "Strategic Structural Design of a Gel Polymer Electrolyte toward a High Efficiency Lithium-Ion Battery," *ACS Applied Energy Materials*, vol. 2, no. 6. American Chemical Society, pp. 3937–3971, Jun. 24, 2019. doi: 10.1021/acsaem.9b00295.

[100] C. Y. Hsu, R. J. Liu, C. H. Hsu, and P. L. Kuo, "High thermal and electrochemical stability of PVDF-graft-PAN copolymer hybrid PEO membrane for safety reinforced lithium-ion battery," *RSC Adv*, vol. 6, no. 22, pp. 18082–18088, 2016, doi: 10.1039/c5ra26345j.

[101] I. Kim *et al.*, "Cross-linked poly(vinylidene fluoride-cohexafluoropropene) (PVDF-co-HFP) gel polymer electrolyte for flexible li-ion battery integrated with organic light emitting diode (OLED)," *Materials*, vol. 11, no. 4, Apr. 2018, doi: 10.3390/ma11040543.

[102] V. P. H. Huy, S. So, and J. Hur, "Inorganic fillers in composite gel polymer electrolytes for high-performance lithium and non-lithium polymer batteries," *Nanomaterials*, vol. 11, no. 3. MDPI AG, pp. 1–40, Mar. 01, 2021. doi: 10.3390/nano11030614.

[103] J. Vohlidal, "Polymer degradation: A short review," *Chemistry Teacher International*, vol. 3, no. 2. Walter de Gruyter GmbH, pp. 213–220, Jun. 01, 2021. doi: 10.1515/cti-2020-0015.

[104] Y. Yao, M. Xiao, and W. Liu, "A Short Review on Self-Healing Thermoplastic Polyurethanes," *Macromolecular Chemistry and Physics*, vol. 222, no. 8. John Wiley and Sons Inc, Apr. 01, 2021. doi: 10.1002/macp.202100002.

[105] S. Aiswarya, P. Awasthi, and S. Shankar Banerjee, "Self-Healing Thermoplastic Elastomeric Materials: Challenges, Opportunities and New Approaches," *Eur Polym J*, p. 111658, Oct. 2022, doi: 10.1016/j.eurpolymj.2022.111658.

[106] K. R. Reddy, A. El-Zein, D. W. Airey, F. Alonso-Marroquin, P. Schubel, and A. Manalo, "Self-healing polymers: Synthesis methods and applications," *Nano-Structures and Nano-Objects*, vol. 23. Elsevier B.V., Jul. 01, 2020. doi: 10.1016/j.nanoso.2020.100500.

[107] M. Diba *et al.*, "Self-Healing Biomaterials: From Molecular Concepts to Clinical Applications," *Adv Mater Interfaces*, vol. 5, no. 17, Sep. 2018, doi: 10.1002/admi.201800118.

[108] Y. Cheng, C. Wang, F. Kang, and Y.-B. He, "Self-Healable Lithium-Ion Batteries: A Review," *Nanomaterials*, vol. 12, no. 20, p. 3656, Oct. 2022, doi: 10.3390/nano12203656.

[109] G. Bauer and T. Speck, "Restoration of tensile strength in bark samples of Ficus benjamina due to coagulation of latex during fast self-healing of fissures," *Ann Bot*, vol. 109, no. 4, pp. 807–811, Mar. 2012, doi: 10.1093/aob/mcr307.

[110] L. Mezzomo *et al.*, "Exploiting Self-Healing in Lithium Batteries: Strategies for Next-Generation Energy Storage Devices," *Advanced Energy Materials*, vol. 10, no. 46. Wiley-VCH Verlag, Dec. 01, 2020. doi: 10.1002/aenm.202002815.

[111] R. P. Wool, "Self-healing materials: A review," *Soft Matter*, vol. 4, no. 3, pp. 400–418, 2008, doi: 10.1039/b711716g.

[112] S. Zhang, N. van Dijk, and S. van der Zwaag, "A Review of Self-healing Metals: Fundamentals, Design Principles and Performance," *Acta Metallurgica Sinica (English Letters)*, vol. 33, no. 9. Chinese Society for Metals, pp. 1167–1179, Sep. 01, 2020. doi: 10.1007/s40195-020-01102-3.

[113] K. Ando, K. Takahashi, and T. Osada, "Structural ceramics with self-healing properties," in *Handbook of Smart Coatings for Materials Protection*, Elsevier Inc., 2014, pp. 586–605. doi: 10.1533/9780857096883.3.586.

[114] X. Feng and G. Li, "Room-Temperature Self-Healable and Mechanically Robust Thermoset Polymers for Healing Delamination and Recycling Carbon Fibers," *ACS Appl Mater Interfaces*, vol. 13, no. 44, pp. 53099–53110, Nov. 2021, doi: 10.1021/acsami.1c16105.

[115] J. C. Cremaldi and B. Bhushan, "Bioinspired self-healing materials: Lessons from nature," *Beilstein Journal of Nanotechnology*, vol. 9, no. 1. Beilstein-Institut Zur Forderung der Chemischen Wissenschaften, pp. 907–935, 2018. doi: 10.3762/bjnano.9.85.

[116] C. Wang *et al.*, "Highly stretchable, non-flammable and notch-insensitive intrinsic self-healing solid-state polymer electrolyte for stable and safe flexible lithium batteries," *J Mater Chem A Mater*, vol. 9, no. 8, pp. 4758–4769, Feb. 2021, doi: 10.1039/d0ta10745j.

[117] C. E. Diesendruck, N. R. Sottos, J. S. Moore, and S. R. White, "Biomimetische Selbstheilung," *Angewandte Chemie*, vol. 127, no. 36, pp. 10572–10593, Sep. 2015, doi: 10.1002/ange.201500484.

[118] L. Rittié, "Cellular mechanisms of skin repair in humans and other mammals," *Journal of Cell Communication and Signaling*, vol. 10, no. 2. Springer Netherlands, pp. 103–120, Jun. 01, 2016. doi: 10.1007/s12079-016-0330-1.

[119] N. Mackman, R. E. Tilley, and N. S. Key, "Role of the extrinsic pathway of blood coagulation in hemostasis and thrombosis," *Arteriosclerosis, Thrombosis, and Vascular Biology*, vol. 27, no. 8. pp. 1687–1693, Aug. 2007. doi: 10.1161/ATVBAHA.107.141911.

[120] E. H. Lee, J. Hsin, O. Mayans, and K. Schulten, "Secondary and tertiary structure elasticity of titin Z1Z2 and a titin chain model," *Biophys J*, vol. 93, no. 5, pp. 1719–1735, 2007, doi: 10.1529/biophysj.107.105528.

[121] B. Willocq, J. Odent, P. Dubois, and J. M. Raquez, "Advances in intrinsic self-healing polyurethanes and related composites," *RSC Advances*, vol. 10, no. 23. Royal Society of Chemistry, pp. 13766–13782, Apr. 05, 2020. doi: 10.1039/d0ra01394c.

[122] R. P. Wool and K. M. O'Connor, "A theory of crack healing in polymers," *J Appl Phys*, vol. 52, no. 10, pp. 5953–5963, 1981, doi: 10.1063/1.328526.

[123] M. O. H. Cioffi, A. S. C. Bomfim, V. Ambrogi, and S. G. Advani, "A review on self-healing polymers and polymer composites for structural applications," *Polymer Composites*. John Wiley and Sons Inc, 2022. doi: 10.1002/pc.26887.

[124] M. Schunack, M. Gragert, D. Döhler, P. Michael, and W. H. Binder, "Low-temperature Cu(I)-catalyzed 'click' reactions for self-healing polymers," *Macromol Chem Phys*, vol. 213, no. 2, pp. 205–214, Jan. 2012, doi: 10.1002/macp.201100377.

[125] H.-P. Wang and Y.-Q. Zhu, "Self-healing Epoxy with Epoxy-amine Dual-capsule Healing System," 2017.

[126] B. Aïssa, D. Therriault, E. Haddad, and W. Jamroz, "Self-healing materials systems: Overview of major approaches and recent developed technologies," *Advances in Materials Science and Engineering*, vol. 2012. 2012. doi: 10.1155/2012/854203.

[127] S. R. Madara, N. S. Sarath Raj, and C. P. Selvan, "Review of research and developments in self healing composite materials," in *IOP Conference Series: Materials Science and Engineering*, Institute of Physics Publishing, May 2018. doi: 10.1088/1757-899X/346/1/012011.

[128] S. R. White, B. J. Blaiszik, S. L. B. Kramer, S. C. Olugebefola, J. S. Moore, and N. R. Sottos, "Self-healing Polymers and Composites: Capsules, circulatory systems and chemistry allow materials to fix themselves." [Online]. Available: https://about.jstor.org/terms

[129] T. Yin, L. Zhou, M. Z. Rong, and M. Q. Zhang, "Self-healing woven glass fabric/epoxy composites with the healant consisting of micro-encapsulated epoxy and latent curing agent," *Smart Mater Struct*, vol. 17, no. 1, Feb. 2008, doi: 10.1088/0964-1726/17/01/015019.

[130] G. Romero-Sabat *et al.*, "Development of a highly efficient extrinsic and autonomous self-healing polymeric system at low and ultra-low temperatures for high-performance applications," *Compos Part A Appl Sci Manuf*, vol. 145, Jun. 2021, doi: 10.1016/j.compositesa.2021.106335.

[131] A. Wolfel, C. Inés, A. Igarzabal, and M. R. Romero, "Imine based self-healing hydrogel triggered by periodate."

[132] S. Burattini, H. M. Colquhoun, B. W. Greenland, and W. Hayes, "A novel self-healing supramolecular polymer system," *Faraday Discuss*, vol. 143, pp. 251–264, 2009, doi: 10.1039/b900859d.

[133] Y. Chujo, K. Sada, and T. Saegusa, "Reversible Gelation of Polyoxazoline by Means of Diels-Alder Reaction1," Wiley, 1990. [Online]. Available: https://pubs.acs.org/sharingguidelines

[134] C. Jiang *et al.*, "Self-healing polyurethane-elastomer with mechanical tunability for multiple biomedical applications in vivo," *Nat Commun*, vol. 12, no. 1, Dec. 2021, doi: 10.1038/s41467-021-24680-x.

[135] T. Park, S. C. Zimmerman, and S. Nakashima, "A highly stable quadruply hydrogen-bonded heterocomplex useful for supramolecular polymer blends," *J Am Chem Soc*, vol. 127, no. 18, pp. 6520–6521, May 2005, doi: 10.1021/ja050996j.

[136] Y. Cheng, X. Xiao, K. Pan, and H. Pang, "Development and application of self-healing materials in smart batteries and supercapacitors," *Chemical Engineering Journal*, vol. 380. Elsevier B.V., Jan. 15, 2020. doi: 10.1016/j.cej.2019.122565.

[137] Y. Cheng, C. Wang, F. Kang, and Y. B. He, "Self-Healable Lithium-Ion Batteries: A Review," *Nanomaterials*, vol. 12, no. 20. MDPI, Oct. 01, 2022. doi: 10.3390/nano12203656.

[138] J. Karvinen and M. Kellomäki, "Characterization of Self-Healing Hydrogels for Biomedical Applications," *Eur Polym J*, p. 111641, Oct. 2022, doi: 10.1016/j.eurpolymj.2022.111641.

[139] T. W. Kwon, Y. K. Jeong, E. Deniz, S. Y. Alqaradawi, J. W. Choi, and A. Coskun, "Dynamic Cross-Linking of Polymeric Binders Based on Host-Guest Interactions for Silicon Anodes in Lithium Ion Batteries," *ACS Nano*, vol. 9, no. 11, pp. 11317–11324, Nov. 2015, doi: 10.1021/acsnano.5b05030.

[140] K. Sugane and M. Shibata, "Self-healing thermoset polyurethanes utilizing host–guest interaction of cyclodextrin and adamantane," *Polymer (Guildf)*, vol. 221, Apr. 2021, doi: 10.1016/j.polymer.2021.123629.

[141] L. Zhang, L. Zhang, L. Chai, P. Xue, W. Hao, and H. Zheng, "A coordinatively cross-linked polymeric network as a functional binder for

high-performance silicon submicro-particle anodes in lithium-ion batteries," *J Mater Chem A Mater*, vol. 2, no. 44, pp. 19036–19045, Nov. 2014, doi: 10.1039/c4ta04320k.

[142] F. Herbst, D. Döhler, P. Michael, and W. H. Binder, "Self-healing polymers via supramolecular forces," *Macromolecular Rapid Communications*, vol. 34, no. 3. pp. 203–220, Feb. 12, 2013. doi: 10.1002/marc.201200675.

[143] L. Zhang, P. Zhang, C. Chang, W. Guo, Z. H. Guo, and X. Pu, "Self-Healing Solid Polymer Electrolyte for Room-Temperature Solid-State Lithium Metal Batteries," *ACS Appl Mater Interfaces*, vol. 13, no. 39, pp. 46794–46802, Oct. 2021, doi: 10.1021/acsami.1c14462.

[144] F. Ding *et al.*, "Dendrite-free lithium deposition via self-healing electrostatic shield mechanism," *J Am Chem Soc*, vol. 135, no. 11, pp. 4450–4456, Mar. 2013, doi: 10.1021/ja312241y.

[145] R. Narayan, C. Laberty-Robert, J. Pelta, J. M. Tarascon, and R. Dominko, "Self-Healing: An Emerging Technology for Next-Generation Smart Batteries," *Advanced Energy Materials*, vol. 12, no. 17. John Wiley and Sons Inc, May 01, 2022. doi: 10.1002/aenm.202102652.

[146] B. Briou, B. Ameduri, B. Boutevin, and B. Améduri, "Trends in Diels Alder in Polymer Chemistry", doi: 10.1039/d0cs01382jï.

[147] S. Billiet, W. van Camp, X. K. D. Hillewaere, H. Rahier, and F. E. du Prez, "Development of optimized autonomous self-healing systems for epoxy materials based on maleimide chemistry," *Polymer (Guildf)*, vol. 53, no. 12, pp. 2320–2326, May 2012, doi: 10.1016/j.polymer.2012.03.061.

[148] Y. Chujo, K. Sada, and T. Saegusa, "Reversible Gelation of Polyoxazoline by Means of Diels-Alder Reaction1," Wiley, 1990. [Online]. Available: https://pubs.acs.org/sharingguidelines

[149] Z. He, H. Niu, and Y. Li, "UV-Light Responsive and Self-Healable Ethylene/Propylene Copolymer Rubbers Based on Reversible [4 + 4] Cycloaddition of Anthracene Derivatives," *Macromol Chem Phys*, vol. 221, no. 12, Jun. 2020, doi: 10.1002/macp.202000096.

[150] D. Y. Wu, S. Meure, and D. Solomon, "Self-healing polymeric materials: A review of recent developments," *Progress in Polymer Science (Oxford)*, vol.

33, no. 5. pp. 479–522, May 2008. doi: 10.1016/j.progpolymsci.2008.02.001.

[151] T. Hughes, G. P. Simon, and K. Saito, "Light-Healable Epoxy Polymer Networks via Anthracene Dimer Scission of Diamine Crosslinker," *ACS Appl Mater Interfaces*, vol. 11, no. 21, pp. 19429–19443, May 2019, doi: 10.1021/acsami.9b02521.

[152] X. Cao *et al.*, "Self-healing solid polymer electrolyte based on imine bonds for high safety and stable lithium metal batteries," *RSC Adv*, vol. 11, no. 5, pp. 2985–2994, Jan. 2021, doi: 10.1039/d0ra10035h.

[153] Z. Xie, B. L. Hu, R. W. Li, and Q. Zhang, "Hydrogen Bonding in Self-Healing Elastomers," *ACS Omega*, vol. 6, no. 14. American Chemical Society, pp. 9319–9333, Apr. 13, 2021. doi: 10.1021/acsomega.1c00462.

[154] J. v. Nardeli, C. S. Fugivara, M. Taryba, M. F. Montemor, and A. v. Benedetti, "Self-healing ability based on hydrogen bonds in organic coatings for corrosion protection of AA1200," *Corros Sci*, vol. 177, Dec. 2020, doi: 10.1016/j.corsci.2020.108984.

[155] K. E. Feldman, M. J. Kade, T. F. A. de Greef, E. W. Meijer, E. J. Kramer, and C. J. Hawker, "Polymers with multiple hydrogen-bonded end groups and their blends," *Macromolecules*, vol. 41, no. 13, pp. 4694–4700, Jul. 2008, doi: 10.1021/ma800375r.

[156] S. Burattini, B. W. Greenland, D. Chappell, H. M. Colquhoun, and W. Hayes, "Healable polymeric materials: A tutorial review," *Chem Soc Rev*, vol. 39, no. 6, pp. 1973–1985, May 2010, doi: 10.1039/b904502n.

[157] S. Dumitrescu, V. Percec, and C. I. Simionescu, "Polymerization of Acetylenic Derivatives. XXVII. Synthesis and Properties of Isomeric Poly-N-ethynylcarbazole *," 1977.

[158] A. J. D'Angelo and M. J. Panzer, "Design of Stretchable and Self-Healing Gel Electrolytes via Fully Zwitterionic Polymer Networks in Solvate Ionic Liquids for Li-Based Batteries," *Chemistry of Materials*, vol. 31, no. 8, pp. 2913–2922, Apr. 2019, doi: 10.1021/acs.chemmater.9b00172.

[159] M. Invernizzi, S. Turri, M. Levi, and R. Suriano, "4D printed thermally activated self-healing and shape memory polycaprolactone-based

polymers," *Eur Polym J*, vol. 101, pp. 169–176, Apr. 2018, doi: 10.1016/j.eurpolymj.2018.02.023.

[160] Y. Lin and G. Li, "An intermolecular quadruple hydrogen-bonding strategy to fabricate self-healing and highly deformable polyurethane hydrogels," *J Mater Chem B*, vol. 2, no. 39, pp. 6878–6885, Oct. 2014, doi: 10.1039/c4tb00862f.

[161] I. Gadwal, "A Brief Overview on Preparation of Self-Healing Polymers and Coatings via Hydrogen Bonding Interactions," *Macromol*, vol. 1, no. 1, pp. 18–36, Dec. 2020, doi: 10.3390/macromol1010003.

[162] N. Wu *et al.*, "Self-Healable Solid Polymeric Electrolytes for Stable and Flexible Lithium Metal Batteries," *Angewandte Chemie*, vol. 131, no. 50, pp. 18314–18317, Dec. 2019, doi: 10.1002/ange.201910478.

[163] F. H. Beijer, R. P. Sijbesma, H. Kooijman, A. L. Spek, and E. W. Meijer, "Strong Dimerization of Ureidopyrimidones via Quadruple Hydrogen Bonding," 1998. [Online]. Available: https://pubs.acs.org/sharingguidelines

[164] G. Zhang, Z. Sun, and M. Li, "Recent developments: self-healing polymers based on quadruple hydrogen bonds," *E3S Web of Conferences*, vol. 290, p. 01037, 2021, doi: 10.1051/e3sconf/202129001037.

[165] B. Zhou *et al.*, "Self-healing composite polymer electrolyte formed via supramolecular networks for high-performance lithium-ion batteries," *J Mater Chem A Mater*, vol. 7, no. 17, pp. 10354–10362, 2019, doi: 10.1039/c9ta01214a.

[166] B. Zhou *et al.*, "Flexible, Self-Healing, and Fire-Resistant Polymer Electrolytes Fabricated via Photopolymerization for All-Solid-State Lithium Metal Batteries," *ACS Macro Lett*, vol. 9, no. 4, pp. 525–532, Apr. 2020, doi: 10.1021/acsmacrolett.9b01024.

[167] H. Gan, Y. Zhang, S. Li, L. Yu, J. Wang, and Z. Xue, "Self-Healing Single-Ion Conducting Polymer Electrolyte Formed via Supramolecular Networks for Lithium Metal Batteries," *ACS Appl Energy Mater*, vol. 4, no. 1, pp. 482–491, Jan. 2021, doi: 10.1021/acsaem.0c02384.

[168] B. Zhou *et al.*, "Self-Healing Polymer Electrolytes Formed via Dual-Networks: A New Strategy for Flexible Lithium Metal Batteries," *Chemistry*

- *A European Journal*, vol. 24, no. 72, pp. 19200–19207, Dec. 2018, doi: 10.1002/chem.201803943.

[169] Y. H. Jo *et al.*, "Self-Healing Solid Polymer Electrolyte Facilitated by a Dynamic Cross-Linked Polymer Matrix for Lithium-Ion Batteries," *Macromolecules*, vol. 53, no. 3, pp. 1024–1032, Feb. 2020, doi: 10.1021/acs.macromol.9b02305.

[170] N. Holten-Andersen *et al.*, "pH-induced metal-ligand cross-links inspired by mussel yield self-healing polymer networks with near-covalent elastic moduli", doi: 10.1073/pnas.1015862108/-/DCSupplemental.

[171] K. Yamauchi, J. R. Lizotte, and T. E. Long, "Thermoreversible poly(alkyl acrylates) consisting of self-complementary multiple hydrogen bonding," *Macromolecules*, vol. 36, no. 4, pp. 1083–1088, Feb. 2003, doi: 10.1021/ma0212801.

[172] J. H. Yang *et al.*, "Understanding and controlling the self-healing behavior of 2-ureido-4[1H]-pyrimidinone-functionalized clustery and dendritic dual dynamic supramolecular network," *Polymer (Guildf)*, vol. 172, pp. 13–26, May 2019, doi: 10.1016/j.polymer.2019.03.027.

[173] M. Nowak, P. Bednarczyk, K. Mozelewska, and Z. Czech, "Synthesis and Characterization of Urethane Acrylate Resin Based on 1,3-Propanediol for Coating Applications," *Coatings*, vol. 12, no. 12, Dec. 2022, doi: 10.3390/coatings12121860.

[174] F. Gao *et al.*, "Properties of UV-cured self-healing coatings prepared with PCDL-based polyurethane containing multiple H-bonds," *Prog Org Coat*, vol. 113, pp. 160–167, Dec. 2017, doi: 10.1016/j.porgcoat.2017.09.011.

[175] P. Ping, Q. Wang, J. Sun, H. Xiang, and C. Chen, "Thermal Stabilities of Some Lithium Salts and Their Electrolyte Solutions With and Without Contact to a LiFePO[sub 4] Electrode," *J Electrochem Soc*, vol. 157, no. 11, p. A1170, 2010, doi: 10.1149/1.3473789.

[176] Z. Wang *et al.*, "High conductivity polymer electrolyte with comb-like structure via a solvent-free UV-cured method for large-area ambient all-solid-sate lithium batteries," *Journal of Materiomics*, vol. 5, no. 2, pp. 195–203, Jun. 2019, doi: 10.1016/j.jmat.2019.04.002.

[177] M. Worzakowska, "Uv polymerization of methacrylates—preparation and properties of novel copolymers," *Polymers (Basel)*, vol. 13, no. 10, May 2021, doi: 10.3390/polym13101659.

[178] D. Callegari *et al.*, "Autonomous Self-Healing Strategy for Stable Sodium-Ion Battery: A Case Study of Black Phosphorus Anodes," *ACS Appl Mater Interfaces*, vol. 13, no. 11, pp. 13170–13182, Mar. 2021, doi: 10.1021/acsami.0c22464.

[179] D. R. Holycross and M. Chai, "Comprehensive NMR studies of the structures and properties of PEI polymers," *Macromolecules*, vol. 46, no. 17, pp. 6891–6897, Sep. 2013, doi: 10.1021/ma4011796.

[180] B. Zhou *et al.*, "Self-Healing Polymer Electrolytes Formed via Dual-Networks: A New Strategy for Flexible Lithium Metal Batteries," *Chemistry - A European Journal*, vol. 24, no. 72, pp. 19200–19207, Dec. 2018, doi: 10.1002/chem.201803943.

[181] Z. Osman, M. I. Mohd Ghazali, L. Othman, and K. B. Md Isa, "AC ionic conductivity and DC polarization method of lithium ion transport in PMMA-LiBF 4 gel polymer electrolytes," *Results Phys*, vol. 2, pp. 1–4, 2012, doi: 10.1016/j.rinp.2011.12.001.

[182] S. Park *et al.*, "In-situ preparation of gel polymer electrolytes in a fully-assembled lithium ion battery through deeply-penetrating high-energy electron beam irradiation," *Chemical Engineering Journal*, vol. 452, Jan. 2023, doi: 10.1016/j.cej.2022.139339.

[183] C. M. Kuntz and A. L. L. East, "An Arrhenius Argument to Explain Electrical Conductivity Maxima versus Temperature," *ECS Trans*, vol. 50, no. 11, pp. 71–78, Mar. 2013, doi: 10.1149/05011.0071ecst.

[184] C. Mo *et al.*, "Rapid Formation of an Artificial Polymer Cladding on a Lithium Metal Anode by in Situ Ultraviolet Curing to Regulate Lithium Ion Flux," *ACS Appl Energy Mater*, vol. 5, no. 7, pp. 9118–9130, Jul. 2022, doi: 10.1021/acsaem.2c01617.

[185] T. Liu *et al.*, "Review—In Situ Polymerization for Integration and Interfacial Protection Towards Solid State Lithium Batteries," *J Electrochem Soc*, vol. 167, no. 7, p. 070527, Jan. 2020, doi: 10.1149/1945-7111/ab76a4.

[186] B. Liu *et al.*, "A novel porous gel polymer electrolyte based on poly(acrylonitrile-polyhedral oligomeric silsesquioxane) with high performances for lithium-ion batteries," *J Memb Sci*, vol. 545, pp. 140–149, 2018, doi: 10.1016/j.memsci.2017.09.077.

[187] K. Shigenobu, K. Dokko, M. Watanabe, and K. Ueno, "Solvent effects on Li ion transference number and dynamic ion correlations in glyme- And sulfolane-based molten Li salt solvates," *Physical Chemistry Chemical Physics*, vol. 22, no. 27, pp. 15214–15221, Jul. 2020, doi: 10.1039/d0cp02181d.

[188] J. Evans, C. A. Vincent, and P. G. Bruce, "Electrochemical measurement of transference numbers in polymer electrolytes."

[189] Y. Wang *et al.*, "Gel Polymer Electrolyte with High Li + Transference Number Enhancing the Cycling Stability of Lithium Anodes," *ACS Appl Mater Interfaces*, vol. 11, no. 5, pp. 5168–5175, Feb. 2019, doi: 10.1021/acsami.8b21352.

[190] B. Boz, H. O. Ford, A. Salvadori, and J. L. Schaefer, "Porous Polymer Gel Electrolytes Influence Lithium Transference Number and Cycling in Lithium-Ion Batteries," *Electronic Materials*, vol. 2, no. 2, pp. 154–173, May 2021, doi: 10.3390/electronicmat2020013.

[191] R. Khurana, J. L. Schaefer, L. A. Archer, and G. W. Coates, "Suppression of lithium dendrite growth using cross-linked polyethylene/poly(ethylene oxide) electrolytes: A new approach for practical lithium-metal polymer batteries," *J Am Chem Soc*, vol. 136, no. 20, pp. 7395–7402, May 2014, doi: 10.1021/ja502133j.

Appendix

List of publications

"UV-cured self-healing gel polymer electrolyte toward safer room temperature lithium metal batteries"

Simone Siccardi, Julia Amici, Samuele Colombi, José Tiago Carvalho, Daniele Versaci, Eliana Quartarone, Luis Pereira, Federico Bella, Carlotta Francia, Silvia Bodoardo, Electrochimica Acta, Volume 433, 2022, 141265, ISSN 0013-4686,

List of oral/poster presentation

Poster: "Self-Healing Polymers for Lithium Metal Batteries"
Simone Siccardi, Julia Amici, Carlotta Francia, Silvia Bodoardo
Jeju Island, South Korea, 72nd Annual Meeting of International Society of Electrochemistry (2021), 29th August – 3rd September; online

Poster: "Self-Healing Polymers for Lithium Metal Batteries"
Simone Siccardi, Julia Amici, Daniele Versaci, Lucia Fagiolari, Federico Bella, Carlotta Francia, Silvia Bodoardo
Prague, Czech Republic, 1st Regional Meeting of International Society of Electrochemistry (2022), 15th August – 19th August

Oral Presentation: "Self-Healing Polymers for Lithium Metal Batteries"
Simone Siccardi, Julia Amici, Daniele Versaci, Lucia Fagiolari, Federico Bella, Carlotta Francia, Silvia Bodoardo
Lisbon, Portugal, 11th European School of Young Material Scientists (2022), 26th September – 27th September